الجمهورية الجزائرية الديمقراطية الشعبية
People's Democratic Republic of Algeria
وزارة التعليم العالي والبحث العلمي
Ministry of Higher Education and Scientific Research

جامعة زيان عاشور بالجلفة
Ziane Achour University of Djelfa

كلية العلوم والتكنولوجيا
Faculty of Science and Technology

Department: Electrical Engineering

DOCTORAL THESIS

3rd Cycle Doctoral (D-LMD)

Presented by

MEDKOUR Maissa

Submitted in Fulfilment of the Requirements for the Degree of 3rd Cycle Doctorate (D_LMD)

Branch: Electromechanical

Specialty: Industrial Maintenance

Topic

Optimisation and Control of Storage in Smart Grids

Supported, on 03 / 06 /2026, before the jury composed of:

Last and first name	Grade	Affiliation	Designation
Mr. CHARRAK Naas	MCA	University of Djelfa	Président
Mr. LAROUSSI Kouider	Professor	University of Djelfa	Supervisor
Mr. AIT ABBAS Hamou	MCA	University of Bouira	Examiner
Mr. M'HAMEDI Benalia	MCA	University of Djelfa	Examiner
Mr. ELBAR Mohamed	MCA	University of Djelfa	Examiner

Djelfa University, FST – 2026-

Sommaire

Figures

Tables

Abbreviations

ABC Artificial Bee Colony

AC Alternating Current

ANN Artificial Neural Network

ARIMA AutoRegressive Integrated Moving Average

BESS Battery Energy Storage System

BMS Battery Management System

CAES Compressed Air Energy Storage

CC Coulomb Counting

CPS Cyber Physical System

DC Direct Current

DE Differential Evolution

DOD Depth of Discharge

DPC Direct Power Control

EIS Electrochemical Impedance Spectroscopy

EKF Extended Kalman Filter

EMS Energy Management System

ESS Energy Storage System

FESS Flywheel Energy Storage System

FOPI Fractional-Order Proportional-Integral

GA Genetic Algorithm

GWO Grey Wolf Optimizer

LCOS Levelized Cost of Storage

Li-ion Lithium-ion

MAE Mean Absolute Error

MASE Mean Absolute Scaled Error

MATLAB Matrix Laboratory

MPPT Maximum Power Point Tracking

OCV Open Circuit Voltage

OCP Open Circuit Potential

PID Proportional-Integral-Derivative

PI Proportional Integral

PWM Pulse Width Modulation

PHS Pumped Hydro Storage

PSO Particle Swarm Optimization

PV Photovoltaic

RBC Rule-Based Control

REF Reference

Rint Internal Resistance Model

RMSE Root Mean Square Error

RUL Remaining Useful Life

SG Smart Grid

SOH State of Health

SOC State of Charge

SMES Superconducting Magnetic Energy Storage

SVM Support Vector Machine

V2G Vehicle to Grid

Acknowledgements

All praise and gratitude are due to Allah, the Almighty, whose guidance and mercy enabled me to reach this milestone.

I sincerely thank my thesis supervisor, ***Professor Laroussi Kouider****, for his guidance, support, and valuable advice throughout this research.*

I would also like to express my deep appreciation to the ***President and members of the examination committee****, namely* ***Dr. Cherak Naas****, President;* ***Dr. Ait Abbas Hamou****, Examiner;* ***Dr. M'hamedi Benalia****, Examiner; and* ***Dr. Elbar Mohamed****, Examiner, for their time, efforts, and constructive remarks that greatly contributed to improving this thesis.*

My sincere gratitude also goes to the ***Applied Automation and Industrial Diagnostics Laboratory (LAADI)*** *for providing a supportive research environment and the necessary facilities during this work.*

I am equally thankful to my colleagues and professors from ***the Faculty of Science and Technology****, especially those from the* ***Department of Electrical Engineering at the University of Djelfa****, for their collaboration, encouragement, and valuable exchanges throughout my research journey*

Finally, I extend my deepest gratitude to my family, my mother, my father, my aunts, and my brothers and sisters for their constant support and encouragement. ***Maissa MEDKOUR***

Table of Publications

	Journal Paper
	MEDKOUR, Maissa, ROUIBAH, Abdelkader, et LAROUSSI, Kouider. Optimal FOPI Control for Energy Storage in a PV Microgrid using Predicted Solar and Load Profiles: Design and Evaluation Jestr r. Journal of Engineering Science and Technology Review, 2025, vol. 18, no 6, p. 142-152.

	IEEE Conferences Papers
1	MAISSA, Medkour et KOUIDER, Laroussi. Direct power control technique for Grid-tied two levels VSI inverter fed by photovoltaic system. In : 2023 1st International Conference on Renewable Solutions for Ecosystems: Towards a Sustainable Energy Transition (ICRSEtoSET). IEEE, 2023. p. 1-5.
2	MAISSA, Medkour, KOUIDER, Laroussi, et ALI, Teta. DPC control for grid-tied inverter powered by PV system under change of parameters and load. In : 2023 2nd International Conference on Electronics, Energy and Measurement (IC2EM). IEEE, 2023. p. 1-7.
3	BOUTOUTA, Fatima, KOUZOU, Abdellah, BELADEL, Abdelkader, et al. Predictive Current Control of a Grid-Connected Photovoltaic Voltage Source Inverter. In : 2023 1st International Conference on Renewable Solutions for Ecosystems: Towards a Sustainable Energy Transition (ICRSEtoSET). IEEE, 2023. p. 1-5.
4	TETA, Ali, MEDKOUR, Maissa, CHENNANA, Ahmed, et al. A Novel Transfer Learning Approach for Detecting Partial Shading in Photovoltaic Systems. In : 2024 IEEE/ACM International Conference on Big Data Computing, Applications and Technologies (BDCAT). IEEE, 2024. p. 290-295.

Abstract :

The high penetration of renewable energy sources, combined with the continuous growth in electricity demand, has led to a significant transformation of electrical power systems. This evolution may cause instability and reliability issues within the power grid. To ensure the stability of the electrical supply system, the integration of renewable energy sources must be carried out in a smooth and controlled manner. Energy storage systems represent an effective solution to facilitate a smooth transition while maintaining power system stability. In this work, the lithium-ion battery plays a dual role. First, it is used as an energy storage system by individual consumers to minimize electricity costs. This is achieved through energy arbitrage based on electricity pricing, power factor correction, peak demand reduction, and energy conservation Second, the lithium-ion battery is also employed to enhance the reliability and stability of the electrical grid. In this case, dynamic regulation and balancing phases are required. This work proposes control and optimization algorithms for energy storage systems to ensure the smooth integration of renewable energy sources while guaranteeing the stability of the electrical power system.

Key words*: Microgrid, Energy Management System (EMS), FOPI Controller, Grey Wolf Optimization, Battery Storage, Prediction*.

Résumé :

La forte intégration des énergies renouvelables, combinée à l'augmentation continue de la consommation électrique, entraîne une transformation profonde des systèmes d'énergie électrique. Cette évolution peut engendrer des problèmes de stabilité et de fiabilité du réseau électrique. Afin de garantir la stabilité du système d'alimentation électrique, l'intégration des sources d'énergie renouvelables doit être réalisée de manière progressive et maîtrisée. Le stockage de l'énergie constitue une solution pertinente pour assurer une transition en douceur, tout en maintenant la stabilité du réseau électrique. Dans ce travail, la batterie lithium-ion joue un double rôle. Premièrement, elle est utilisée comme système de stockage d'énergie par les consommateurs individuels afin de minimiser le coût de l'électricité. Cette optimisation repose sur l'arbitrage énergétique en fonction du prix de l'électricité, la correction du facteur de puissance, la réduction de la demande de pointe et la préservation de l'énergie. Deuxièmement, la batterie lithium-ion contribue à l'amélioration de la fiabilité et de la stabilité du réseau électrique. Dans ce contexte, une régulation dynamique et une phase d'équilibrage sont nécessaires. Ce travail propose ainsi des algorithmes de commande et d'optimisation du stockage d'énergie visant à assurer une intégration harmonieuse des énergies renouvelables tout en garantissant la stabilité du système d'alimentation électrique.

Mots clés *: Micro-réseau, Système de Gestion de l'Énergie (SGE), Contrôleur FOPI, Optimisation par Loup Gris, Stockage par Batterie, Prévision.*

الملخص

أدى الإدماج المتزايد لمصادر الطاقة المتجددة، إلى جانب النمو المستمر في استهلاك الطاقة الكهربائية، إلى إحداث تحولات جوهرية في أنظمة الطاقة الكهربائية. وقد تؤدي هذه التحولات إلى زعزعة استقرار وموثوقية شبكة التغذية الكهربائية. ولضمان استقرار نظام التغذية الكهربائية، يجب أن يتم دمج مصادر الطاقة المتجددة بشكل تدريجي ومنضبط يُعد تخزين الطاقة أحد الحلول الفعالة لضمان انتقال سلس، مع الحفاظ على استقرار الشبكة الكهربائية. في هذا العمل، تلعب بطارية الليثيوم-أيون دورًا مزدوجًا.أولاً، تُستخدم كنظام لتخزين الطاقة من قبل المستهلكين الأفراد بهدف تقليل تكلفة الكهرباء، وذلك من خلال الموازنة الطاقوية المعتمدة على سعر الكهرباء، وتصحيح معامل القدرة، وتقليل ذروة الطلب، والحفاظ على الطاقة.ثانيًا، تُستخدم بطارية الليثيوم-أيون أيضًا لتحسين موثوقية واستقرار الشبكة الكهربائية. وفي هذه الحالة، تصبح عملية التنظيم الديناميكي ومرحلة الموازنة ضرورية. يقترح هذا العمل خوارزميات تحكم وتحسين لأنظمة تخزين الطاقة، تهدف إلى ضمان دمج سلس لمصادر الطاقة المتجددة مع الحفاظ على استقرار نظام التغذية الكهربائية.

كلمات مفتاحية: الشبكة المصغرة، نظام إدارة الطاقة، المتحكم *FOPI*، تحسين الذئب الرمادي، تخزين البطاريات، التنبؤ.

General Introduction

The continuous growth of global energy demand, coupled with the urgent need to mitigate climate change and reduce dependence on fossil fuels, has profoundly transformed the structure and operation of modern electrical power systems. In recent decades, renewable energy sources such as photovoltaic (PV) and wind energy have experienced rapid development and large-scale deployment. Although these resources are environmentally sustainable, their intrinsic intermittency and uncertainty pose significant technical challenges to power system stability, reliability, and energy quality.

To address these challenges, the concept of smart grids has emerged as a key paradigm for next-generation power systems. Smart grids combine advanced sensing, communication, and control technologies to enable bidirectional power and information flows between generation units, storage systems, and consumers. This intelligent infrastructure enhances operational flexibility, improves energy efficiency, and facilitates the large-scale integration of renewable energy sources. However, the effective operation of smart grids requires robust energy management strategies capable of coordinating multiple heterogeneous components under dynamic and uncertain conditions.

Energy storage systems (ESS) constitute a cornerstone of smart grid architectures by providing the ability to decouple energy generation from consumption. They contribute to peak shaving, frequency regulation, voltage support, and the mitigation of renewable energy fluctuations. Among the various storage technologies, lithium-ion (Li-ion) batteries have emerged as the most promising solution for both stationary and mobile applications due to their high energy density, superior efficiency, fast response time, and long cycle life. Nevertheless, Li-ion batteries are highly sensitive to operating conditions such as overcharging, deep discharging, temperature variations, and high current rates, which can accelerate ageing and reduce their lifespan.

Consequently, the development of advanced energy management and control strategies is essential to fully exploit the advantages of lithium-ion batteries while ensuring their safe and durable operation. Conventional control approaches, including proportional–integral (PI) and proportional–integral–derivative (PID) controllers, are widely implemented in industrial applications due to their simplicity and ease of tuning. However, these methods often exhibit

limited performance when dealing with nonlinear dynamics, system uncertainties, and rapid variations in renewable generation and load demand.

In recent years, fractional-order controllers have gained increasing attention as a powerful alternative to classical integer-order controllers. By introducing non-integer differentiation and integration orders, fractional-order PI (FOPI) controllers provide additional degrees of freedom, enabling improved robustness, better transient response, and enhanced steady-state accuracy. At the same time, metaheuristic optimization algorithms inspired by natural phenomena have proven effective in tuning controller parameters in complex and nonlinear systems. Among these algorithms, the Grey Wolf Optimizer (GWO) stands out for its simplicity, fast convergence, and strong global search capability.

Within this context, this thesis proposes a novel energy management strategy for a grid-connected photovoltaic microgrid equipped with a lithium-ion battery storage system. The proposed approach combines a FOPI controller with the Grey Wolf Optimizer to optimally regulate the bidirectional DC–DC converter interfacing the battery with the DC bus. The objective is to enhance system stability, reduce energy losses, minimize battery degradation, and improve overall energy efficiency under varying operating conditions.

The contributions of this work include the detailed modeling of the photovoltaic system, power electronic converters, and lithium-ion battery, the design and optimization of a FOPI-based control scheme using GWO, and an extensive simulation-based performance evaluation. The results demonstrate the effectiveness of the proposed strategy compared to conventional PI control, highlighting its potential for practical implementation in future smart grid and microgrid applications.

This thesis is structured as follows. **Chapter 1** presents a comprehensive state of the art on smart grids, with a particular focus on renewable energy integration and energy storage systems, highlighting the role and challenges of lithium-ion batteries within smart grid architectures. **Chapter 2** is devoted to the modeling of the lithium-ion battery, including its electrical characteristics, performance analysis, and integration within smart grid and microgrid environments. **Chapter 3** addresses energy management and control systems, covering conventional and advanced control approaches, and details the proposed control and optimization methodology adopted in this work, namely the fractional-order PI controller optimized using the Grey Wolf Optimizer. **Chapter 4** presents the simulation results and performance evaluation of the proposed strategy under various operating conditions, followed

by a detailed discussion and comparative analysis with classical control methods. Finally, the thesis concludes with a summary of the main contributions and perspectives for future research.

Chapter 1: State of the Art on Smart Grids and Energy Storage Systems

1.1. INTRODUCTION

The worldwide energy transition towards sustainable and resilient power systems is increasingly predicated on the advancement of smart grids and the efficient integration of renewable energy sources. Nonetheless, these advancements provide various obstacles regarding forecasting, adaptability, security, and power quality.

The initial chapter presents a systematic literature review to establish the conceptual and technological underpinnings essential for comprehending the challenges associated with the control and optimization of energy storage in this environment.

Subsequently, emphasis is placed on energy storage systems (ESS), which are crucial for reconciling production and consumption, alleviating the variability of renewable energies, and improving grid stability. The many families of technologies mechanical, electrical, electrochemical, or hybrid, are delineated, emphasizing their operational principles, performance metrics, and application domains.

Among these technologies, lithium-ion batteries occupy an important place due to their high energy density, good efficiency and high cyclability, thus justifying their adoption in many distributed storage systems.

Finally, the chapter presents advanced control and optimisation approaches that enable intelligent energy flow management, focusing on conventional methods (PI control), heuristic approaches and artificial intelligence techniques, while identifying current limitations such as managing intermittency, premature battery wear and challenges related to multi-objective optimisation.

This critical review paves the way for the contributions proposed in this work, which aim to develop robust and adaptive control strategies to extend battery life, improve overall energy efficiency, and address the specific constraints of modern smart grids.

Chapter 1 of this thesis provides a structured literature review, establishing a solid conceptual and technological foundation for addressing the challenges associated with controlling and optimising energy storage in smart grids.

The first section is devoted to an in-depth analysis of smart grids, detailing their architecture, key components, and capacity to integrate renewable energy sources, which are crucial elements for the energy transition and decarbonisation of electricity systems.

The second section examines energy storage technologies such as Li-ion batteries, supercapacitors and flywheels.

Among these technologies, lithium-ion batteries are the focus of particular attention due to their high energy density, long service life and high efficiency. They will be at the heart of the experimental study developed in the following chapters, where their behaviour will be analysed through an optimised energy management system.

The third section explores advanced control and optimisation methodologies, focusing on energy flow management strategies and optimisation approaches, particularly those based on heuristic algorithms and artificial intelligence techniques.

Finally, the last section identifies the limitations of existing work, including challenges related to managing the intermittency of renewable energies, storage flexibility and algorithm efficiency, in order to propose areas for improvement and position the contributions of this thesis within a clearly defined scientific and technical framework.

This systematic progression aims to contextualise the issues and guide the reader towards the specific topics addressed in the following chapters.

1.2. EVOLUTION OF ELECTRICITY NETWORKS: FROM TRADITIONAL NETWORKS TO SMART GRIDS

In 2019, despite the fact that 770 million people worldwide still lack access to electricity, electricity grids have continued to expand in size and capacity since the construction of the first long-distance transmission line in 1896. However, current infrastructure, designed at the end of the 19th century, is not suited to modern challenges such as behaviour prediction, resilience, consumer participation and responsiveness.

The transition to smart grids addresses these challenges by optimising electricity generation, distribution, transmission and marketing in response to real-time changes.

Smart grids provide faster responses through automated monitoring and control, facilitating more efficient integration of renewable energy while ensuring energy security.

Furthermore, they enable active consumer participation via smart devices, electric vehicles and solar roofs, thereby transforming a centralised network into a decentralised and optimised system based on distributed generation. [1]

1.3. INTRODUCTION TO SMART GRIDS

Smart grids, as illustrated in Figure 1.1, are electricity distribution systems that provide decentralised and automated energy management. They are an example of a cyber-physical system (CPS), integrating various monitoring, communication and data processing components, generating a significant volume of power and information to be transmitted and processed for the proper functioning of the system.

The main objective of smart grids is to provide real-time information and load control to consumers, distributors and network operators throughout the electricity production, transmission and distribution phases, in order to reduce costs while improving energy efficiency and system reliability. [2]

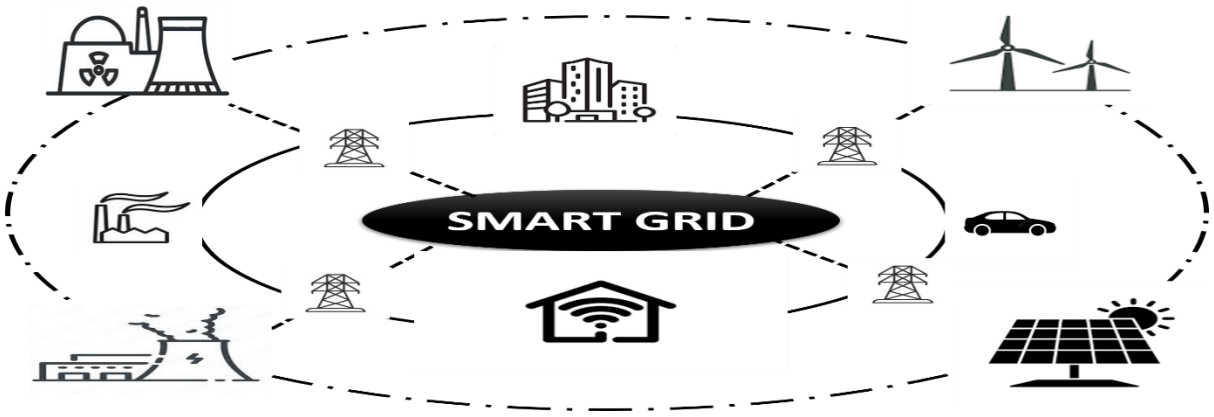

Figure 1.1 *Overview of Smart Grid Architecture*

1.4. KEY STRUCTURE AND COMPONENTS

The structure of a smart grid is based on several interconnected elements that work together to optimise electricity distribution, improve energy efficiency and ensure system reliability. The main components are as follows:

1.4.1. Energy production:

Electricity generation has undergone a transformation since the late 19th century, shifting from centralised systems to autonomous and decentralised systems. Technological advances have enabled the exploitation of renewable sources such as solar and wind power, thereby

promoting the decentralisation of production. Although renewable energies are proliferating, traditional sources will remain dominant until 2020, with a shift expected by 2050 [3].

1.4.2. Energy storage systems (ESS):

ESS are technologies designed to store energy for later use. Available in various forms,electrical, thermal or chemical, these systems play a key role in improving grid flexibility and reliability by capturing energy during periods of low demand and releasing it during peak consumption or when backup power is needed [4].

1.4.3. Transmission and distribution systems:

Transmission involves transporting electricity from production sites to distribution networks using equipment such as power quality monitors, protective relays and substation meters. Distribution, on the other hand, connects the transmission network to end consumers, with a focus on energy storage, control and management [5].

1.4.4. Smart meters:

These are advanced electronic devices that enable remote monitoring of electricity consumption. They offer features such as dynamic pricing and load management, facilitating energy control for both suppliers and users [6].

1.4.5. Energy management systems (EMS):

The EMS balances energy production and consumption within a microgrid, whether in grid-connected or isolated mode. It uses optimisation techniques such as PSO (Particle Swarm Optimisation) and DE (Differential Evolution) to minimise costs by efficiently managing resources such as photovoltaics, wind power, diesel and natural gas [7].

1.4.6. Communication networks:

Communication in smart grids refers to the exchange of information between the various actors and equipment in the network. It is crucial for the efficient management of data generated by sensors and its transmission to electricity companies [8].

1.4.7. Control and optimisation technologies:

Smart grid control relies on techniques such as droop control and proportional-integral (PI) controllers, which manage voltage regulation and reactive power distribution while ensuring accurate load sharing and stable power flow, even under different microgrid configurations [9].

1.4.8. Smart consumers:

Electricity consumers can be divided into four main sectors:

- Residential: individual and collective housing
- Commercial: public and private establishments
- Industrial: factories, agriculture, construction, etc.
- Transport: mainly based on fossil fuels but increasingly incorporating electric and rechargeable hybrid vehicles, as well as rail networks and trolleybuses connected continuously to the electricity grid [10].

1.5. ENERGY STORAGE TECHNOLOGIES

Energy storage systems play a strategic role in power grid management by mitigating fluctuations between intermittent generation and variable demand [11].

These technologies include mechanical, electrical, electrochemical, and hybrid storage systems [12], as illustrated in Figure 01.

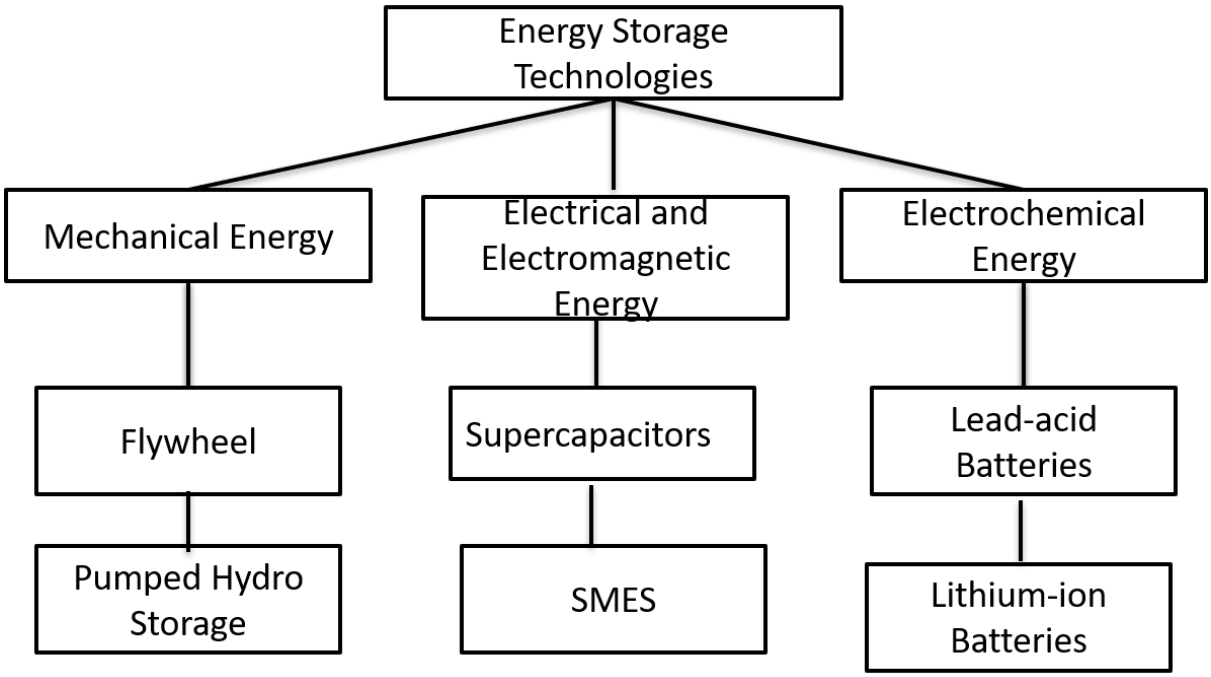

Figure 1.2 *Taxonomy of Energy Storage Technologies*

They fall into several categories, each based on distinct physical or chemical principles that address specific needs in terms of performance, response time, or storage capacity.

1.5.1. Mechanical Energy

1.5.1.1 Flywheel

The flywheel energy storage system converts electrical energy into mechanical energy (and vice versa) through an electromechanical motor/generator. The energy is stored as kinetic energy in a rotating rotor, whose capacity depends on its shape, the maximum allowable stress, and the density of the material.

Modern systems use a rotating cylinder with magnetic levitation, ensuring low maintenance and a long service life (over 20 years). They offer a specific energy of 5 to 25 Wh/kg, with peak power reaching up to 2 kW/kg for short durations (about one minute), and very high cyclability, exceeding 100,000 cycles [13].

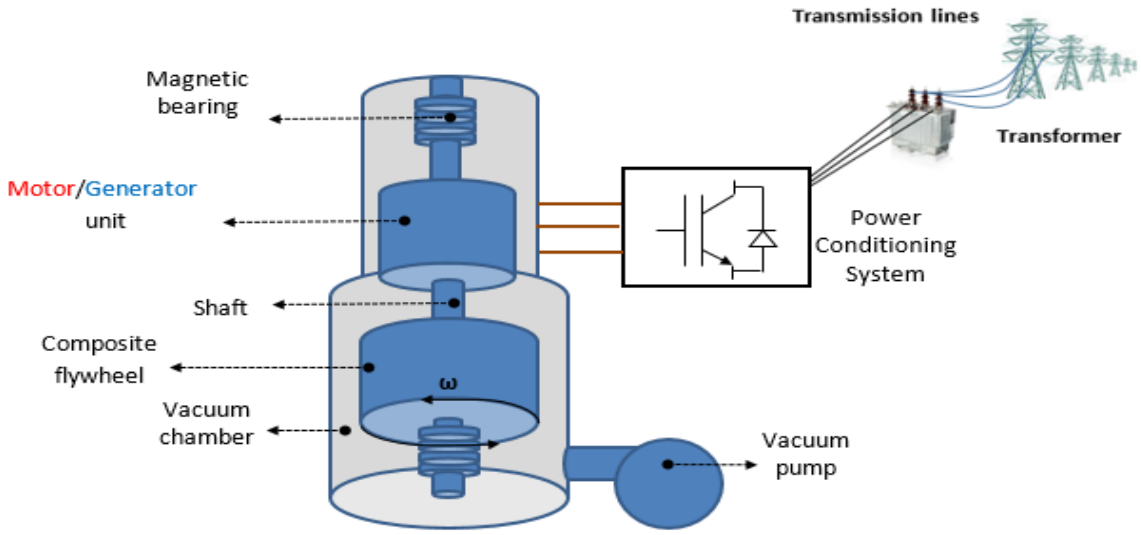

Figure 1.3 *Flywheel Energy Storage System (FESS)*

- ***Operating principles of a flywheel energy storage system:***

Inertial energy storage systems (IESS) are based on a reversible energy conversion: electricity is converted into mechanical energy via an electric motor, then stored as kinetic energy in a flywheel. During discharge, this energy is converted back into electricity by a generator, often a single asynchronous machine performing both functions (motor/generator), controlled by a power converter [14].

- IESS are characterised by:
- High power capacity,
- Very short response time (a few milliseconds),
- Long service life, primarily dependent on the cooling system.

1.5.1.2 Pumped Hydroelectric Storage (PHS)

The PHS system allows excess electricity during periods of low demand to be stored by pumping water to an elevated reservoir, then released as energy during peak consumption by letting it flow back through turbines. This method, used since the 1890s, today represents the primary means of large-scale energy storage (99% of global capacity). It comes in various sizes (pico, micro, small, and large PHS) with power ranging from a few kW to several thousand MW. Its energy efficiency varies between 70% and 85%, and its lifespan exceeds 40 years.

Although effective and durable, PHS is limited by high costs and geographic constraints. It can be coupled with renewable sources such as solar or wind to maximize energy efficiency [15].

Pumped hydro storage (PHS) is one of the most mature and widespread technologies for large-scale energy storage. Like any technological solution, it offers notable advantages that explain its adoption in many energy systems, but also presents limitations that must be considered during planning and deployment [16].

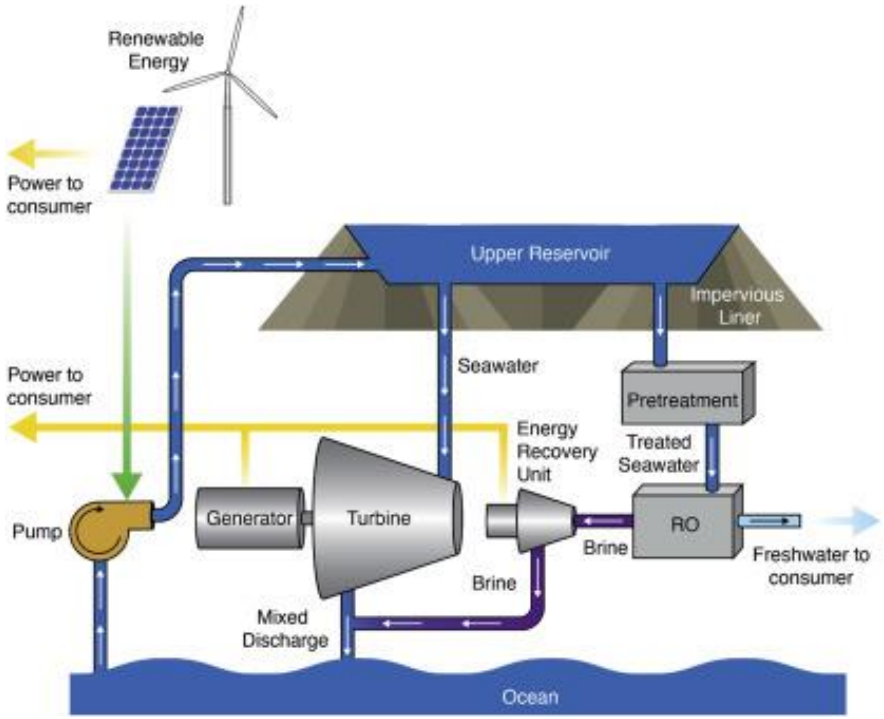

Figure 1.4 *Pumped Hydro Storage (PHS) System*

- ***Advantages of PHS:***

Among the main advantages of pumped storage are:

- Large-scale storage capacity, enabling the meeting of high energy demand.
- Low response time (ramp-up), ranging from a few seconds to a few minutes.
- Stable integration with variable renewable energy sources (such as wind or solar).
- Relatively low and stable levelized cost of storage (LCOS) over the long term.
- Low operating and maintenance costs once the system is installed.
- Long lifespan, often exceeding 50 years.
- Mature technology with a high degree of reliability.
- High round-trip efficiency, generally above 80%.

- Ability to respond quickly to fluctuations in electricity supply and demand.
- Capability to store large amounts of energy compared to other technologies.
- Low or even zero emissions after the construction phase.
- Flexible construction options, whether on rivers or off-stream.
- Contribution to energy system resilience, particularly during periods of high variability.

- ***Limitations of PHS:***

However, several technical, economic, and environmental constraints are associated with this technology:

- Very high initial investment cost, constituting a major barrier.
- This cost also represents a socio-economic obstacle, limiting adoption in certain contexts.
- Strong site topography constraints, restricting potential installation locations.
- Potential environmental impact, especially for on-river installations, which can affect local ecosystems.
- Sometimes insufficient transport and transmission infrastructure, particularly in remote areas.

1.5.1.3 Compressed Air Energy Storage (CAES)

CAES is an energy storage system that uses compressed air to generate electricity. Air is stored under pressure and then released into a turbine coupled to a generator to produce energy. To improve air expansion, a fuel (often natural gas) is used. The electricity produced is then injected into the grid [17].

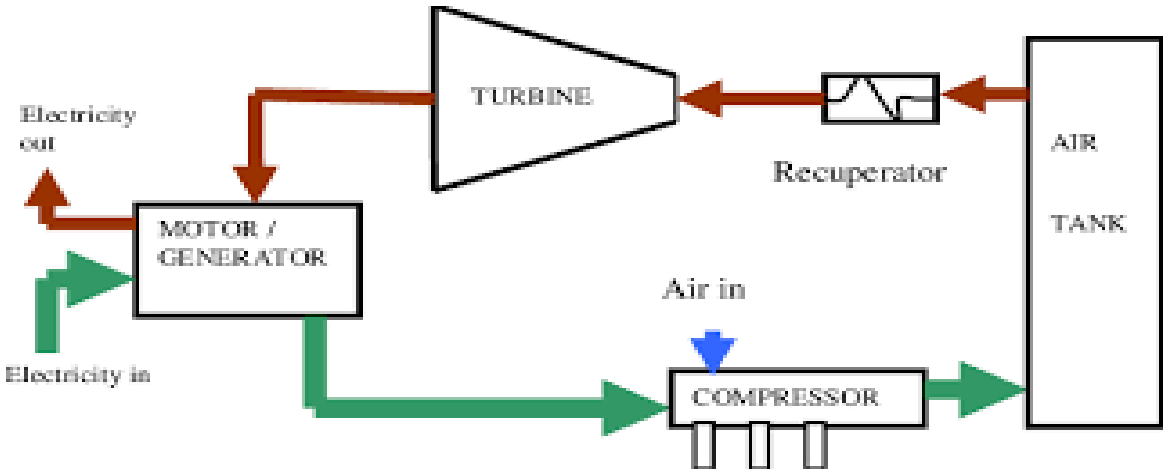

Figure 1.5 *Schematic Diagram of a CAES System*

According to [18], compressed air energy storage (CAES) systems have the following advantages and disadvantages:

- ***Advantages:***

• Medium- and large-scale storage capacity (from a few MW to several thousand MW).

• Energy density of approximately 12 kWh/m³.

• Efficiency of up to 70% with humidification and heat recovery.

• Fast start-up time (9 minutes in emergency mode, 12 minutes under normal conditions).

• Ability to compete with combined cycle gas turbines.

• Can be deployed close to consumption centres thanks to small-scale installations.

- ***Disadvantages:***

• Moderate efficiency without recovery (approximately 54%).

• High energy consumption for compression (0.7 to 0.8 kWh consumed for 1 kWh recovered).

• Requires approximately 5,800 kJ of fuel per kWh recovered.

• Risk of self-discharge losses in the event of air leaks.

• Complex infrastructure requiring compression, high-pressure storage and thermal conversion devices.

1.5.2. Electrical and Electromagnetic Energy

1.5.2.1 Supercapacitors

Supercapacitors store electrical energy without electrochemical reactions, enabling them to achieve very high charging and discharging speeds. Although their energy density is lower than that of batteries, their high reactivity makes them ideal for applications requiring instantaneous power peaks [19].

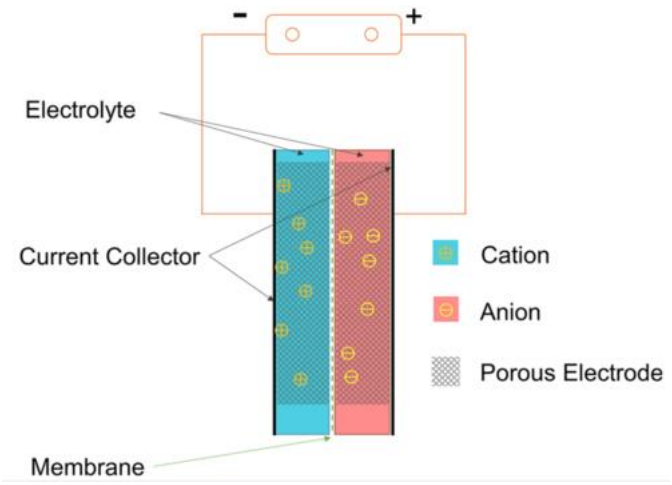

Figure 1.6 *Supercapacitor: Electrical Energy Storage by Double-Layer Effect*

- ***Advantages and disadvantages of supercapacitors:***

Supercapacitors have several notable advantages that justify their increasing use in modern systems. They offer very high charge and discharge currents, very short response times, and an exceptionally long service life of up to 100,000 cycles. They have high power density and their state of charge is easy to manage, making them particularly suitable for applications requiring rapid and repeated responses. However, these devices have certain limitations, such as low energy density, relatively low maximum voltage per cell (2.7 V), and the use of potentially hazardous electrolytes such as acetonitrile, which can pose safety and integration issues [20].

1.5.2.2 Superconducting Magnetic Energy Storage (SMES)

Superconducting Magnetic Energy Storage (SMES) allows electricity to be stored directly as magnetic energy using a superconducting coil with no resistance loss. This system

is characterised by its very high instantaneous power output, although it is less useful for reactive power. Since the 2000s, several pilot projects have been carried out in Japan and France, demonstrating the technical feasibility and effectiveness of SMES in compensating for voltage dips. It combines high power density with good energy density, as illustrated in the comparative figure [21].

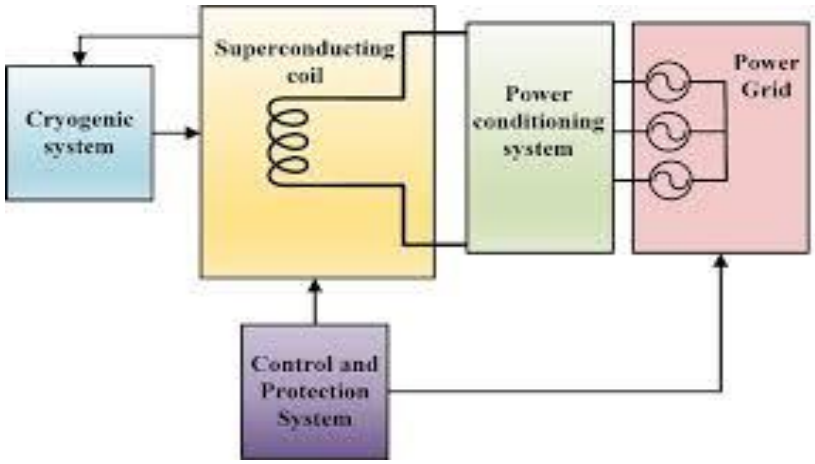

Figure 1.7 *Schematic Diagram of an SMES System*

- ***Advantages and disadvantages of SMES:***

SMES systems offer numerous technological advantages that set them apart from other forms of energy storage. They offer excellent efficiency (over 93%), extremely short response times enabling an almost instantaneous reaction to disturbances, and exceptional cyclability with no loss of performance over cycles. Furthermore, thanks to the absence of the Joule effect, they allow very high current densities, significantly reducing energy losses.

However, their deployment is hampered by several major disadvantages. The high cost of superconducting materials, cryogenic systems and associated electronics is a significant obstacle to their widespread use. Furthermore, their storage capacity remains limited to a few megawatts, and the very high current intensities generated can damage certain components. Finally, the use of powerful magnetic fields raises environmental and electromagnetic compatibility issues [22].

1.5.3. Electrochemical energy

1.5.3.1 Lead-acid batteries

Lead-acid electrochemical batteries account for more than 80% of the lead used worldwide

and are the most iconic object associated with lead. The main principles related to their operation, use and recycling are discussed in this section [23].

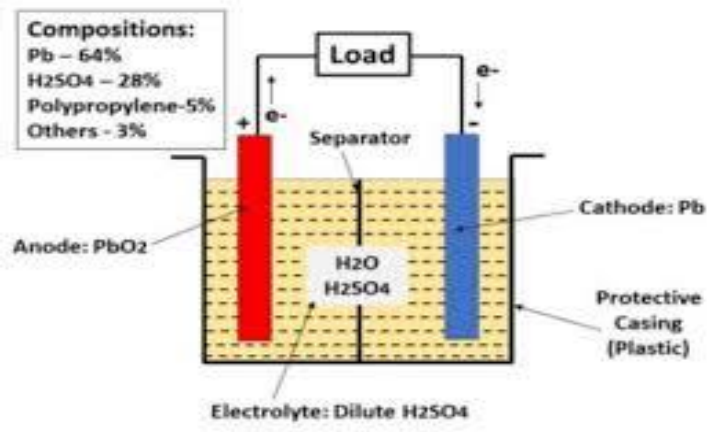

Figure 1.8 *Lead-Acid Battery: Components and Working Mechanism*

Advantages and disadvantages of lead-acid batteries:

Among conventional storage technologies, lead-acid batteries stand out for their simplicity of manufacture and low cost. However, they also have several technical limitations [24]:

Advantages of lead-acid batteries:

• Relatively low cost, making them economical for many applications.

• Wide availability on the market, with proven technology.

Disadvantages of lead-acid batteries:

• Limited life cycle, approximately 400 cycles in hybrid applications.

• Low specific energy, resulting in high weight for high-power applications, which is uneconomical for hybrid vehicles.

• Reduced performance at low temperatures, affecting their efficiency in cold climates.

1.5.3.2 Lithium battery

Lithium-ion batteries, developed in the 1970s and 1980s by Goodenough, Whittingham and Yoshino (2019 Nobel Prize in Chemistry), operate through the reversible exchange of

lithium ions between the cathode and anode. They offer good performance in terms of specific capacity, service life and nominal potential. Their efficiency depends on the active materials used, particularly their storage capacity. They work by moving ions through an electrolyte and a separator, allowing electrons to be transferred via an external circuit. The charge/discharge current is quantified by the C-rate, which influences the speed of the process [25].

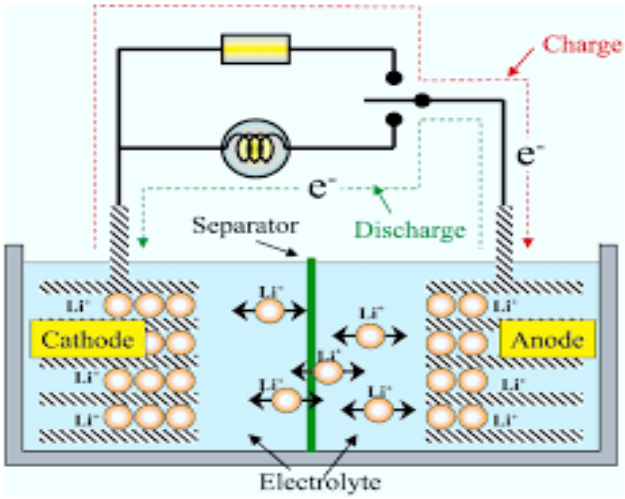

Figure 1.9 *Schematic Representation of a Lithium-Ion Battery Cell*

The characteristic parameters of lithium-ion batteries are divided into internal (related to materials, structure and chemistry) and external (electrically observable) parameters. Among the main external parameters are open-circuit voltage, which is influenced by the type of materials and the charge level, and nominal voltage, which is measured at half charge. The nominal capacity (in Ah) indicates the maximum charge that the battery can provide, while the residual capacity reflects the energy still available. The state of charge (SOC) expresses the remaining energy level, and the state of health (SOH) measures wear and tear compared to a new battery. Internal resistance, which increases with age and use, affects performance. Finally, the remaining useful life (RUL) refers to the number of cycles or time remaining before the battery becomes unusable [26].

- ***Advantages of lithium-ion (Li-ion) batteries:***

Due to their advanced technical characteristics, lithium-ion batteries offer numerous advantages, including [27]:

1. High voltage: Theoretical voltage of approximately 4 V, very close to the actual operating voltage, enabling stable electrical performance.

2. High specific energy: Ability to store a large amount of energy per unit of mass (up to 150 Wh/kg in practice), useful for mobile or embedded systems.
3. High energy density: Between 250 and 700 Wh/L, enabling efficient integration even in confined spaces, such as electric vehicles or compact systems.
4. Good energy and ocular efficiency: Low energy losses during charge/discharge cycles, ensuring optimal use of stored energy.
5. Suitable operating temperature range: Stable operation between -20°C and +60°C, allowing for use in various climatic environments.
6. Extended lifetime: Resistant to ageing and repeated cycles, ensuring considerable longevity.
7. Reasonable charging time: Enable fast charging, especially with good current control, without significantly compromising battery life.
8. Reliable state of charge (SOC) monitoring: Accurately measurable state of charge, facilitating intelligent management and safety of the energy system.
9. Controlled discharge: Stable power supply down to deep discharge levels, without sudden voltage fluctuations.

1.6. ENERGY MANAGEMENT SYSTEMS (EMS) IN SMART GRIDS

1.6.1. Architecture of an EMS:

The architecture of an Energy Management System (EMS) corresponds to the general organisation of its components and devices. It plays a fundamental role in the proper functioning and efficiency of the system. There are three main parts:

supervision, which enables energy analysis and planning control, responsible for regulating flows in real time according to instructions; and data acquisition, provided by sensors and measuring devices. A good understanding of this architecture is essential in order to anticipate potential malfunctions and implement appropriate solutions [28].

1.6.2. Integration of storage units in EMS:

The integration of energy storage into microgrids helps to compensate for the intermittency of renewable sources and better manage energy demand. The EMS coordinates between production units, loads and storage devices to optimise energy flows. The management system determines the optimal periods for charging and discharging batteries based on economic and technical criteria and the availability of renewable resources. This

intelligent management maximises self-consumption, smooths out peaks in demand and contributes to the stability of the local grid [29].

1.7. ENERGY STORAGE CONTROL METHODS

The charge controller is an essential component of a solar energy storage system (Solar-BESS), as it regulates the energy from the photovoltaic panels to power the load and manage the charging and discharging of the battery, thus ensuring stable operation and extending its lifetime. Its role is to prevent both overcharging and deep discharging through an optimised strategy, determined according to the system's objectives and specifications, and generally validated by several simulations. Its operation can be summarised in four main modes: night mode, where no power is generated due to the absence of solar irradiation; charge mode, activated when demand exceeds solar production (P_load > P_PV) and the battery is at risk of deep discharge, leading to the load being powered via the grid; MPPT mode, where an algorithm keeps the panels at maximum power point when the battery can be charged or discharged without risk; and finally, non-MPPT mode, used when solar production exceeds demand and the battery cannot safely absorb the surplus, causing the controller to limit the power of the PV generator, except when the surplus can be fed into the grid [30].

1.8. CRITICAL REVIEW OF EXISTING STUDIES:

The addition of energy storage systems is crucial for the future, both for grid security and for the decarbonisation of the energy sector, as highlighted in several comprehensive reviews, notably Rahman, Md Mustafizur et al. [31], Olabi, Abdul Ghani et al. [32], and Gür, Turgut M. [33].

Zhang, Chao et al. [34] highlight the potential of batteries for large-scale energy storage. They discuss the characteristics of current and future batteries, emphasising the advantages and disadvantages of different technologies. Lithium-ion batteries are distinguished by their high energy density and efficiency, while vanadium flow batteries offer high discharge flexibility and a long service life. Lead-acid and aluminium-ion batteries remain competitive due to their low cost.

Itani, Khaled and De Bernardinis, Alexandre [35] provide an overview of next-generation battery technologies, emphasising material advances and innovation. In particular, they highlight the need to replace cobalt in lithium-ion batteries for environmental and geopolitical reasons, and to improve the stability of organic electrolytes to enhance safety. The authors also

highlight the potential of solid-state batteries (SSBs) due to their high ionic conductivity, although challenges remain, such as interfacial resistance and dendrite formation. Finally, the integration of IoT, cloud, AI and digital technologies is identified as a key factor in the evolution of batteries and smart grids.

Lithium-ion batteries (LIBs) currently dominate electrochemical storage thanks to their high energy density, power, reliability and long service life.

LIBs are particularly attractive for grid-scale energy storage. Chen, Tianmei et al. [36] highlight their energy efficiency, energy density and long service life, as well as their ability to provide key grid services such as frequency regulation and peak smoothing. Hesse, Holger C. et al. [37] confirm their usefulness for residential photovoltaic solutions, while noting that other technologies such as lead-acid batteries may be more suitable depending on the context, particularly for reasons of cost or reliability.

Förstl, Markus et al. [38] evaluated the impact of different energy management strategies on the lifespan of LFP batteries in residential PV-BESS systems. The results show that strategies such as Feed-in Damping (FID) can extend battery life compared to other methods such as maximising self-consumption or mixed linear programming.

In the domestic sphere, Song, Ziye et al. [39] propose an energy management system (HEMS) combined with a PV-BESS to optimise the use of appliances and smooth out consumption peaks, thereby reducing electricity costs and power peaks. Sayfutdinov, Timur and Vorobev, Petr [40] develop a MILP tool to optimise the operation of LFP batteries while taking into account their degradation, offering significant savings on the overall project.

Yoo, Y. and Ha, Y. [41] analyse the BESS market in Southeast Asia and point out that its development is limited by regulatory and economic constraints. Subsidies and international partnerships could improve the market's attractiveness, as also noted by Pandey, A.K. et al. [42] and Moon, H.E. et al. [43].

Globally, several large-scale energy storage projects already exist, including Vistra Moss Landing (350 MW, California) [44], Victorian Big Battery (300 MW, Australia) [45], EnspireME (48 MW, Germany) [46] and Pillswood BESS (98 MW, United Kingdom) [47]. Smaller-scale systems are also being studied, such as buildings equipped with PV-BESS, which show positive economic and environmental potential despite high initial costs (Li, B. et al. [48]; Liu, J. et al. [48]; Ouedraog, K.E. et al. [49]; Zhao, G. et al. [50]).

Finally, several advanced energy management strategies have been studied. Obaid, D. S. et al. [51] optimised a proportional-integral (PI) controller for a three-phase inverter in a PV-battery system. Hafsi, O. et al. [52] compared six energy management techniques, including conventional PI, state machines, fuzzy logic, artificial neural networks (ANN), ECMS and EEMS. Moghimi, M. et al. [53] proposed a rule-based strategy to optimise battery usage in a residential microgrid. Attou, N. et al. [54] explored management integrating PV, wind, BESS and V2G stations for flexible operation. Aboubaida, H. et al. [55] developed an optimal distribution approach based on DC bus voltage control, while Muriithi, G. and Chowdhury, S. [56] developed a reinforcement learning (Q-learning) based strategy to dynamically optimise battery charging and discharging while reducing costs and extending battery life.

1.8.1. Limitations of existing control approaches

For this study, I chose to use a lithium-ion battery, based on the positive results and experimental feedback reported in previous work. This technology, which dominates electrochemical storage, is distinguished by its high energy density, reliability and long service life, making it an ideal choice for applications requiring effective energy control and management. However, to fully exploit the potential of lithium-ion batteries, it is crucial to implement effective energy management strategies. Despite progress in this area, certain limitations remain: conventional methods, such as proportional-integral (PI) control, lack robustness in the face of rapid or non-linear load variations; rule-based approaches are not very adaptive and do not take into account future uncertainties, such as the variability of photovoltaic production or the behaviour of electric vehicles; finally, intelligent methods, such as neural networks or fuzzy logic, require large amounts of data and high computing power, while sometimes suffering from a lack of transparency in decision-making.Furthermore, fractional controllers associated with optimisation algorithms, such as GWO, remain largely unexplored despite their high potential in terms of accuracy and stability. In this context, lithium-ion batteries represent an optimal solution for combining energy performance and reliability in energy management and control systems.

1.8.2. Proposed contribution

To overcome the limitations identified in conventional approaches, we propose an innovative strategy based on a fractional PI controller (FOPI), whose parameters are automatically optimised using the Grey Wolf Optimizer (GWO) algorithm. The FOPI has the advantage of allowing finer tuning of the system dynamics thanks to its adjustable fractional

orders, thus offering a more stable and accurate response than conventional PI controllers. For its part, the GWO is an effective bio-inspired optimisation method capable of identifying the optimal controller parameters even in non-linear and disturbed environments, thus ensuring greater robustness and adaptability of the energy management system.

This method significantly reduces static error, overshoot, and stabilisation time, while maintaining low computational complexity, making it suitable for embedded applications such as residential microgrids.

1.9. CONCLUSION

This first chapter presented an in-depth analysis of the evolution of electrical networks, energy storage technologies, and control and optimisation approaches adopted in smart electrical systems. The study identified the growing needs associated with the massive integration of renewable energies, as well as the major challenges posed by their intermittency, grid flexibility, and the durability of storage equipment.

Particular attention was paid to the various storage technologies, whether mechanical, electrical, electromagnetic or electrochemical. Among these, lithium-ion batteries stand out as a preferred solution due to their high energy density, good efficiency and strong potential for integration into modern microgrids. Understanding its internal and external parameters is essential for designing control strategies capable of preserving its service life while ensuring optimal operation.

The chapter also presented the operating principles of energy management systems (EMS) and the control and optimisation methods currently in use. Although conventional approaches (such as PI control or deterministic rules) are simple to implement, they quickly reveal their limitations when faced with the non-linear and variable dynamics of renewable sources. Advanced techniques, such as artificial intelligence or heuristic methods, offer improved performance but can suffer from a lack of transparency, high computational requirements or poor adaptability.

This critical review highlights a significant gap in the literature: the lack of approaches that exploit the advantages of fractional controllers combined with recent optimisation algorithms. It is in this context that the contribution proposed in this thesis is based on a FOPI controller optimised by the Grey Wolf Optimizer (GWO) algorithm, which improves the accuracy, stability and robustness of the system. Subsequent developments will therefore build

on the theoretical elements established in this chapter to propose a high-performance solution adapted to the real constraints of smart microgrids.

Chapter 2: Modelling, Performance Evaluation and Microgrid Integration of Lithium-Ion Batteries

2.1 INTRODUCTION

With the rise of mobile applications, electric mobility, and stationary storage, lithium-ion (Li-ion) batteries now occupy a prominent place among electrochemical storage technologies. Their success can be explained by their high energy density, low self-discharge, good cycling performance, and energy efficiency superior to that of many other technologies.

This chapter begins with an overview of Li-ion batteries. It covers the principles of operation, essential terminology such as state of charge (SOC) and state of health (SOH), and the physical and electrochemical phenomena that govern their performance. Particular attention is paid to intrinsic limitations, including sensitivity to overvoltage, deep discharge, thermal ageing, and safety risks.

Li-ion battery modelling is also presented, as it is an essential tool for predicting the dynamic and thermal behaviour of the system. This modelling enables the development of intelligent management algorithms, the optimisation of storage system sizing, and the design of appropriate control strategies.

In order to justify the choice of Li-ion technology for this study, a technical and economic comparison is made (Table 2.1) [57] between several existing battery technologies: lead-acid, nickel-cadmium, nickel-metal hydride, sodium-sulphur, and lithium-ion. This comparison highlights the superiority of Li-ion batteries in terms of energy density, efficiency, and service life, despite certain constraints such as higher unit cost and limited availability of raw materials.

In addition, this chapter includes a section dedicated to the integration of Li-ion batteries within a hybrid microgrid. This section presents the system studied, comprising a photovoltaic farm, a bidirectional Boost/Buck converter, a three-phase inverter, and a connection to the electricity grid. It details the modelling of each of the components (PV modules, converters, inverter and Li-ion battery) and explains how the battery interacts with the system to store and release energy according to the state of charge and load requirements. The inclusion of this practical case study provides a concrete context for understanding the behaviour of Li-ion

batteries in real-world applications and illustrates the importance of modelling them for energy management in hybrid systems.

This chapter, therefore aims to provide the necessary understanding to grasp the challenges associated with the use of Li-ion batteries in demanding applications, while setting out the foundations that will guide the rest of this research.

2.2 WHY LITHIUM-ION?

Lithium-ion technology currently offers one of the best compromises between high energy density, power/energy flexibility, and energy efficiency, as shown by the Ragone diagram and comparisons with other batteries. Although it is more recent than lead-acid technologies, it is becoming increasingly popular due to its high efficiency (95–99%), good cycling performance, low self-discharge, and negligible memory effect.

Despite historically high costs, estimated at between €459 and €560/kWh according to various sources, trends show a steady decline thanks to industrial progress and economies of scale. For example, for stationary storage of 500 kWh with a lifespan of 3,000 cycles, the current cost of use is estimated at around £0.12/kWh stored, and could fall further in the medium term.

At the same time, the future of lithium-ion storage is supported by active research into new electrode and electrolyte materials to increase energy density, particularly through lithium-sulphur (Li-S) and lithium-air (Li-O_2) technologies. The integration of silicon anodes, improved ionic conductivity, and thermal stability are also key developments aimed at overcoming current physical and chemical limitations.

These prospects confirm the strong potential for evolution of lithium-ion batteries, justifying their central role in energy storage solutions for stationary applications and electric mobility [58].

Table 2.1 compares different battery technologies according to several technical and economic criteria, highlighting the advantages and limitations of each, and justifying the choice of lithium-ion batteries for this study due to their high energy density, long service life, high efficiency, and low self-discharge.

Table 2.1 *Technical and Economic Characteristics of Various Battery Types*

Criterion	**Pb-acid**	**Ni-Cd**	**Ni-MH**	**NaS**	**Li-ion**
Cost (€ / kWh)	25 – 200	80 – 1000	275 – 1500	300 – 500	459 – 560
Power density (W/kg)	1 – 300	10 – 1000	10 – 1500	150 – 230	4 – 4500
Energy density (Wh/kg)	30 – 50	40 – 60	50 – 80	150 – 240	75 – 250
Number of cycles	300 – 1500	500 – 2000	500 – 2000	2500 – 4500	1000 – 10000
Operating temperature (°C)	20 – 40	40 – 50	40 – 50	250 – 350	20 – 60
Energy efficiency (%)	70 – 92	60 – 80	50 – 80	75 – 85	95 – 99
Self-discharge (%/day)	0.1 – 0.3	0.2 – 0.6	1	20	0.1 – 0.3
Memory effect	No	Yes	Yes	No	Low

2.3 LI-ION BATTERY MODELLING :

2.3.1 Terminology and design parameters :

2.3.1.1 Battery cells and packs

A Li-ion cell is a reversible electrochemical device that stores and releases energy through the movement of lithium ions between a negative electrode (graphite) and a positive electrode (metal oxides) through an electrolyte. Depending on requirements, these cells are assembled into modules and then into packs, incorporating sensors, cooling, and a management system (BMS) to ensure safety and performance in applications such as electric vehicles [59]. The cells are connected in series and parallel to form a battery pack that meets voltage and capacity requirements [59]. Each cell has its own State-of-Charge (SOC), which can lead to an internal imbalance.

2.3.1.2 Internal resistance

Internal resistance consists of an ohmic component and a polarisation component [60][61]. It limits the available power and increases with the age of the battery. For a complete pack, the resistance can be 50–100% higher than the nominal value [62].

2.3.1.3 Terminal voltage and open-circuit voltage

The terminal voltage is measured under load and drops at low SOC [63]. The open circuit voltage (OCV) is measured without load and increases with SOC [64]. The cut-off voltage defines the discharge limit [65].

2.3.1.4 Nominal capacity and C_{rate}

Capacity Q, expressed in ampere-hours (Ah), corresponds to the amount of electrical charge that a battery can store during charging and release during discharging [66]

The nominal capacity Q_{nom} Is calculated by:

$$Q_{nom}[AH] = I_{discharge} * t_{discharge} \qquad (2.1)$$

It decreases at higher C_{rate}. The C_{rate} is defined by:

$$C_{rate} = \frac{I_{discharge}}{Q_{nom}} \ [H^{-1}] \qquad (2.2)$$

2.3.1.5 State of Charge (SOC)

The state of charge (SOC) represents the amount of energy still available in the battery [67] at a given moment, expressed in relation to its nominal capacity [68] (2.3):

$$SOC = \frac{Q_{actual}}{Q_{nom}} * 100 \qquad (2.3)$$

It can be estimated by counting coulombs:

$$SOC = SOC_{intial} - (\frac{1}{Q_{nom}}) \int Idt \qquad (2 .4)$$

With a correction factor [69] :

$$SOC = SOC_{intial} - \eta(\frac{1}{Q_{nom}}) \int Idt \qquad (2.5)$$

SOC testing methods

The discharge test is reliable in the laboratory for checking SOC but remains limited for on-board use [70].

2.3.1.6 State-of-Health (SOH)

State of health (SOH) is an indicator that assesses performance loss due to battery degradation. It is defined as the ratio between the battery's current capacity and its maximum capacity when new [71].

The SOH expresses the current state of the battery [72][73]:

$$SOH = \frac{Q_{actual}}{Q_{nom}} * 100 \qquad (2.6)$$

It is influenced by internal impedance, active material loss, and temperature [74].

2.3.1.7 OCP (Open-Circuit Potential) and OCV (Open-Circuit Voltage)

They refer respectively to the electrochemical potential of an electrode at equilibrium (OCP) and the voltage of the battery when it is at electrochemical and thermal equilibrium (OCV), the latter being defined as the difference between the open-circuit potentials (OCP) of the cathode and anode [75].

2.3.2 Equivalent electrical models (Rint, Thevenin)

2.3.2.1 Rint model

The Rint model, illustrated in Figure 2.1, includes an ideal voltage source U_{OC}, which defines the open-circuit voltage of the battery. The parameters R_0 (series resistance) and U_{OC} (open-circuit voltage) are constant.I_L represents the charging current, which takes a positive value during discharge and a negative value during charging.U_L corresponds to the voltage across the battery terminals. However, this model has a limitation in its ability to respond to high current demands during charging and discharging (dynamics). To overcome this limitation, it is necessary to add parallel RC branches that will simulate these dynamics [76].

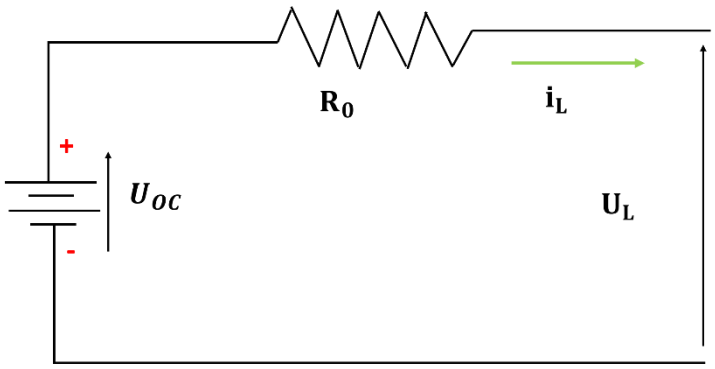

Figure 2.1 *Electrical Circuit Representative of the Rint Model*

2.3.2.2 RC model

The RC model, originally introduced by SAFT Battery Company, is an equivalent electrical model commonly used to describe the dynamic behavior of a battery. Its schematic diagram is shown in Figure 2.6. The model consists of a large capacitor Cb, which represents the stored capacity, and a small capacitor Cc, which accounts for polarization effects [77].

The following system of equations describes the electrical behavior of the RC circuit:

$$\begin{bmatrix} \frac{dV_b}{dt} \\ \frac{dV_c}{dt} \end{bmatrix} = \begin{bmatrix} \frac{-1}{C_b+(R_e+R_c)} & \frac{1}{C_b+(R_e+R_c)} \\ \frac{1}{C_c+(R_e+R_c)} & \frac{-1}{C_c+(R_e+R_c)} \end{bmatrix} \begin{bmatrix} V_b \\ V_c \end{bmatrix} + \begin{bmatrix} \frac{R_c}{C_b+(R_e+R_c)} \\ \frac{R_c}{C_c+(R_e+R_c)} \end{bmatrix} I_L \qquad (2.7)$$

The terminal voltage is given by:

$$V_L = \begin{bmatrix} \frac{R_c}{R_e+R_c} & \frac{R_e}{R_c+R_e} \end{bmatrix} \begin{bmatrix} V_b \\ V_c \end{bmatrix} + \begin{bmatrix} -\frac{R_c R_e}{R_e+R_c} \end{bmatrix} I_L \qquad (2.8)$$

Where R_t, R_c, and R_e The terminal resistance, RC branch resistance, and end resistance are denoted as R, R1, and R2, respectively, and I_L represents the load current.

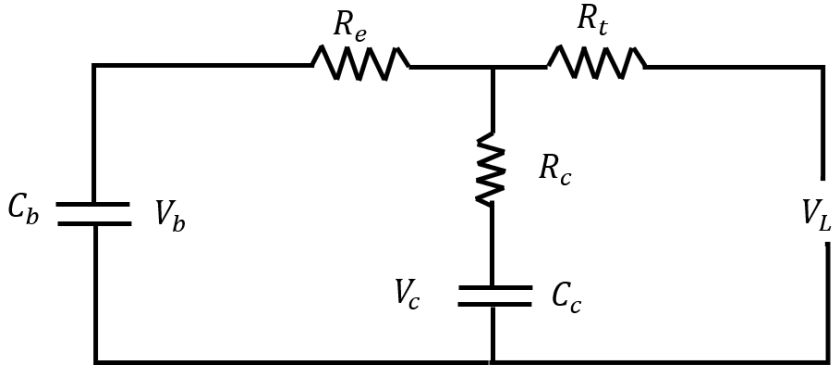

Figure 2.2 *Equivalent circuit of RC battery model*

2.3.2.3 Thevenin model

Thévenin's electrical model represents the elementary cell as an ideal voltage source, corresponding to the open-circuit voltage depending on SOC and temperature, associated with a series resistor and an R/C circuit (resistor and capacitor in parallel) connected in series. This simplified model makes it possible to reproduce the dynamic evolution of the internal impedance while remaining easy to configure for industrial applications. In our study, this model is the adapted version chosen to represent the electrical behaviour of the cell, as it offers an optimal compromise between accuracy, ease of implementation, and low computational

cost. This choice is justified by its ability to capture the essential dynamic phenomena (including the transient response related to internal impedance) while maintaining a structure that is sufficiently lightweight for real-time integration into a control or diagnostic platform. The figure illustrates this equivalent circuit, where temperature is considered a constant input parameter (T_0)) during operation [78].

The cell voltage is given by:

$$V_{cell}(t) = V_0(SOC, T_0) - I(t) \times R_{dyn}(SOC, T_0, C_{rate}) - V_{RC}(t) \qquad (2.9)$$

where:

- V_0 (SOC, T_0): open-circuit voltage (dependent on state of charge and temperature)
- R_{dyn}: dynamic series resistance
- V_{RC}(t): voltage drop across the network terminals R_1 // C

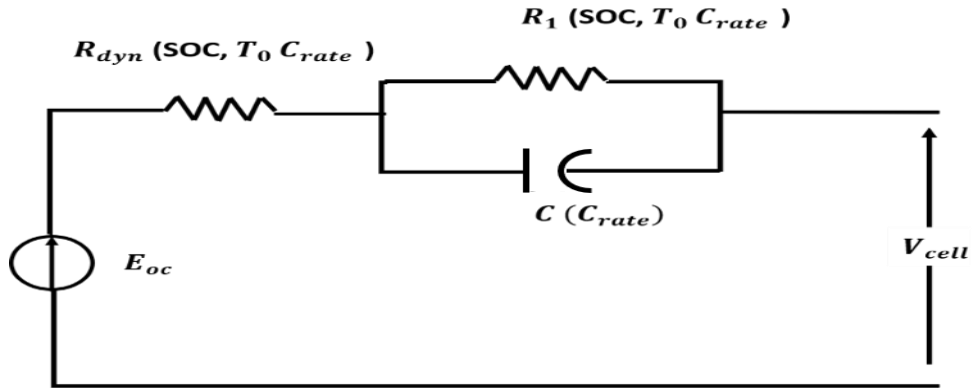

Figure 2.3 *Equivalent circuit of the Thevenin battery model*

The RC circuit terminal voltage follows the law:

$$dV_{RC}(t)/dt = -\frac{1}{(R_1(SOC,T_0,C_{rate})} \times C(C_{rate}))] \times V_{RC}(t) + \frac{I(t)}{C(C_{rate})} \qquad (2.11)$$

The current supplied by the source is distributed:

$$I(t) = I_{RS}(t) + I_{RC}(t) \qquad (2.12)$$

In practical terms, we replace:

$$I_{RC}(t) = C \times \frac{dV_{RC}(t)}{dt} + \frac{V_{RC}(t)}{R_1} \qquad (2.13)$$

The state of charge is updated according to the current supplied/requested:

$$SOC(t) = SOC(0) - [\frac{1}{Q_{nom}}] \times \int_0^t I(\tau)\, d\tau \qquad (2.14)$$

with:

• Q_{nom} : nominal capacity of the cell (Ah)

Summary

Dependent variables:

• R_{dyn} and R_1 vary with SOC, T_0 and C_{rate}(charge/discharge rate).

• C may depend on C_{rate} (relaxation frequency).

Fixed parameters:

• T_0 is assumed to be constant here.

Compact form System in condensed form:

$$V_{cell} = V_0 - I \times R_{dyn} - V_{RC} \quad (2.15)$$

$$\frac{dV_{RC}}{dt} = -[\frac{1}{R_1 C}] \times V_{RC} + \frac{I}{C} \quad (2.16)$$

$$SOC(t) = SOC(0) - [\frac{1}{Q_{nom}}] \quad (2.17)$$

2.4 BATTERY PERFORMANCE ASSESSMENT

Assessing battery performance by accurately determining SOC and SOH is essential to ensuring optimal management of any system that uses batteries. SOC provides information on the available charge level, while SOH indicates the overall condition of the battery and its ability to maintain performance over time. The BMS relies on these two parameters to ensure safety, extend battery life and provide a reliable estimate of remaining energy [79]. In many applications, Li-ion batteries consist of complex assemblies of cells in series and/or parallel, requiring continuous monitoring of thermal balance as well as changes in SOC and SOH. However, accurately estimating these indicators remains a challenge due to their dependence on several factors such as temperature, current and ageing. Approaches to address these difficulties will be presented in the following sections.

2.5 LI-ION BATTERY AGEING

Li-ion batteries undergo a gradual loss of performance over time, mainly due to changes in the physical and chemical properties of their internal components. These mechanisms are collectively referred to as ageing.

There are generally two main forms of ageing, which are closely related to the storage and usage conditions of the battery.

2.5.1 Calendar ageing

Even when not in use, a battery can degrade due to internal reactions, such as corrosion or other slow electrochemical phenomena. This process, known as calendar ageing, defines the length of time a battery can remain in storage without excessive loss of performance. This degradation typically results in an increase in internal resistance and a reduction in available capacity. As shown in the figure, these variations are strongly influenced by the storage temperature and the state of charge (SOC) during this period [80].

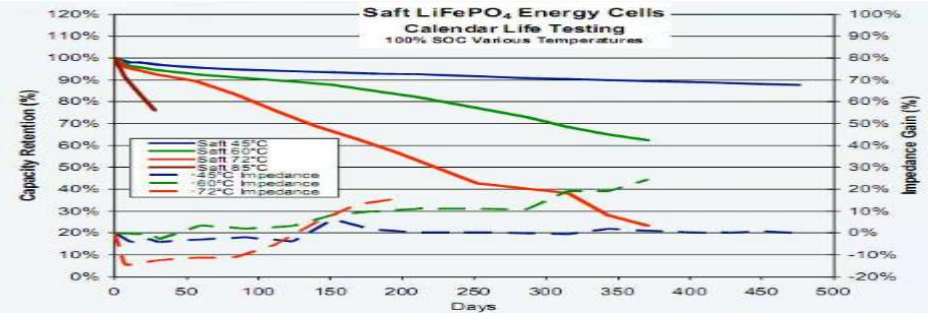

Figure 2.4 *Temperature-dependent variation in the internal resistance and capacity of a Li-ion battery, case of calendar ageing,[80]*

2.5.2 Cycle life

The cycle life of a Li-ion battery is strongly influenced by the applied charge and discharge profile, the SOC range used, and the operating temperature. It is generally expressed as the number of cycles performed or the total amount of charge exchanged over time. In the automotive sector, numerous studies have helped to better characterise this phenomenon and develop models for predicting changes in capacity and internal resistance based on intensive cycling scenarios.

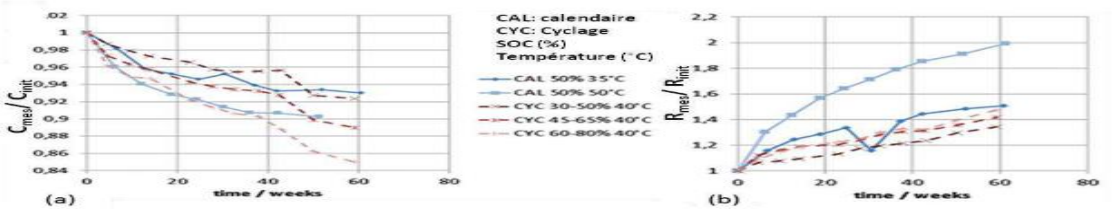

Figure 2.5 *Comparison of variations in capacity (a) and resistance (b) between calendar ageing and cycling ageing as a function of SOC and temperature,[80]*

2.5.3 Influence of combined stresses on ageing

The lifespan and performance of lithium-ion batteries depend heavily on the interaction and accumulation of mechanical, electrochemical, thermal, and electrical stresses. Calendar ageing is mainly caused by electrochemical and thermal stresses during storage, while cycling ageing results mainly from mechanical and electrochemical stresses generated by repeated intercalation/deintercalation cycles. Controlling these stresses is essential to optimise cell life according to the intended application [81].

2.6 METHODS FOR ESTIMATING SOC AND SOH

Estimating SOC and SOH in batteries is based on two main categories: direct methods and indirect methods.Among the direct methods, Coulomb counting (CC) is simple and widely used, but it suffers from an accumulation of errors. Several studies have proposed improvements, such as the integration of filters (Kalman, particle) or neural networks, although these solutions are often more complex or sensitive to temperature variations. The OCV method, based on measuring open-circuit voltage, is accurate but requires a significant rest time, which limits its use in continuous operation. Electrochemical impedance spectroscopy (EIS) provides a very accurate assessment of SOC, but requires specialised equipment and long measurement times, which complicates its integration into embedded systems.Indirect methods, which are suitable for continuously operating systems, are based on advanced models and algorithms. The extended Kalman filter (EKF) is one of the most widely used methods due to its ability to handle the non-linearities of lithium-ion batteries, although it requires significant computing power. Machine learning methods (SVM, BNN, LSTM) provide robust estimates, particularly in the presence of noise, but require large volumes of data and high computational capabilities. Hybrid approaches combining several techniques are also used to improve accuracy.There are several categories of SOH estimation methods: direct methods (based on remaining capacity), differential analyses, model-based methods (electrochemical or electrical equivalents) and data-driven techniques. Rapid SOH estimation methods, using for example internal resistance or material properties, provide results in a short time but often require specialised equipment. No single method is universal: the choice depends on the constraints of the application, the level of accuracy required and the resources available [82].

2.7 INTEGRATION OF BATTERIES INTO A MICROGRID

In this section, we present the integration of a bidirectional Boost/Buck converter within a hybrid microgrid, illustrated in Figure 2.6. The system comprises a photovoltaic (PV) array,

a bidirectional converter, an inverter, an alternating current (AC) load, and a connection to the electricity grid. The PV output is used to power the load and recharge the converter, while an intelligent energy management system (EMS) dynamically coordinates the flows to minimise unnecessary cycling, extend the system's lifespan, and ensure continuous power to critical loads. When the state of charge (SOC) of the converter falls below the 80% threshold, excess energy is distributed between powering the loads and recharging the converter, and is only fed into the grid when the SOC reaches 80%. In the event of a photovoltaic deficit, the converter remains inactive if its SOC is below 20%, with the load being supplied by the grid, and recharging only resumes when PV production exceeds load demand.

This section will describe the modelling of the main components of the microgrid, including the PV farm, the boost/buck converter, the inverter, the load, and their interaction with the grid.

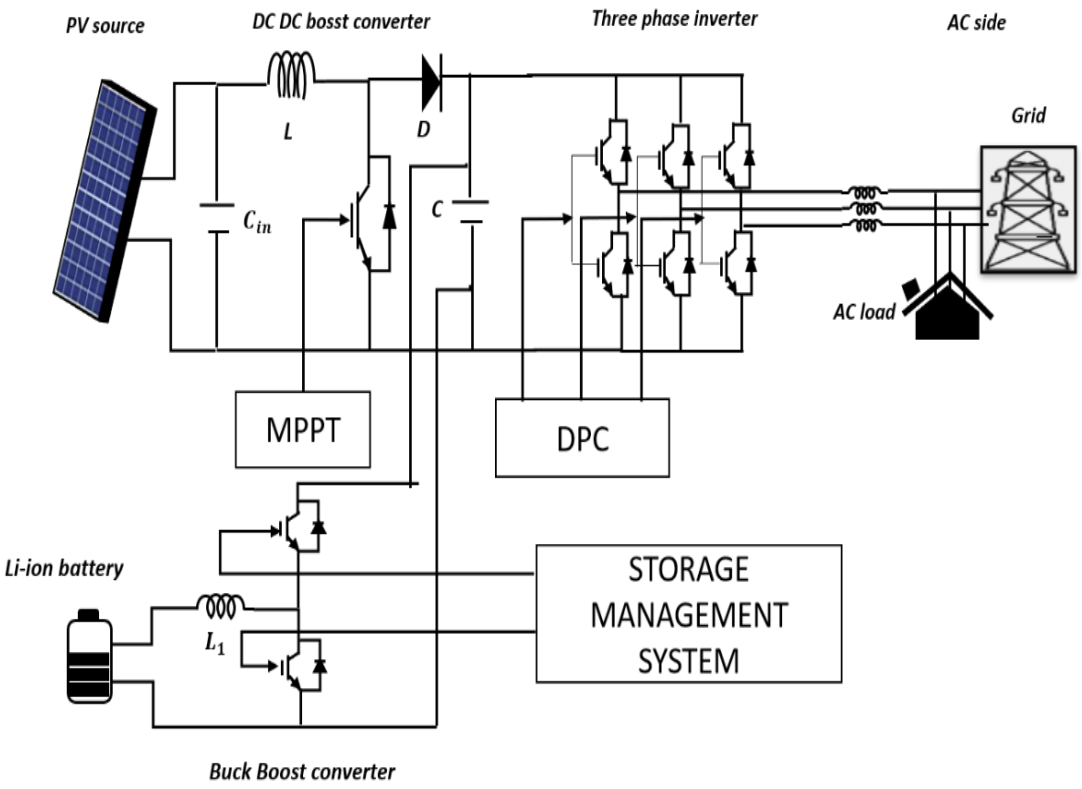

Figure 2.6 *Schematic of the hybrid energy system*

To provide a clear overview of the system components, the key parameters of the Boost and Buck-Boost converters used in the system are summarized in Table 2.2.

Table 2.2 *Technical Parameters of the Boost and Buck-Boost Converters*

Parameter	Value
L	0,0002 H
C_{in}	0,001 F
C	0,0011 F
L_1	0,005 H

2.7.1 PV cell modeling

The single-diode model (Figure 2.7) is widely used to represent the electrical characteristics of a photovoltaic (PV) cell, as it provides a simple yet sufficiently accurate description of the physical phenomena governing its operation. In this model, the photogenerated current (I_{ph}) is the main source of current and depends mainly on solar irradiance, while being only slightly influenced by temperature. The internal losses of the cell are taken into account through the series resistance (R_s), which includes ohmic losses due to contacts, conductive materials, and interconnections, as well as the shunt resistance (R_{sh}), which represents leakage currents (I_p) related to junction imperfections or manufacturing defects. The diode integrated into the model reproduces the behaviour of the PN junction, and the current flowing through it (I_D) reflects the diffusion and recombination phenomena of charge carriers, which strongly influence the voltage and overall efficiency of the cell. This model is therefore an essential tool for analysing, simulating and optimising the performance of photovoltaic systems [83].

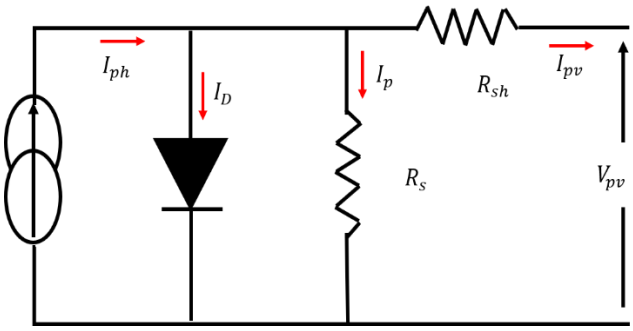

Figure 2.7 *Electrical equivalent circuit of a photovoltaic cell*

The following equation is used to determine the output current generated by the photovoltaic cell and forms the analytical basis of the single-diode model. The expression

presented in equation (1) reflects the balance between the photo-generated current, the current flowing through the diode and losses due to internal resistances, thus providing a complete representation of the electrical behaviour of the PV cell. This mathematical relationship is essential for predicting the cell's response to variations in irradiance, temperature or load, and serves as a starting point for modelling and simulating the performance of the photovoltaic system.

$$I_{pv} = I_{ph} - I_D - I_p \tag{2.18}$$

Substituting the diode equation, the expression becomes:

$$I_{pv} = I_{ph} - I_0\left(e^{\frac{V_{pv}+I_{pv}R_S}{nkT}} - 1\right) - \frac{V_{pv}+I_{pv}R_S}{R_{sh}} \tag{2.19}$$

n: diode ideality factor

k: Boltzmann constant

T: cell temperature (K)

q: electron charge

I_0: diode reverse saturation current

I_{ph}: photocurrent (light-generated current)

I_D: diode current

I_{sh}: shunt leakage current

R_s: series resistance

R_{sh}: shunt resistance

V_{pv}: photovoltaic cell output voltage

I_{pv}: photovoltaic cell output current

When ignoring the effects of series and shunt resistances, the equation simplifies to:

$$I_{pv} = I_{ph} - I_0 e^{AV_{pv}} \tag{2.20}$$

Where A = q / (n k T)

The system studied was developed and simulated using MATLAB/Simulink, which allows the dynamic behaviour of the photovoltaic device to be accurately represented. The PV

module selected for this study is the ENN Solar Energy EST-120, whose electrical parameters are listed in Table 2.3, serving as the basis for its modelling.

Table 2.3 *PV parameters*

Parameter	Value
Number of parallel strings (N_p)	30
Number of modules in series (N_s)	7
Maximum power (P_{max})	121 W

The non-linear characteristics of the photovoltaic output curves highlight the essential role of MPPT algorithms in ensuring optimal power extraction, as illustrated in Figure 2.7.

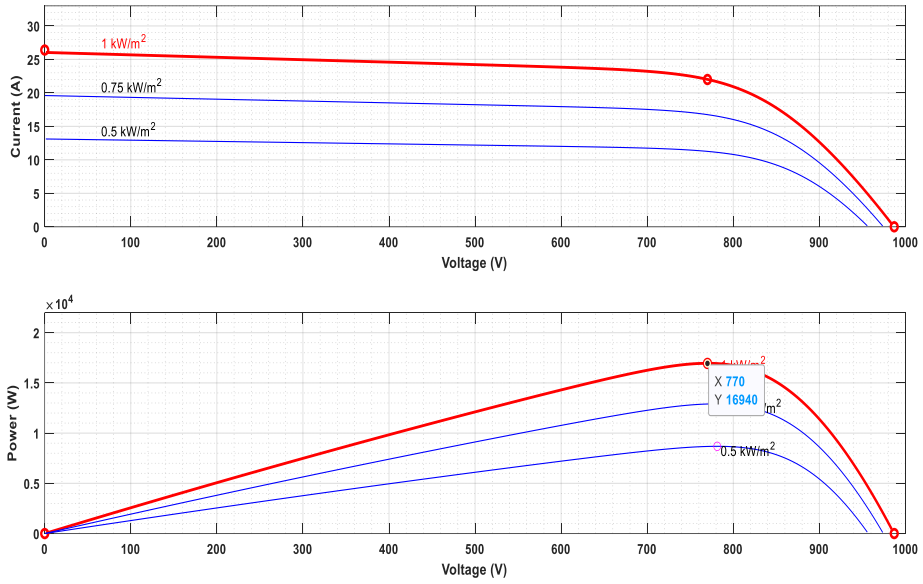

Figure 2.8 *The characteristics of the PV panel*

2.7.2 DC-DC boost converter

The boost converter (see figure 2.8) is a static DC-DC converter that raises the voltage of a DC source to a higher level. It is widely used in solar panels, wind turbines, switching power supplies, and electric vehicles. The behaviour of the converter can be analysed by applying the mesh law to the loop containing the inductance and the node law to the capacitor branch. Its operation depends directly on the switching states of the switch, alternating between

open and closed, which allows control of the voltage elevation and regulation of the energy transmitted to the load [84].

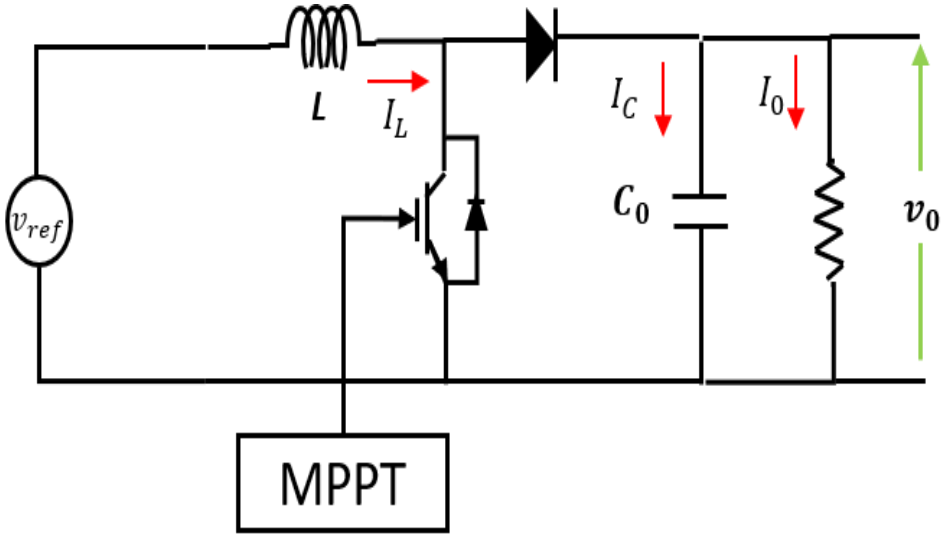

Figure 2.9 *DC-DC Boost Converter*

The sizing of converter components is essential to ensure the proper functioning of the grid-connected PV system. The inductance L of the boost chopper is defined according to the duty cycle (α), the switching frequency (f_s) and the current ripple (ΔI_L). The capacitor (C_{pv}) placed at the output of the PV panel is calculated based on the voltage ripple (Δv_{pv}), while the DC bus capacitor (C_{DC}) depends on the power produced by the photovoltaic panel, the average DC bus voltage (v_{DC}), the voltage ripple (Δv_{DC}) and the grid frequency (ω). These relationships allow the system parameters to be precisely adjusted to ensure optimal power flow stability [85].

$$L = \frac{v_{pv}\,\alpha}{f_s \Delta I_L} \qquad (2.21)$$

$$C_{pv} = \frac{\alpha^2 v_{pv}}{8 f_s \Delta v_{pv} L} \qquad (2.22)$$

$$C_{DC} = \frac{P_{pv}}{\omega v_{DC} \Delta v_{DC}} \qquad (2.23)$$

2.7.3 Li-ion battery modeling

The Li-ion battery model chosen for this work is Thévenin's electrical model, as mentioned earlier in this chapter. We use a set of 10 batteries connected in series to increase

the voltage while maintaining the same current. The battery parameters are summarised in the expanded table 2.1.

Table 2.4 *Battery Parameters*

Parameter	Value
Nominal voltage	50 V
Rated capacity	6 Ah
Internal resistance	0.008 Ω

2.7.4 Bidirectional DC-DC Converter (Buck-Boost)

The bidirectional Buck-Boost converter illustrated in Figure 2.9 is an evolution of the unidirectional converter, achieved by replacing its power switches with bidirectional switches. This modification allows power to flow in both directions while retaining the ability to convert voltage in both boost and buck modes. It can thus increase or decrease the voltage in direct mode and regulate the power flow in the opposite direction with the same flexibility. In certain configurations, it can also provide a negative output voltage. Thanks to this versatility and its bidirectional power transfer capability, this topology is widely used in the modern design of bidirectional DC-DC converters [86].

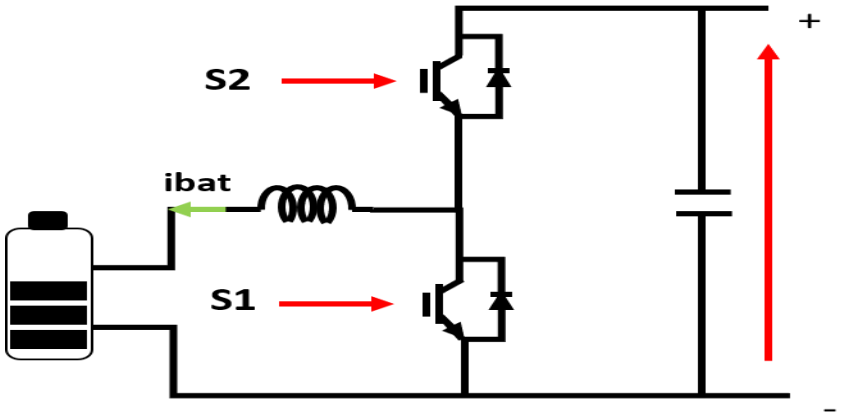

Figure 2.10 *The bidirectional Buck-Boost Converter*

2.7.5 Three-phase 2-level inverter

We opted for a two-level three-phase inverter (Figure 2.11) to provide the interface between the DC side and the electricity grid.The three-phase voltage inverter consists of three single-phase half-bridge inverters sharing the same DC bus and supplying a star-connected inductive load. The output voltages form a balanced three-phase system, and pulse width modulation (PWM) is used to obtain a three-level voltage between two phases and a five-level phase-to-neutral voltage, thereby reducing the harmonic distortion ratio and voltage gradient. The fundamental voltage depends on the amplitude modulation index (ma): for ma ≤ 1, the relationship is linear, while for ma > 1, overmodulation causes low-order harmonics. The maximum phase-to-neutral fundamental voltage is Vdc/2 for ma = 1 and can reach 2/π Vdc at full wave, at the cost of an increase in harmonic content. The inverter can thus be modelled as an amplifier of the reference signal, neglecting imperfections and PWM switching [87].

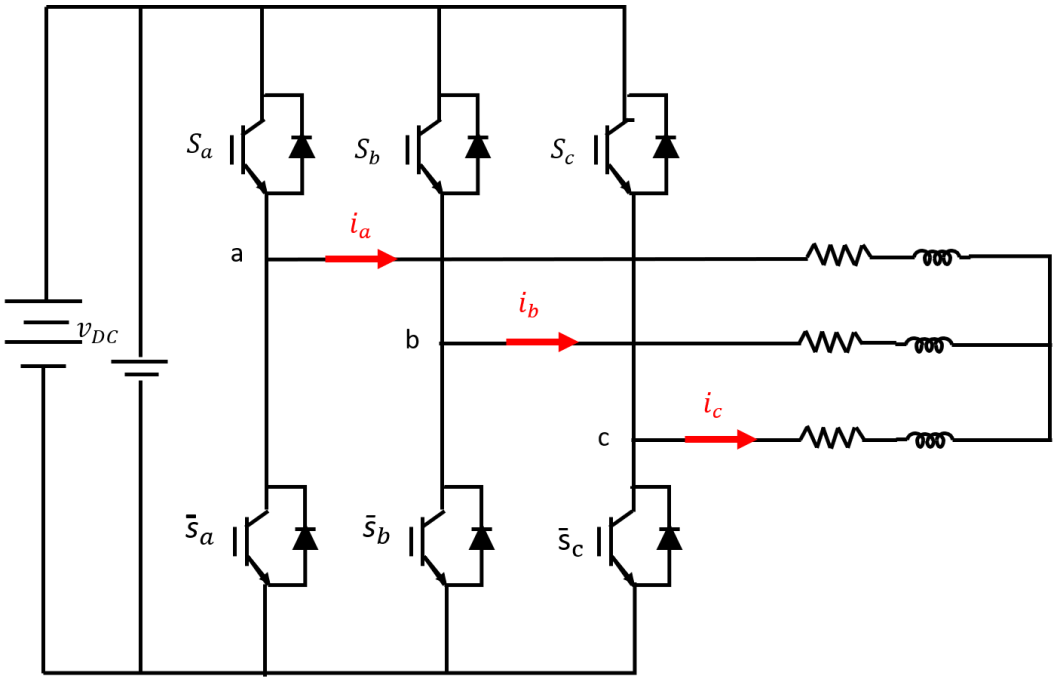

Figure 2.11 *Topology of a three-phase voltage inverter*

2.8 CONCLUSION

This chapter presented a comprehensive analysis of lithium-ion batteries, from their operating principles to their modelling, including their performance and limitations. Comparison with other storage technologies confirmed the suitability of Li-ion for applications requiring high energy density and efficiency.

Detailed modelling of batteries, converters and photovoltaic infrastructure has made it possible to accurately represent the dynamic behaviour of the system under study. The integration of batteries into a hybrid microgrid has highlighted their strategic role in energy management, flow optimisation and power continuity, while limiting component ageing.

This approach, combining theory, modelling and practical application, provides a solid framework for future work on the design, energy optimisation and development of smart, high-performance storage systems that meet the growing challenges of renewable energy.

Chapter 3: Energy Management Strategy Based on FOPI Controller Optimized by Grey Wolf Optimizer

3.1 INTRODUCTION

The evolution of smart energy systems has led to growing interest in high-performance control strategies capable of ensuring stability, efficiency and robustness in microgrids incorporating renewable sources. In this context, choosing the right controller is crucial to ensuring optimal voltage, power and storage management. This chapter presents a detailed study of different control approaches, ranging from conventional controllers such as PI and PID, which are widely used in industry, to advanced methods based on artificial intelligence and metaheuristic techniques. The aim is to highlight their principles, optimisation capabilities and areas of application in PV-battery-grid systems. The chapter also introduces the proposed energy management system, based on a FOPI controller optimised by the Grey Wolf Optimizer (GWO) algorithm, designed to ensure dynamic, robust and efficient control of the bidirectional converter.

3.2 CONVENTIONAL AND INTELLIGENT CONTROLLER

3.2.1 Conventional Controller

3.2.1.1 PID Control

The PID (Proportional, Integral, Derivative) controller remains the most widely used control algorithm. The majority of feedback loops are controlled by this algorithm or its variants. It can be deployed in various forms, whether as a stand-alone controller, integrated into a DDC (Direct Digital Control) system, or within a hierarchical and distributed process control architecture. Every day, thousands of instrumentation and control engineers around the world use this type of controller.

PID control is one of the most widely used algorithms in industry and automatic control systems. It regulates and stabilises the behaviour of a system based on the difference between the desired output and the actual output [88].

The term proportional produces a control action proportional to the instantaneous error. The greater the error, the greater the correction applied. This control improves response speed and reduces steady-state error, but can cause oscillations around the target value [88].

$$P = k_p \cdot e(t) \tag{3.1}$$

The integral term generates a control action proportional to the integral of the error over time, allowing accumulated errors to be corrected and steady-state error to be eliminated. It improves long-term accuracy but can introduce oscillations or undesirable effects [89].

$$I = k_i \cdot \int_0^t e(\tau) d\tau \tag{3.2}$$

The derivative term produces a control action proportional to the variation of the error over time, anticipating future changes in the system. It improves stability and transient response, but can amplify signal noise [90].

$$D = k_d \cdot \frac{de(t)}{dt} \tag{3.3}$$

The PID equation combines these three actions to minimise the difference between the desired output and the actual output:

Error:

$$e(t) = x(t) - y(t) \tag{3.4}$$

The mathematical relationship expressing the total control is written as follows:

$$u(t) = P + I + D = k_p e(t) + k_i \int e(t) dt + k_d \frac{de(t)}{dt} \tag{3.5}$$

The operation of the various actions is shown in a block diagram (Figure 3.1), while Figure 3.2 illustrates the evolution of the error when a PID controller is applied.

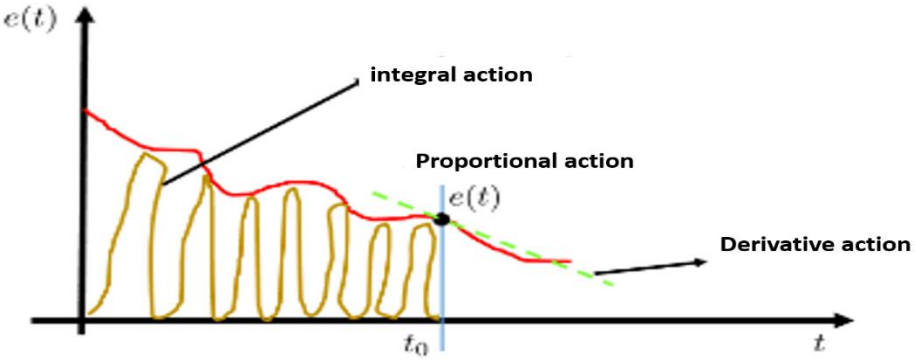

Figure 3.1 *Graphical representation of the error evolution [91]*

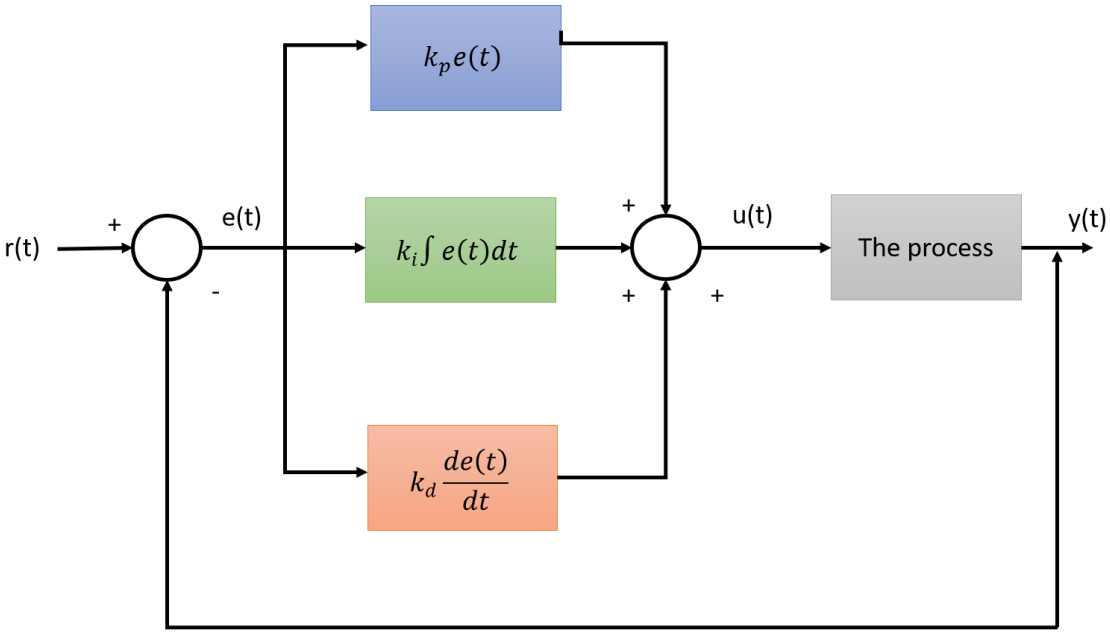

Figure 3.2 *Representation of the PID controller using a block diagram [92]*

3.2.1.2 PI Control

The PI controller, widely used in industrial systems, is designed to maintain the setpoint despite disturbances. It combines a proportional action, which improves response speed, with an integral action, which reduces steady-state error [93].

In its parallel form (Figure 3.3),

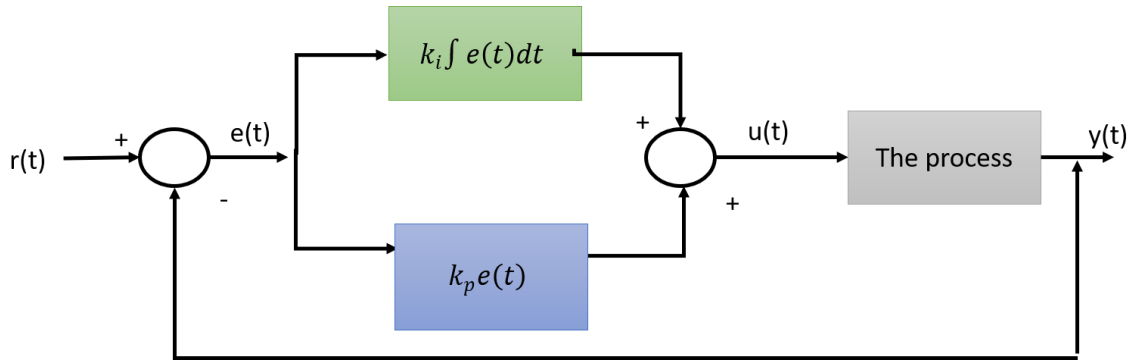

Figure 3.3 *Diagram of system control via PI control*

It is defined by:

$$u(s) = k_p e(t) + k_i \int e(t)dt \tag{3.6}$$

With:

$$e(s) = r(s) - y(s) \tag{3.7}$$

The gains are kp (proportional) and ki (integral). The transfer function becomes:

$$u(s) = e(s)\left[k_p e(t) + \int e(t)dt\right] \tag{3.8}$$

3.2.2 AI techniques

3.2.2.1 Fuzzy logic-based control

Conventional control methods have their limitations when dealing with complex, non-linear systems, which are often difficult to model accurately. Fuzzy control, therefore, appears to be an effective alternative: based on Zadeh's fuzzy logic, it uses linguistic rules to represent uncertainty and unpredictable behaviour. As it does not require an exact mathematical model, it is particularly well suited to non-linear and partially known systems [94].

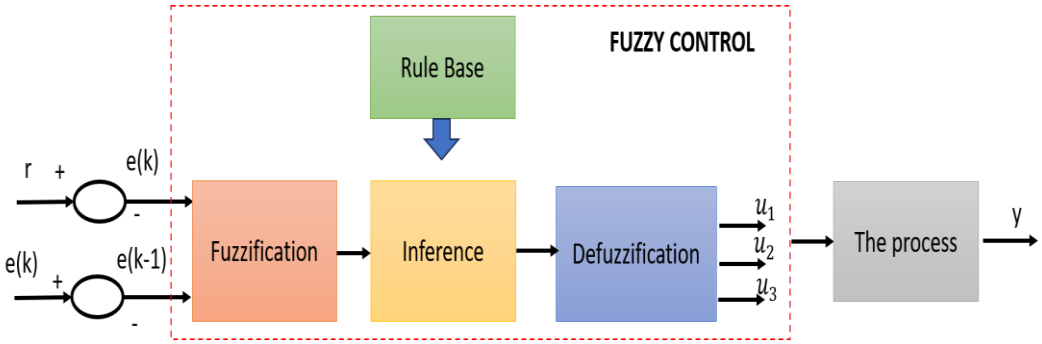

Figure 3.4 *Functional diagram of a fuzzy regulator*

Fuzzification is the first step in a fuzzy system. It transforms digital inputs into fuzzy values using linguistic variables (small, medium, large). This conversion is performed using membership functions, which describe the degree to which a value belongs to a fuzzy set. The most common shapes are triangular, trapezoidal, and Gaussian, as illustrated in Figure 3.5 [95].

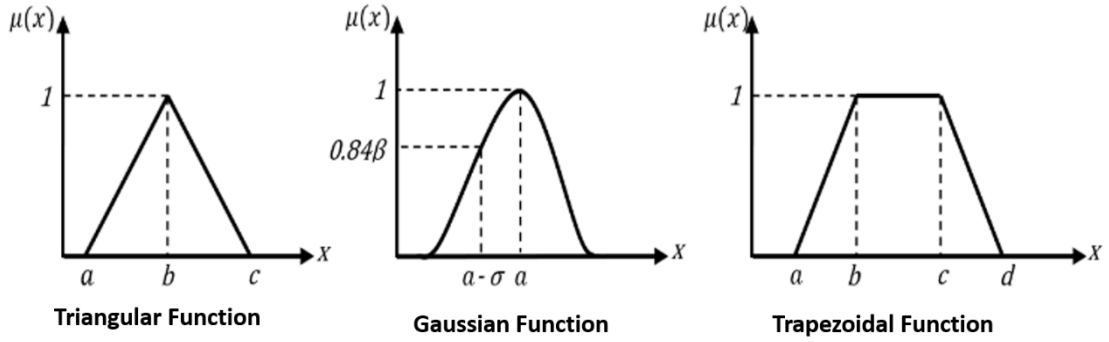

Figure 3.5 *Different forms of membership functions of a fuzzy system*

The corresponding expressions are:

Triangular function:

$$trim\ f(x;a;b;c) = \begin{cases} 0 & if\ x \le a \\ \frac{x-a}{b-a} & if\ a \le x \le b \\ \frac{c-x}{c-b} & if\ b \le x \le c \\ 0 & if\ x \ge c \end{cases} \tag{3.10}$$

Trapezoidal function:

$$trapm\ f(x;a;b;c;d) = \begin{cases} 0 & if\ x \le a \\ \frac{x-a}{b-a} & if\ a \le x \le b \\ 1 & if\ b \le x \le c \\ \frac{d-x}{d-c} & if\ c \le x \le d \\ 0 & if\ x \ge d \end{cases} \tag{3.11}$$

Gaussian function:

$$gaussmf(x;\sigma,a) = e^{\frac{(x-a)^2}{2\sigma^2}} \tag{3.12}$$

Inference establishes the link between fuzzy inputs and fuzzy outputs using rules that employ the logical operators AND, OR, and THEN. The most commonly used methods are those developed by Mamdani, Larsen, and Sugeno.

Mamdani (Min–Max):

$$R_i = If\ x_1\ is\ A_i\ and\ x_2\ is\ B_i, then\ z = C_i \tag{3.13}$$

$$\mu R_i = Min(x_1 \in A_i, x_2 \in B_i) \tag{3.14}$$

$$\mu_{C_i}(z) = Max\{Prod[\mu_{A_i}(x1), \mu_{B_i}(x_2)]\} \tag{3.15}$$

Sugeno (Sum–Product): combination by sum and product.

A summary of the methods is shown in Table 3.1.

Table 3.1 *Summary of the Different Inference Methods*

Methods	**Condition**	**Conclusion**	**Rule Conclusions**
Min — Max (Mamdani)	AND: Min OR: Max	THEN: Min	OR: Max
Max — Prod (Larsen)	AND: Min OR: Max	THEN: Prod	OR: Max
Sum — Prod (Sugeno)	AND: Prod OR: Sum	THEN: Prod	OR: Sum

Defuzzification converts the fuzzy output into a clear-cut value. The most common method is the centre of gravity method, which calculates the representative value of the output.

$$yres = \frac{\sum_{i=1}^{n} x_i\, \mu(x_i)}{\sum_{i=1}^{n} \mu(x_i)} \tag{3.16}$$

3.2.2.2 Artificial neural networks

Artificial neural networks (ANNs) are mathematical models inspired by biological neural networks, designed to process information intelligently and adaptively. They can learn complex relationships and solve non-linear problems, with greater resilience to noise and robustness than traditional methods. An ANN is composed of interconnected neurons organised in layers.

Each neuron receives inputs from the previous layer, and applies synaptic weights W_{jk} and a bias b_k, and transmits the output to the next layer [96].

Figure 3.7 illustrates a feedforward network, the most common type.

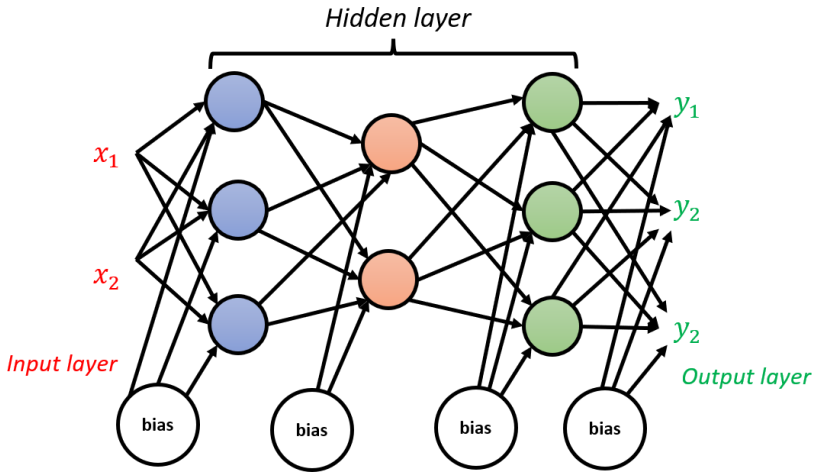

Figure 3.6 *Feedforward neural network*

Neuron j in layer i is described mathematically by (3.17):

$$y_j(i) = f\left(\sum_k j_k(i)x_k + b_j(i)\right) \tag{3.17}$$

where f is the activation function. The mean squared error for the output layer is:

$$Erreur = 0.5\sum_{s=1}^{R}(y_s - y_{s-desired})^2 \tag{3.18}$$

where R is the number of neurons in the output layer.

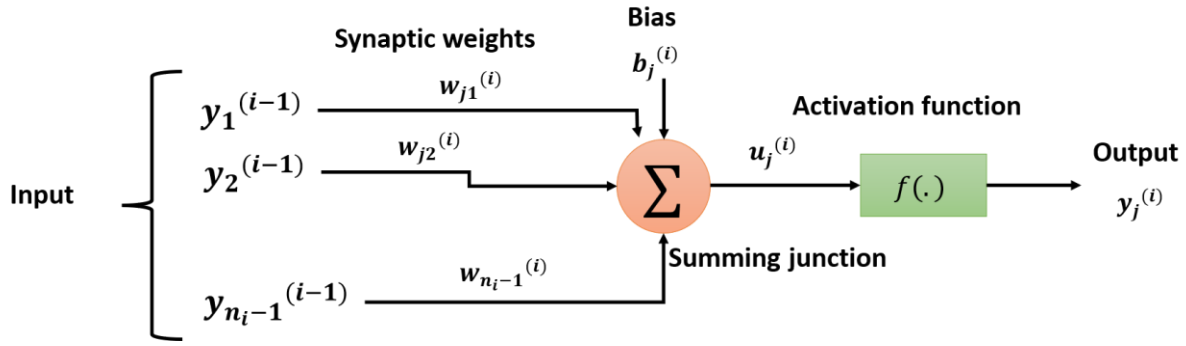

Figure 3.7 *Basic structure of a neuron*

ANNs do not require explicit programming or a pre-established knowledge base. They learn through various strategies, such as:

- Supervised learning: adjusting weights to minimise the error between input and target output.
- Unsupervised learning: self-organisation based on the similarity of input data.
- Reinforcement learning: an autonomous agent learns to maximise a cumulative reward.

Activation functions (non-linear) are essential to enable the network to model complex behaviours. The choice of function type depends on the type of data being processed (Table 3.2).

Table 3.2 *Activation function*

Name	**Matlab Function**	**Equation**
Identity / Ramp	purelin (Linear)	$f(x) = x$
Step / Heaviside Function	heaviside	$f(x) = \begin{cases} 0 \; if \; x < 0 \\ 1 \; if \; x \geq 0 \end{cases}$
Logistic (Sigmoid)	logsig	$f(x) = \frac{1}{1 + e^{-x}}$
Hyperbolic Tangent	tansig	$f(x) = tanh(x) = \frac{2}{1 + e^{-2x}} - 1$
Rectified Linear Unit (ReLU)	poslin (Positive linear)	$f(x) = \begin{cases} 0 \; if \; x < 0 \\ x \; if \; x \geq 0 \end{cases}$

Learning algorithms optimise weights and biases. A fundamental example is gradient descent:

$$x_{k+1} = x_k - \alpha_k g_k \tag{3.19}$$

where

x_k is the vector of current weights and biases, g_k is the gradient, and α_k is the learning rate.

Multi-layer feedforward networks (MLPs) are composed of:

- An input layer
- One or more hidden layers
- An output layer

Each neuron calculates a weighted sum of the inputs, applies an activation function, and passes the result to the next layer. ANNs are able to generalise from the training data to produce correct outputs even on unseen inputs.

3.3 METAHEURISTIC METHODS

3.3.1 The Particle Swarm Optimisation

The Particle Swarm Optimisation (PSO) algorithm is a bio-inspired method developed in 1995 by Kennedy and Eberhart, based on social behaviour observed in nature, such as schools of fish or flocks of birds. It is widely used to solve complex optimisation problems [95]. The algorithm considers a swarm of particles, each particle representing a potential solution characterised by its position x_i and velocity v_i. The evolution of each particle at each iteration depends on its current position and velocity, its best individual position $p_{i,best}$ (cognitive component), and the best collective solution gbest (social component) [97].

The corresponding equations are:

$$v_i\,(t+1) = wv_i\,(t) + \; c_1 r_1 \left(p_{i,best} - x_i\,(t)\right) + c_2 r_2 \left(g_{best} - x_i(t)\right) x_i\,(t+1) = x_i\,(t) + v_i(t+1) \tag{3.20}$$

where w is the inertia factor,c_1 and c_2 are the learning coefficients, and r_1 and r_2 are uniform random numbers.

Figure 3.8 illustrates the particle movement strategy:

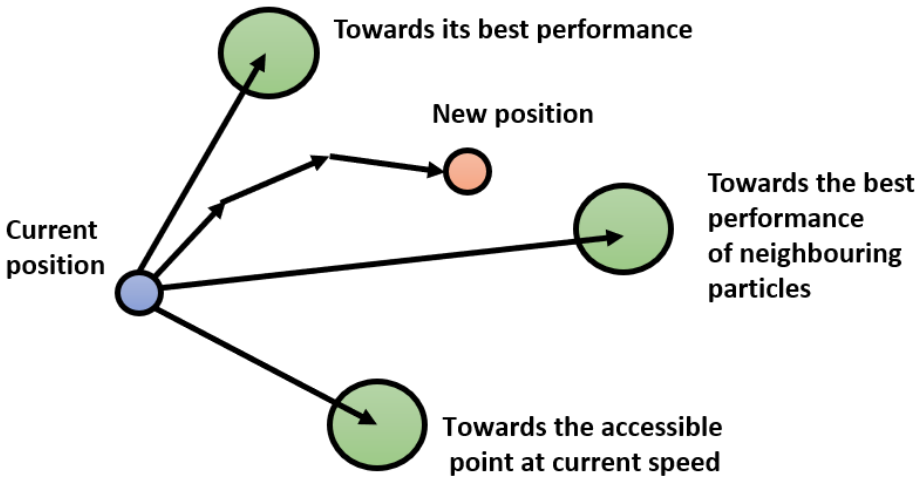

Figure 3.8 *Particle movement strategy*

3.3.2 Genetic algorithms

Genetic algorithms (GAs), inspired by natural selection and evolution, are part of evolutionary algorithms [98] and are widely used for optimising complex, non-linear parameters. They are recognised for their robustness and effectiveness in exploring any search space, even large ones, and can handle conflicting objectives. They work by first generating an initial population of potential solutions (chromosomes), then evaluating each individual according to a fitness function representing the performance of the system. The best-performing individuals are selected for reproduction, and new individuals are created via crossover and mutation, thus exploring the parameter space. This process is repeated over several generations until optimal or near-optimal solutions are obtained [98].

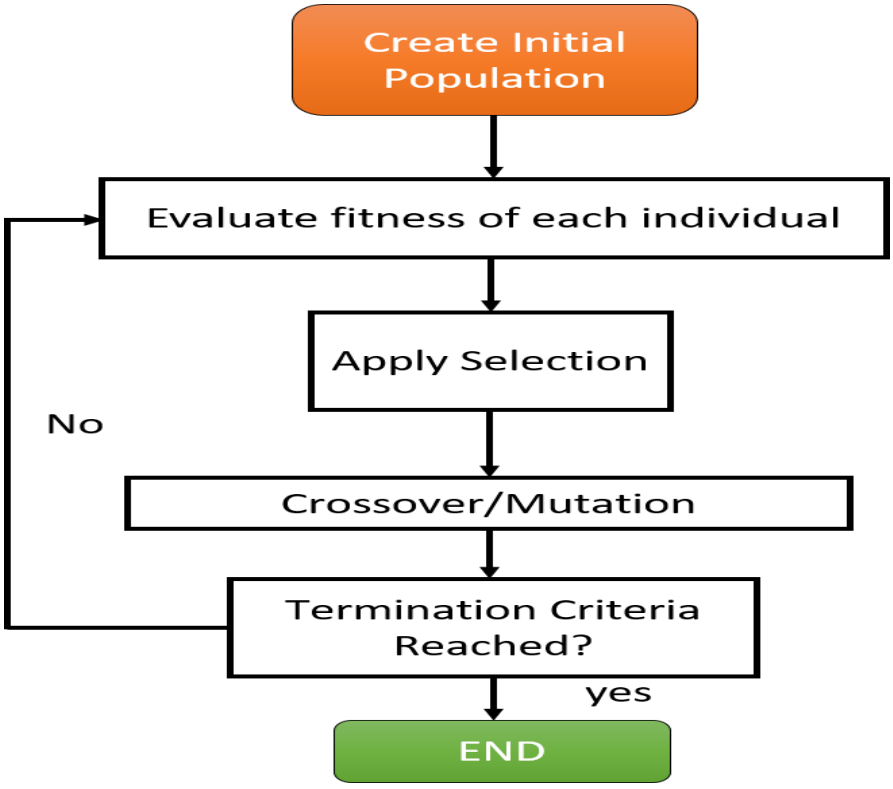

Figure 3.9 *The Flowchart of Genetic Algorithm [97]*

3.3.3 The Artificial Bee Colony (ABC) algorithm

The Artificial Bee Colony (ABC) algorithm simulates the foraging behaviour of bees to solve optimisation problems. It starts with a random initialisation of SN candidate solutions x_i=($x_{i,1}$,…,$x_{i,D}$) according to (3.21) [99]:

$$x^0{}_{i,j} = x_{l,j} + rand(0,1)(x_{u,j} - x_{l,j}) \tag{3.21}$$

where $x_{l,j}$,and $x_{u,j}$ represent the bounds of each dimension.

In the employed phase, each bee generates a new position using the search equation (3.22)

$$v_{i,j} = x^t{}_{i,j} + \theta_{i,j}(x^t{}_{i,j} - x^t{}_{k,j}) \tag{3.22}$$

with $k \neq i$ chosen randomly and $\theta_{i,j} \in [-1,1]$. The new solution is accepted according to a greedy selection.

$$x_i^{t+1} = \begin{cases} v_i \, , if \; f(v_i) < f(x_i^t) \\ x_i^t \qquad\qquad\qquad , else \end{cases} \tag{3.23}$$

The onlooker phase intensifies exploration around promising sources. Fitness is calculated via (3.24)

$$fit_i^{t+1} = \begin{cases} \frac{1}{1+f_i^{t+1}} \, , f_i^{t+1} > 0 \\ 1 + \left| f_i^{t+1} \right| , else \end{cases} \tag{3.24}$$

and the solutions are selected with probability

$$p_i^{t+1} = \frac{fit_i^{t+1}}{\sum_{m=1}^{SN} fit_m^{t+1}} \tag{3.25}$$

The onlookers then generate new solutions.

Finally, in the scout phase, any stagnant solution whose counter exceeds the limit is replaced by a new solution generated by the initialisation equation.

The entire process is illustrated in the flowchart in Figure 3.11.

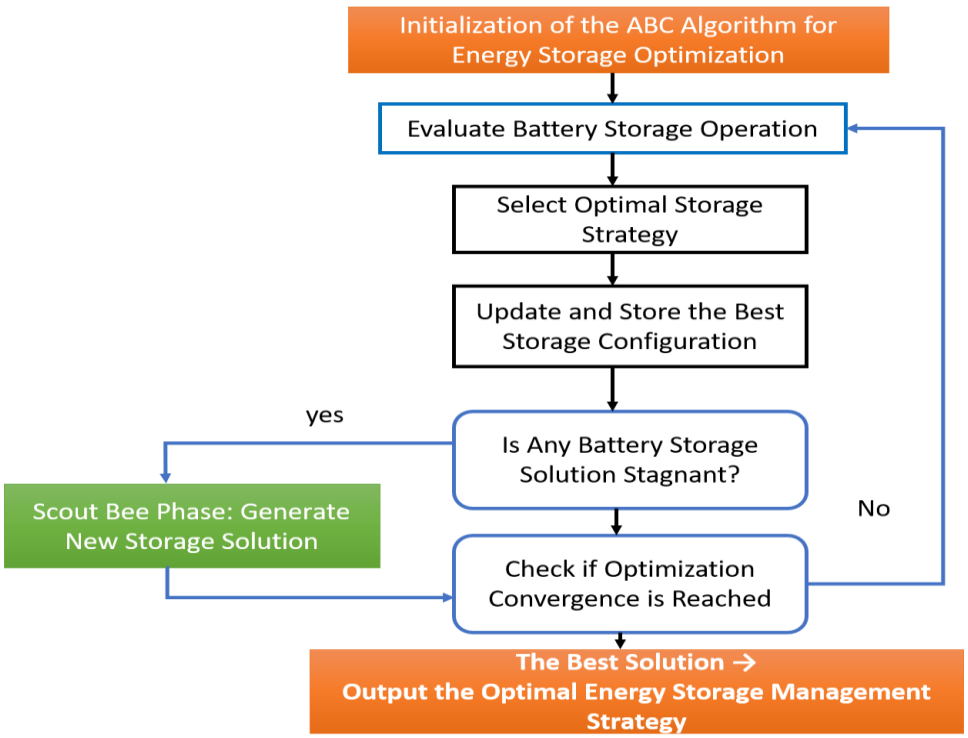

Figure 3.10 *The Flowchart of the standard ABC algorithm*

3.3.4 Grey wolf optimizer (GWO)

GWO provides notable advantages over traditional methods like PSO and GA, due to its multi-leader guidance mechanism and its ability to adapt the search range dynamically [100]. The process typically begins with the definition of parameters, constraints, and performance criteria. Depending on the problem type, optimization may involve single or multiple objectives, with or without constraints. A wide range of traditional and metaheuristic techniques has been employed to address such challenges in engineering systems.

The Grey Wolf Optimizer (GWO) is a metaheuristic algorithm inspired by the hunting mechanisms and social hierarchy of grey wolves. The algorithm replicates the natural structure of a wolf pack, where the alpha wolf leads the decision-making process, supported by beta and delta wolves, while the remaining omega wolves follow. The hunting process includes three key stages: tracking, encircling, and attacking the prey, as illustrated in Figure 3.12 These behaviors are mathematically formulated to guide the optimization process efficiently and often outperform conventional methods .

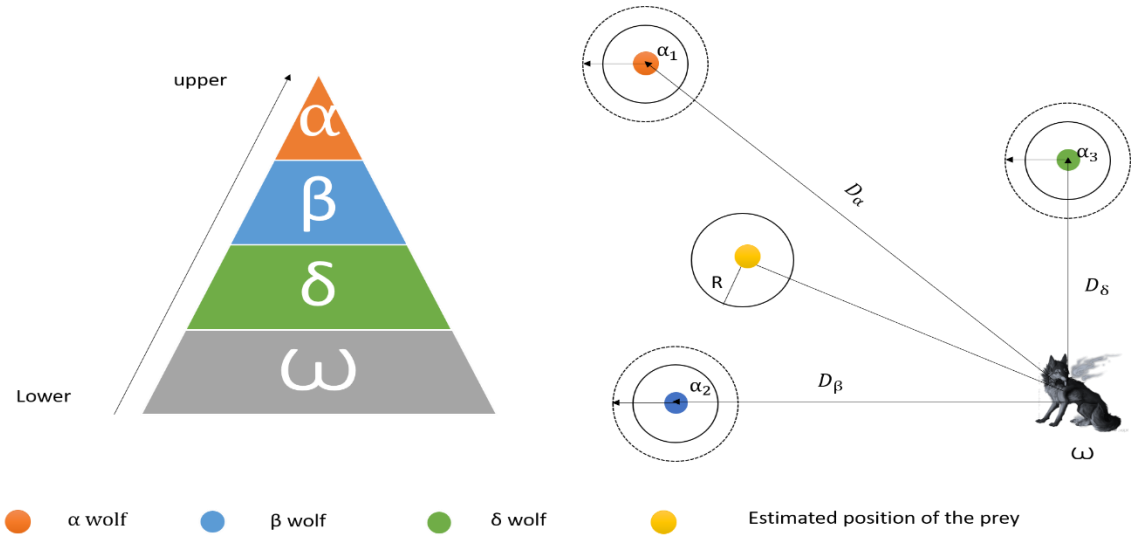

Figure 3.11 *Schematic representation of the grey wolf hunting strategy used in the GWO algorithm, including tracking, encircling, and attacking phases*

The GWO algorithm simulates the hierarchy by assigning roles to candidate solutions: Alpha (best solution), Beta (second-best), Delta (third-best), and Omega (remaining search agents) . The search agents update their positions relative to the leading wolves using the following equations:

$$D = |C.X_{best} - X| \tag{3.26}$$

$$X = X_{best} - A.D \tag{3.27}$$

Here, D represents the distance to the optimal solution, X_{best} denotes the best position, and A and C are coefficient vectors, which are defined as follows:

$$A = 2a.r_1 - a \tag{3.28}$$

$$C = 2.r_2 \tag{3.29}$$

In this process, the parameter 'a' gradually decreases from 2 to 0, allowing the algorithm to balance exploration and exploitation. To encircle their prey, wolves update their positions using the following equation:

$$X = X_{best} - A|C.X_{best} - X| \tag{3.30}$$

GWO was selected in this study due to its ability to effectively balance global exploration and local exploitation, which is critical for tuning fractional-order control parameters in

nonlinear hybrid energy systems. Its low parameter dependency, fast convergence behavior, and robustness in high-dimensional, non-convex search spaces make it well-suited for real-time optimization of control systems. Compared to other metaheuristics, GWO requires fewer control parameters and demonstrates consistent performance with reduced computational complexity. These advantages justify its selection for optimizing the FOPI controller parameters in the proposed PV-battery-grid system.

This iterative process continues until a predefined termination condition is met, such as the maximum number of iterations or convergence criteria. The overall optimization process is summarized in the flowchart shown in Figure 3.13.

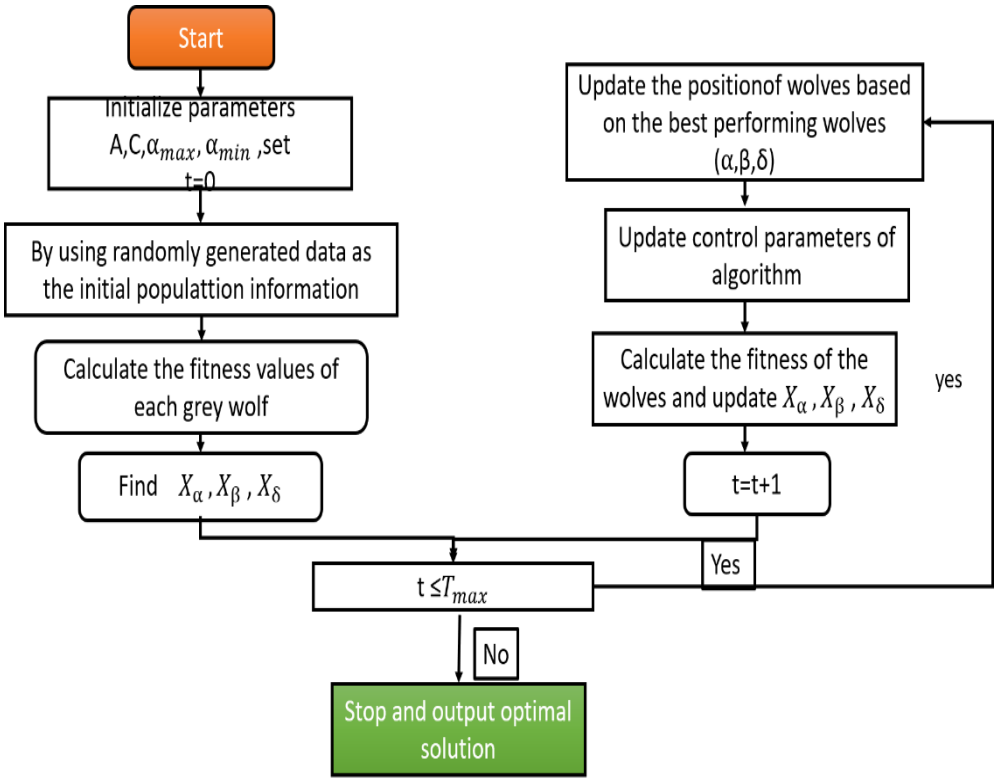

Figure 3.12 *Flowchart of the Grey Wolf Optimization (GWO) algorithm*

3.4 RULE-BASED CONTROL STRATEGIES

Rule-based strategies (RBC) are based on simple logical instructions such as IF... THEN. They are valued for their robustness and low computational complexity. They enable: the reduction of consumption peaks, the optimisation of self-consumption, the exploitation of tariff variations, the improvement of thermal comfort or the autonomy of the microgrid. They are often used to coordinate PV, batteries, loads, and the grid, with savings of up to 20% according to studies [101].

Figure 3.14 illustrates an example flowchart that explains the concept.

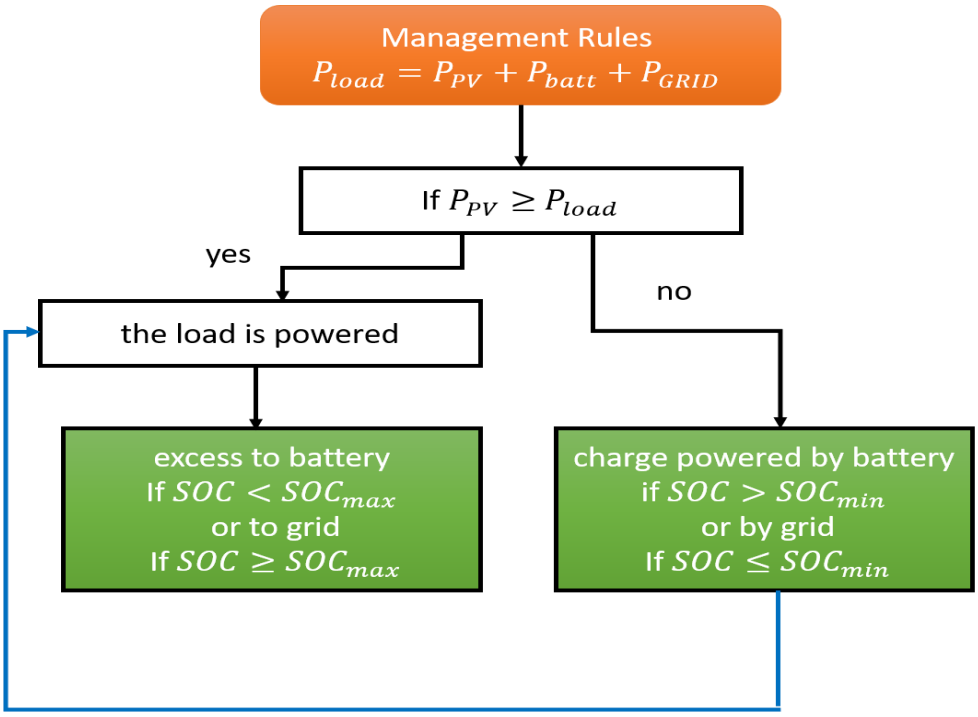

Figure 3.13 *Flowchart of the Rule-Based Energy Management Strategy*

3.5 PROPOSED ENERGY MANAGEMENT SYSTEM

The system studied comprises a photovoltaic generator connected to a set of batteries connected to the electricity grid. In order to interface these different components, appropriate power electronics are used, as described in Chapter 2. A boost converter is connected to the photovoltaic array to implement the Maximum Power Point Tracking (MPPT) strategy, while a bidirectional converter is connected to the battery and regulated by a Fractional Order Proportional-Integral controller optimised by the Grey Wolf Optimisation (FOPI-GWO) algorithm. Finally, an inverter provides the link between the DC bus and the AC grid, controlled by Direct Power Control (DPC). This section provides a detailed description of these different controls.

3.5.1 Maximum Power Point Tracking (MPPT)

Maximum Power Point Tracking (MPPT) controllers are essential for optimising the output of photovoltaic systems. They adjust the voltage and current of solar panels to extract maximum power despite variations in sunlight and temperature. MPPT works by tracking the maximum power point of the current-voltage (P-V) curve, thus ensuring energy efficiency. There are different methods for reaching this point, each with trade-offs in terms of accuracy,

speed and complexity [102]. Among the classic methods for tracking the maximum power point is the Hill Climbing algorithm, an optimisation process that starts with an initial solution, chosen randomly or according to heuristics, and proceeds by successive adjustments to improve it. The algorithm evaluates each solution using an evaluation function and generates neighbouring solutions through small modifications. If a neighbouring solution has a better value, it replaces the current solution. This iterative process continues until no further improvement is possible, leading to the local maximum. Hill climbing is particularly effective for determining the optimal position of a photovoltaic panel to maximise the system's power [103], [104]. Figure 3.15 illustrates this process in a flowchart, from initialisation to the final optimised result.

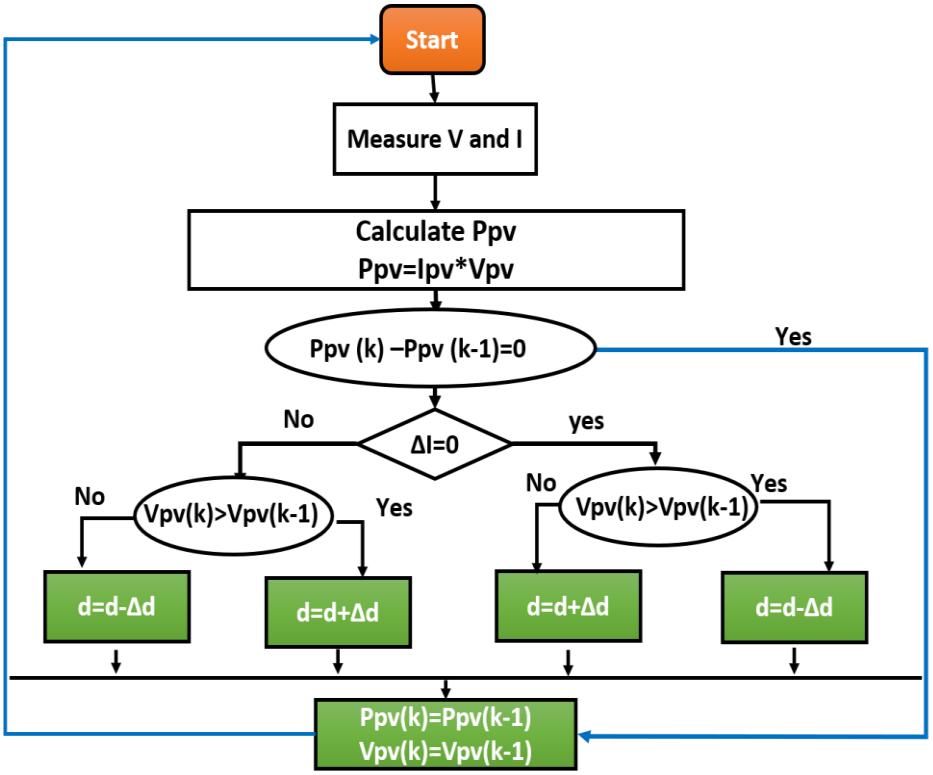

Figure 3.14 *Flowchart of the Hill Climbing Algorithm*

Solar radiation and ambient temperature data were extracted from the public NASA POWER Data Access Viewer database. They cover a continuous period of ten days, from 1 to 10 August 2022, for a geographical region located in the wilaya of Djelfa (Algeria). A forecasting procedure was developed in MATLAB to generate realistic and consistent data for the hybrid system simulation.

Five forecasting techniques were applied to the variables studied: the ARIMA (Autoregressive Integrated Moving Average) model, widely used for the analysis and forecasting of time series with trends or recurring patterns, whose main parameters are p (autoregressive order), d (degree of differentiation) and q (order of the moving average) [105]; linear regression, a simple and interpretable method assuming a linear relationship between the input variables and the target variable [106]; moving average, which consists of calculating the average of the last n observed values in order to smooth out short-term fluctuations and estimate future values [107]; support vector machines (SVM), an effective supervised learning method for regression and classification, suitable for small data sets and non-linear relationships through the use of kernel functions such as the Gaussian kernel (RBF) [108]; and finally, the artificial neural network (ANN), inspired by the functioning of the human brain, whose multilayer structure and learning capacity enable accurate predictions to be made in complex systems [109].

The performance of the forecasting models was evaluated using three statistical indicators: mean absolute error (MAE), mean absolute standardised error (MASE) and root mean square error (RMSE), whose mathematical expressions are presented in equations (3.31), (3.32) and (3.33) [110]. These indicators make it possible to quantify the accuracy of the predicted values in relation to the actual observations.

$$RMSE = \sqrt{\frac{1}{N}\sum_{i=1}^{N}(x_i - \hat{x_i})^2} \tag{3.31}$$

$$MAE = \frac{1}{N}\sum_{i=1}^{N}|x_i - \hat{x_i}| \tag{3.32}$$

$$MASE = \frac{MAE}{MAE_{naive}} * 100 \tag{3.33}$$

Where:

N is the total number of data points,

x_i is the actual (measured) value at time step iii,

$\hat{x_i}$ is the predicted value at the same time step,

MAE_{naive} is the mean absolute error obtained using a naïve forecasting model, typically based on persistence.

3.5.2 Direct Power Control (DPC)

For inverter control, the Direct Power Control (DPC) strategy was adopted due to the satisfactory performance reported in study [111]. This method is based on a switching table

(Table 3.3) that uses the errors between the reference active and reactive powers and their measured values as inputs in order to keep these errors within a hysteresis band.

Table 3.3 *Switching table of DPC*

n		1	2	3	4	5	6	7	8	9	10	11	12
dp	dq												
1	1	7	7	0	0	7	7	0	0	7	7	0	0
1	0	0	6	7	1	2	7	0	3	7	4	0	5
0	1	1	2	2	3	3	4	4	5	5	6	6	1
0	0	6	1	1	2	2	3	3	4	4	5	5	6

The DC bus regulation block provides the reference active power P_{ref} , expressed as:

$$P_{ref} = I_{ref}.V_{dc} \tag{3.34}$$

The reference reactive power q_{ref} is set to zero, while the instantaneous measured powers p and q are calculated from the grid voltages and currents according to [112].

$$p = V_{\alpha}.I_{\alpha} + V_{\beta}.I_{\beta} \tag{3.35}$$

$$q = I_{\alpha}.V_{\beta} - I_{\beta}.V_{\alpha} \tag{3.36}$$

Hysteresis comparators then generate digital signals S_p and S_q from the errors between the reference powers and the estimated powers. The mains voltage is converted into a digital signal to determine the corresponding sector [113], defined by the following relationship

$$(n-2)\frac{\pi}{6} \leq \theta n \leq -n-1)\frac{\pi}{6} \quad n = 1,2,\ldots.,12 \tag{3.37}$$

The diagram of the direct power control is shown in Figure 3.16.

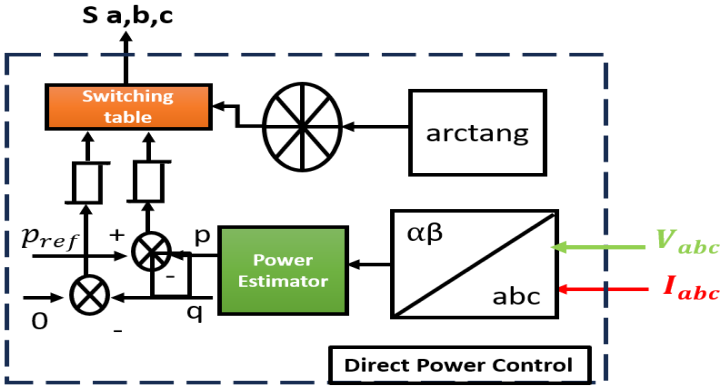

Figure 3.15 *Direct power control diagram*

3.5.3 Proposed Storage Management System

An energy management system based on a FOPI controller, optimised using the Grey Wolf Optimizer (GWO) algorithm, has been developed to ensure efficient regulation of the charging and discharging phases of the Li-ion battery. This control system is structured in two stages, each using a fractional-order proportional-integral corrector to ensure stability, accuracy and robustness. The first FOPI controller compensates for the difference between the measured voltage and the reference voltage to ensure the stability of the DC bus. The second adjusts the signal according to the battery current in order to correctly regulate the power exchanged. The signals from this double loop are then converted into pulse width modulation (PWM) to drive the bidirectional DC-DC converter.

The FOPI controller is defined by the following transfer functions, (3.38):

$$G(s) = \frac{U(s)}{E(s)} = K_p + K_i . \frac{1}{S^{\lambda}} \tag{3.38}$$

with $0 < \lambda < 1$, where:

K_p: proportional gain

K_i: integral gain

λ: fractional order

In order to improve storage durability and avoid excessive cycling, two operating conditions have been incorporated into the overall control scheme. Figure 3.16 shows the architecture of the FOPI controller, including these conditions, which limit the negative effects of deep discharge and overcharge, thereby extending battery life.

The corresponding control laws are given by (3.39) and (3.40):

$$u(s_1) = \begin{cases} k_p + k_i . \frac{1}{s^{\lambda}} \; if \; SOC > 20 \\ 0 \qquad\qquad otherwise \end{cases} \tag{3.39}$$

$$u(s_2) = \begin{cases} k_p + k_i . \frac{1}{s^{\lambda}} \; if \; SOC \leq 80 \\ 0 \qquad\qquad otherwise \end{cases} \tag{3.40}$$

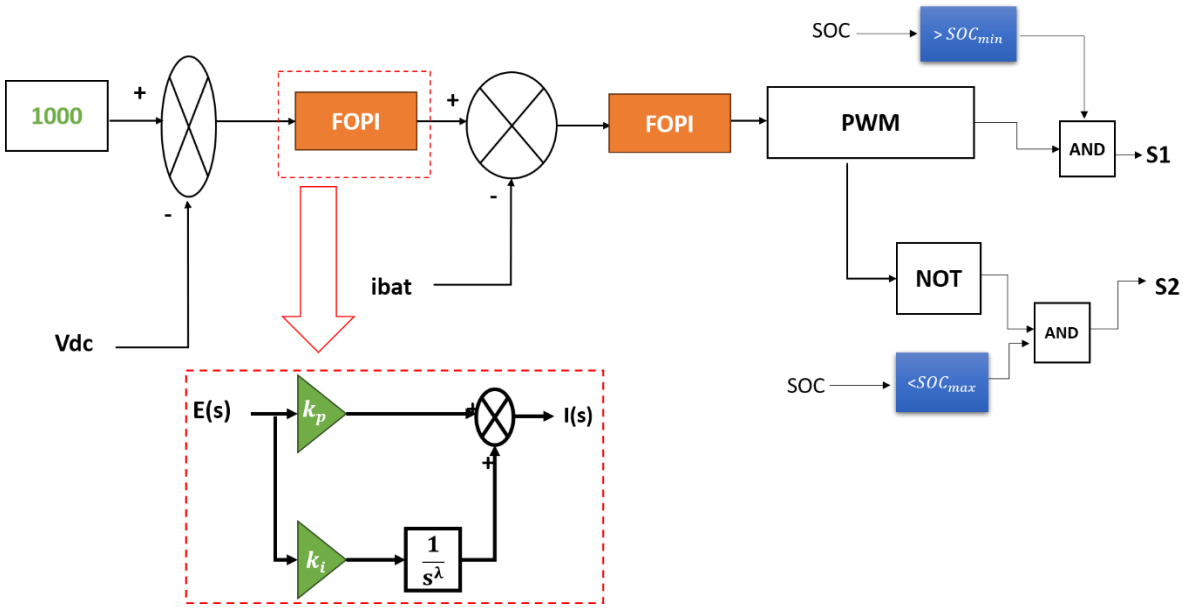

Figure 3.16 *Functional diagram of the FOPI controller with conditions*

To achieve optimal performance, the parameters k_p, k_i and λ were adjusted using GWO, which improves dynamic response, reduces voltage deviations and limits overcurrents. The objective function used is defined by (3.41):

$$J = \frac{w\_1.std(v\_dc\ [A:B])}{v_{ref}} + w_2 . \frac{|\max(v_{dc}) - v_{ref}|}{v_{ref}} + w_3 . \frac{|\max(i_{bat}) - I_{ref}|}{I_{ref}} \qquad (3.41)$$

It combines three weighted criteria:

w_1: stability of the DC bus voltage,

w_2: maximum deviation from the reference voltage,

w_3: maximum deviation of the battery current from its setpoint.

3.6 CONCLUSION

This chapter has presented a comprehensive overview of control methods applied to microgrids, covering both conventional techniques and intelligent and metaheuristic approaches. After reviewing the fundamentals of PID and PI controllers, we highlighted the contributions made by fuzzy logic, neural networks and optimisation algorithms such as PSO, GA, ABC and GWO. Particular attention was paid to the GWO-optimised FOPI controller, which was integrated into the management strategy for the PV-battery-grid system studied. This control architecture provides an interesting compromise between stability, dynamic performance and robustness in the face of variations in irradiation and load profile.

The following chapter will be devoted to modelling and simulating the complete system, presenting the results obtained and interpreting them in order to evaluate the actual performance of the control strategies developed.

Chapter 4: Simulation Results, Performance Analysis, and Discussion

4.1 INTRODUCTION

This final chapter is devoted to presenting and analysing the simulation results obtained in the MATLAB/Simulink environment, with the aim of validating the forecasting, control and energy management strategies proposed for the hybrid microgrid under study. These simulations are a key step in the work, as they enable the dynamic behaviour of the system to be assessed under realistic operating conditions, characterised by the variability of renewable resources and consumption profiles.

Initially, forecasting methods were implemented to estimate the essential input parameters of the system, namely solar irradiance, ambient temperature, and electricity consumption. Several predictive approaches, including ARIMA models, linear regression, moving averages, support vector machines (SVM), and artificial neural networks (ANN), were compared using recognised performance indicators (RMSE, MAE, and MASE). The best-performing models for each variable were then selected to generate realistic time profiles, which were used as excitation signals in Simulink.

Based on these forecast data, a comprehensive model of the photovoltaic microgrid, incorporating a lithium-ion battery and a connection to the electricity grid, was developed. The simulations enable detailed analysis of the performance of the conversion system, the stability of the DC bus voltage, and the effectiveness of the proposed control and optimisation strategies. Particular attention is paid to comparing different metaheuristic optimisation approaches, notably the Grey Wolf Optimizer (GWO) and Particle Swarm Optimization (PSO), as well as comparing them with a conventional PID controller.

Finally, this chapter highlights the overall energy behaviour of the microgrid, including battery management under state of charge (SOC) constraints, power distribution between different sources, and the impact of control strategies on system stability, reliability, and sustainability. The results obtained not only demonstrate the superiority of the proposed method but also highlight its potential for application in photovoltaic microgrids in real-world contexts, particularly in regions with high solar potential such as Algeria.

4.2 DATA AND PROFILES USED FOR THE SIMULATION

The data used covers a ten-day period from 1 to 10 August 2022, corresponding to the Djelfa region in Algeria. It includes solar irradiance and ambient temperature data from the NASA POWER database, as well as a synthetic electricity consumption profile representative of a residential load, varying between 3 kW at night and 4 kW during the day. Based on these hourly series, 24-hour forecast profiles were generated to feed into the Simulink model of the microgrid. The simulation covers a full daily cycle under realistic conditions, with photovoltaic production reaching approximately 16 kW at midday and a maximum temperature close to 40°C. The battery state of charge is maintained between 20% and 80%, ensuring safe operation, bus voltage stability around 1000 V, and efficient charge and discharge management according to variations in sunlight and demand.

4.3 MODELLING OF THE MICROGRID USING MATLAB/SIMULINK

In order to evaluate the performance of the proposed energy control and management strategies, a comprehensive model of the hybrid microgrid was developed using MATLAB/Simulink. This model aims to accurately reproduce the dynamic behaviour of the system under real operating conditions, while allowing for the integration of forecast data on irradiance, temperature and consumption.

The microgrid studied consists mainly of a photovoltaic generator, a lithium-ion battery, a DC link, an inverter, an electrical load and a connection to the public electricity grid. The overall architecture of the system ensures a reliable power supply to the load, while optimising the use of solar energy and limiting the load on the grid.

Figure 4.1 illustrates the overall structure of the microgrid implemented in MATLAB/Simulink. It shows the interconnection of the various subsystems, as well as the power and control flows between the photovoltaic source, the storage system, the electricity grid and the load. This representation highlights the central role of the DC link and the controller in coordinating energy exchanges.

The photovoltaic generator is modelled based on its electrical characteristics, taking into account the influence of solar irradiance and ambient temperature on the power produced. Forecast hourly profiles are applied as input signals, enabling the natural variability of photovoltaic production to be simulated over an extended daily cycle.

The lithium-ion battery plays a central role in the energy management of the microgrid. It is modelled by integrating the dynamics of voltage, current and state of charge (SOC). Operational constraints are imposed to maintain the SOC within a safe range of 20% to 80%, which prevents overcharging and deep discharging, thereby extending the battery's service life. The model clearly distinguishes between charging and discharging phases, based on the balance between photovoltaic production, load demand and exchange with the grid.

The continuous bus is the coupling element between the various sources and the load. Its voltage is regulated around a reference value set at 1000 V using a FOPI-type controller, whose parameters are optimised by metaheuristic algorithms. The stability of this voltage is a key indicator of the overall performance of the system, as it ensures the safe and efficient operation of the inverter and connected loads.

The connection to the electricity grid is modelled to allow bidirectional power exchange. The grid intervenes when photovoltaic production and the energy stored in the battery are insufficient to meet demand, or conversely, it absorbs excess production when the battery reaches its charge limits. This configuration makes it possible to analyse the impact of the proposed strategies on reducing grid dependence and improving self-consumption.

Finally, the electrical load is represented by a variable consumption profile, reflecting typical residential or tertiary usage. This profile is applied as a dynamic constraint to the system, making it possible to evaluate the microgrid's ability to respond effectively to fluctuations in demand.

All of these sub-models are integrated into Simulink to form a consistent and flexible simulation platform. This modelling forms the basis for the analyses presented in the following sections, where the performance of optimisation algorithms, control strategies and energy management are evaluated and compared in different operating scenarios.

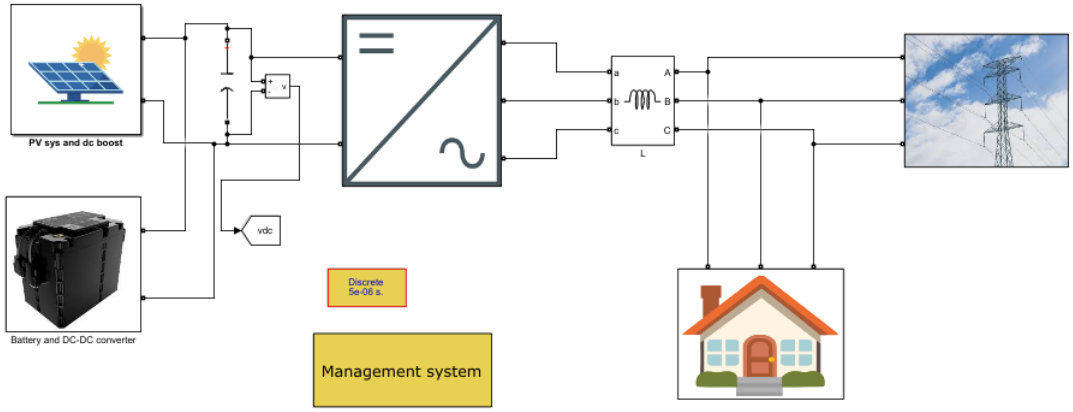

Figure 4.1 *Overall architecture of the hybrid microgrid implemented in MATLAB/Simulink*

4.4 PREDICTION RESULTS AND MODEL SELECTION

Forecasting methodologies were employed in MATLAB to estimate the primary input parameters of the hybrid system, specifically solar irradiance, ambient temperature, and electrical consumption, to replicate the system's behaviour under actual operating conditions. A variety of prediction methodologies were formulated and assessed using standard statistical metrics, including RMSE, MAE, and MASE, facilitating the identification of the most appropriate technique for each parameter. After identifying the appropriate prediction models, the obtained data were assembled into a SIMIN input file and incorporated into Simulink as time-series data to conduct simulations utilising realistic forecast-based inputs.

The first ten days of solar irradiance, ambient temperature, and electrical load consumption all of which were used to train and assess forecasting models are shown in Figure 4.2. The data used for model training and parameter optimisation is represented by the learning segment, which is shown in black. This enables the identification of the common daily and hourly patterns present during the study period. The additional extension of the curves matches the anticipated values that the suggested models produce, which surpass the historical record.

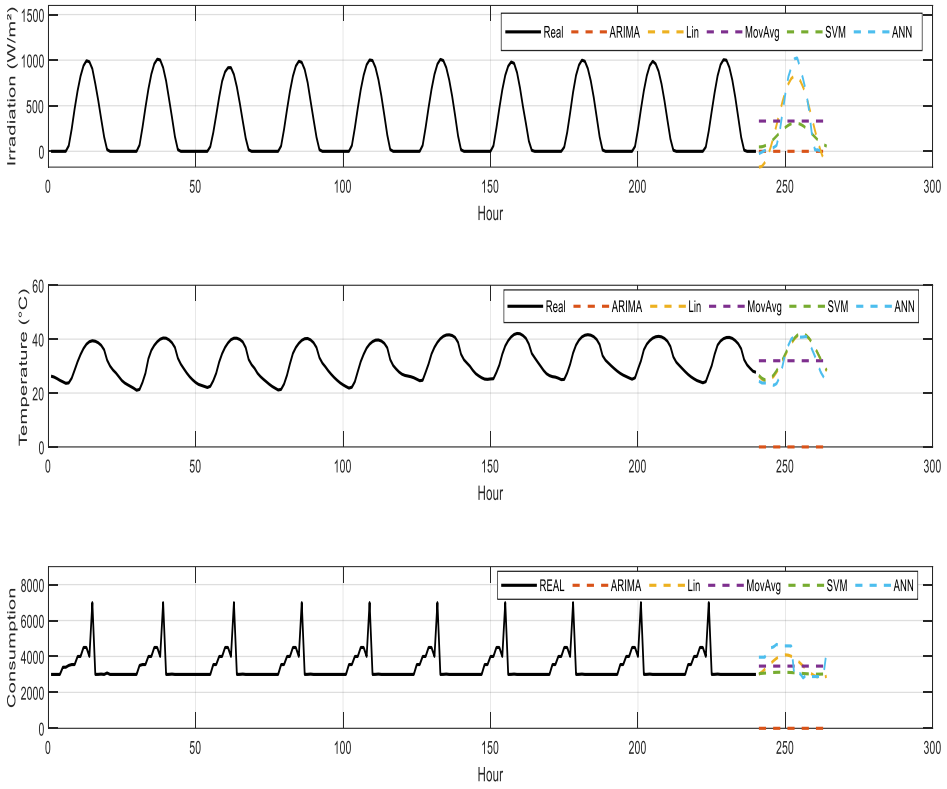

Figure 4.2 *Raw Hourly Irradiance, Temperature, and Consumption Data with Predictions from Multiple Forecasting Methods*

The accuracy of forecasting models in predicting solar radiation, ambient temperature, and electricity consumption is illustrated in Figure 4.3 and Tables 4.1, 4.2, and 4.3. The forecasting techniques examined include ARIMA, linear regression, moving average, support vector machine (SVM), and artificial neural network (ANN). To compare and evaluate each model, we used statistical measures such as mean absolute error (MAE), mean absolute standardised error (MASE), and root mean square error (RMSE), which allow us to objectively assess the accuracy and reliability of the models and identify the best ones for describing the temporal evolution of each variable. The results indicate that the ANN model excels at predicting temperature and irradiance, while the linear model is more effective at predicting electricity consumption. This conclusion is based on a comparative analysis of the models' performance and their ability to capture the temporal variations and dynamic behaviours of the different variables. By providing real, high-quality input data, this performance evaluation confirms the relevance and accuracy of the models selected for the MATLAB/Simulink hybrid simulation of the photovoltaic-battery microgrid.

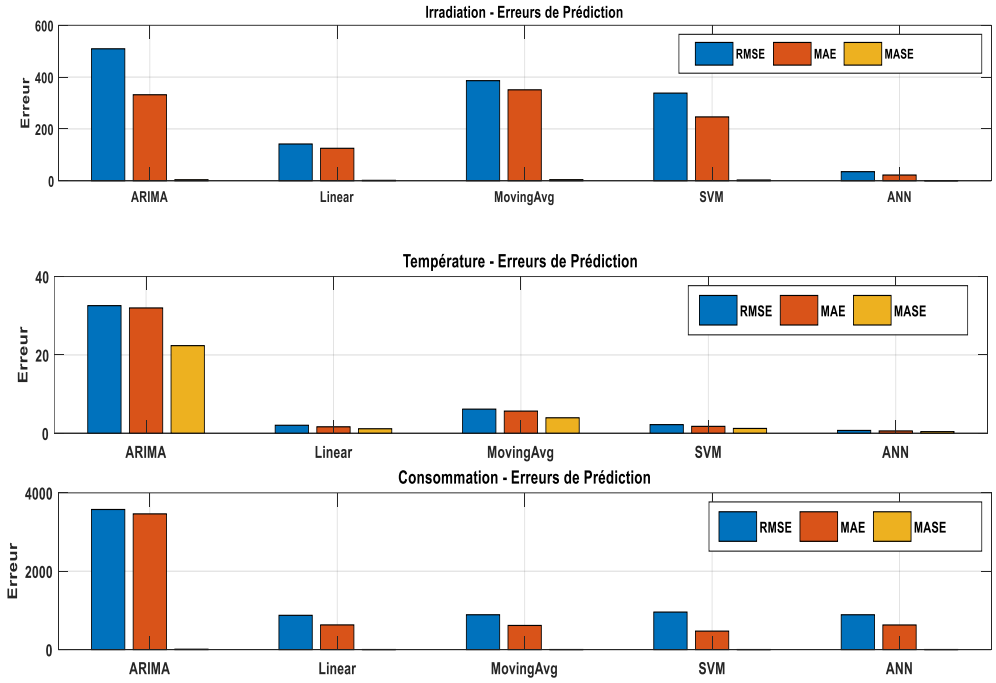

Figure 4.3 *Error Distribution Plots of Predicted Variables (Irradiance, Temperature, and Consumption)*

Table 4.1 *Performance Evaluation of Forecasting Methods for Irradiance: ARIMA, Linear, Moving Avg, SVM, and ANN Based on RMSE, MAE, and MASE Metrics*

Methods	**RMSE**	**MAE**	**MASE**
ARIMA	509.236	331.858	3.798
Linear	141.760	125.152	1.432
Moving Avg	386.254	350.900	4.016
SVM	338.189	246.304	2.819
ANN	45.194	33.544	0.384

Table 4.2 *Performance Evaluation of Forecasting Methods for Temperature: ARIMA, Linear, Moving Avg, SVM, and ANN Based on RMSE, MAE, and MASE Metrics.*

Methods	RMSE	MAE	MASE
ARIMA	32.576	31.988	22.369
Linear	2.043	1.655	1.158

Moving Avg	6.160	5.658	3.957
SVM	2.206	1.766	1.235
ANN	1.525	1.254	0.877

Table 4.3 *Performance Evaluation of Forecasting Methods for consumption: ARIMA, Linear, Moving Avg, SVM, and ANN Based on RMSE, MAE, and MASE Metrics.*

Methods	RMSE	MAE	MASE
ARIMA	3575.615	3463.432	9.389
Linear	874.303	629.555	1.707
Moving Avg	888.629	616.087	1.670
SVM	957.177	471.140	1.277
ANN	909.273	508.787	1.379

4.5 CONTROL SYSTEM RESULTS

4.5.1 Description of the system studied and entry profiles

The system studied is a local microgrid consisting of a photovoltaic generator connected to the electricity grid and coupled with a lithium-ion battery for energy storage. In the absence of solar radiation, particularly at night, the battery takes over to provide a continuous direct current (DC) supply to local loads, thus ensuring continuity of service.

In order to evaluate the efficiency of the proposed controller under realistic conditions of varying sunlight, the predicted values of irradiance, temperature and consumption shown in Figure 4.4 were used as excitation signals for the system. These data cover a complete 24-hour cycle repeated over a period of ten consecutive days, allowing the behaviour of the system to be observed over a wide range of weather and load conditions.

Irradiance is zero during the night, begins to increase from 7 a.m., reaches its maximum around noon, and then gradually decreases until sunset. The ambient temperature follows a similar trend, with a gradual rise in the morning and a peak of around 40°C in the middle of the afternoon before falling again in the evening. Electricity consumption, meanwhile, remains relatively stable at around 3000 W during the night, gradually increases during the day to reach a peak of 4000 W, then decreases again in the evening, reflecting the typical profile of a residential or tertiary load.

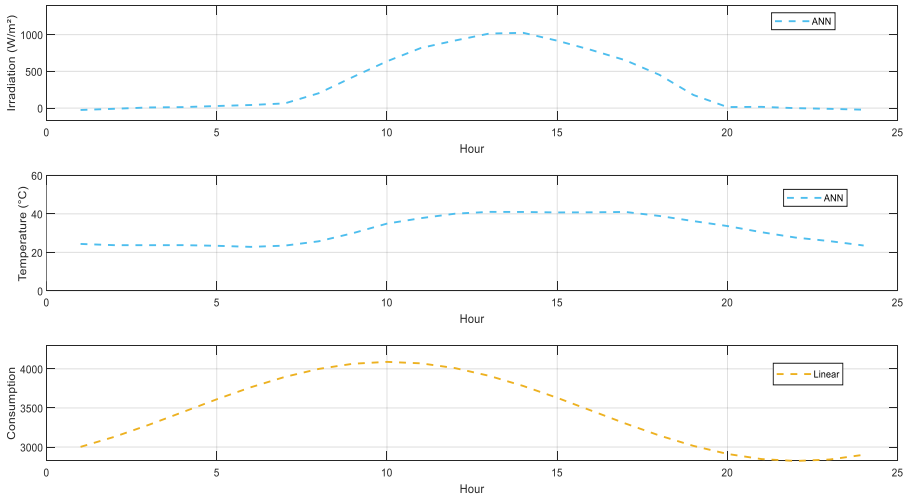

Figure 4.4 *Hourly Profile of Irradiance, Temperature, and Consumption*

4.5.2 Evolution of the objective function of optimisation algorithms

Figure 4.5 illustrates the evolution of the objective function over iterations for the two optimisation algorithms studied, namely the Grey Wolf Optimizer (GWO) and Particle Swarm Optimization (PSO). This objective function measures the quality of the solution obtained at each stage of the optimisation process and evaluates each algorithm's ability to reach the desired global minimum.

We can see that the GWO algorithm converges much more quickly, reaching stability after only about four iterations. The value of the objective function decreases rapidly to a minimum of around 50, then remains almost constant, reflecting remarkable stability and good optimisation accuracy. This performance highlights the GWO's ability to effectively balance the exploration and exploitation phases of the search space, enabling it to avoid local minima and ensure robust convergence.

In contrast, the PSO algorithm shows slower and less regular convergence. The decrease in the objective function only becomes significant from the ninth iteration onwards, reaching a final value of around 150, which is significantly higher than that obtained by GWO. This difference reflects the lower efficiency of PSO in finding the global minimum, probably due to less balanced exploration and a tendency to get trapped prematurely in local solutions.

Thus, the comparison clearly highlights the superiority of GWO in terms of convergence speed, stability and accuracy, which justifies its adoption for controller optimisation in the context of energy management for the microgrid studied.

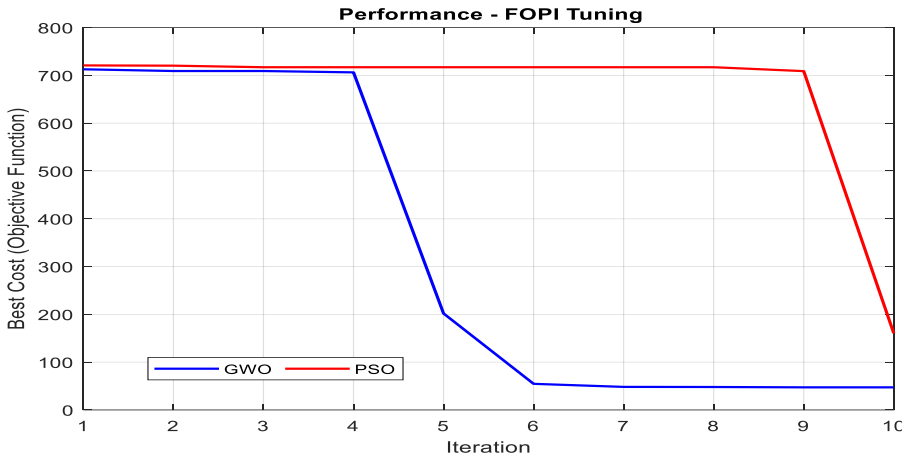

Figure 4.5 *Objective Function Evolution for GWO and PSO Algorithms*

4.5.3 DC bus voltage regulation (Vdc)

Figure 4.6 shows the growth of the DC voltage (Vdc). Over a 24-hour period, compare the performance of two optimization approaches, GWO and PSO, using a reference (REF) to represent the desired target value. The three curves remain about around 1000 V, showing good overall stability. The GWO-based controller closely follows the reference with insignificant variations, whereas PSO, while generally stable, shows a tiny positive drift between 8 a.m. and 10 a.m., reaching around 1010 V. This shows a little increased dynamic regulation capacity, albeit at the expense of a minor divergence from the reference value. Both approaches effectively adjust voltage (Vdc).GWO demonstrated higher stability.

These results confirm that the Grey Wolf Optimizer (GWO) achieves faster and more consistent convergence than Particle Swarm Optimization (PSO). This behavior aligns with theoretical expectations, as GWO maintains a stronger balance between exploration and exploitation through its multi-leader hierarchy. Recent research on optimization in renewable energy systems has highlighted similar advantages, further reinforcing the relevance of GWO for nonlinear control applications.

Figure 4.7 provides an additional comparison with a conventional PID controller to further validate the proposed strategy. It can be observed that the PID response is slower than that of the GWO-optimized FOPI controller. Although the PID eventually reaches the reference value, the initial transient highlights the enhanced robustness and faster response of the proposed FOPI-GWO controller.

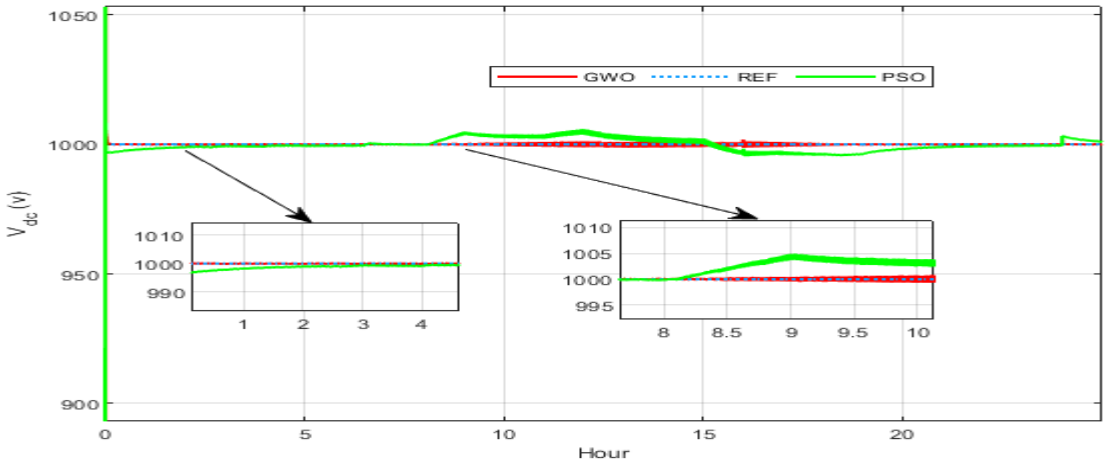

Figure 4.6 *DC link voltage*

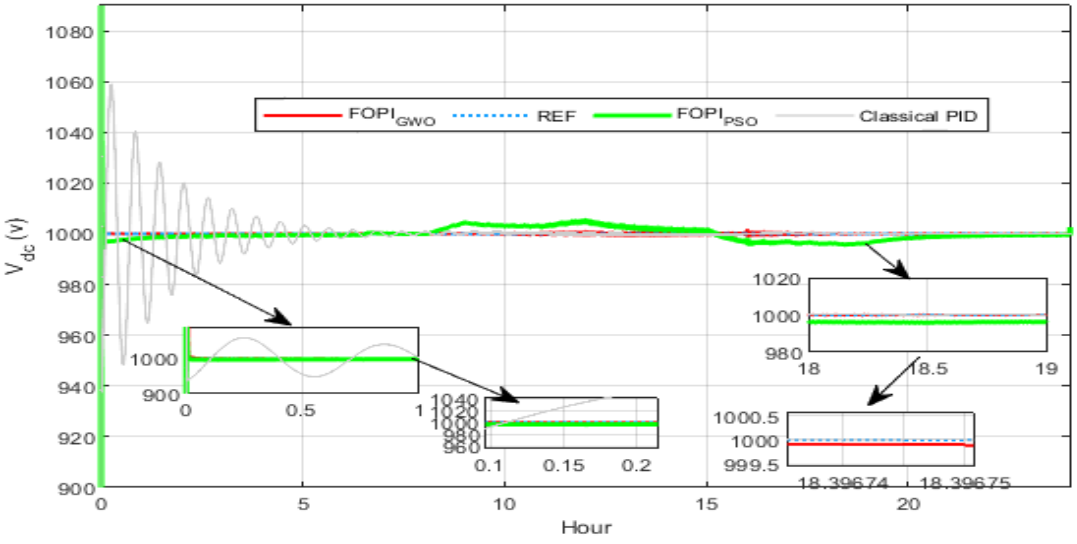

Figure 4.7 *Comparative Analysis of DC Link Voltage Control Using Classical PID, FOPI-GWO, and FOPI-PSO Controllers*

4.5.4 Analysis of battery behaviour

4.5.4.1 Battery voltage and current

Figures 4.8 and 4.9 show the growth of battery voltage and current over a 25-hour period, comparing two optimization techniques: Particle Swarm Optimization and Grey Wolf Optimization. The battery voltage gradually increases, peaking at 545 V at hour 15, somewhat higher than PSO's 543 V. Following this apex, GWO exhibits a rapid voltage decline, whereas PSO has a gradual reduction. GWO has significant stability at around 0 A, indicating a balanced charge and discharge mechanism. In contrast, PSO demonstrates significant fluctuation, with

a prominent discharge phase around hour 15, during which the current lowers to approximately -7 A.GWO improves stability by buffering unexpected variations in voltage and current, reducing thermal stress and increasing battery longevity. Although both strategies achieve similar peak voltage performance, GWO's dynamic resilience and ability to avoid high power peaks make it a more reliable and efficient approach to optimal energy management.

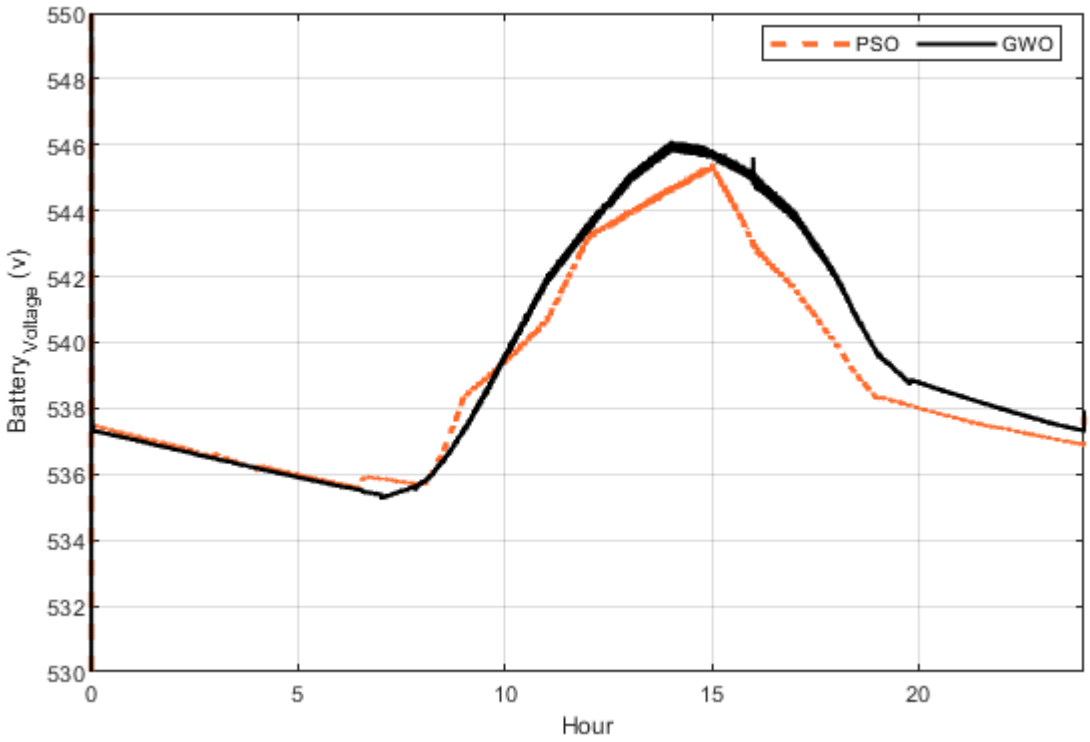

Figure 4.8 *Battery Voltage Behavior at 20% < SOC < 80%*

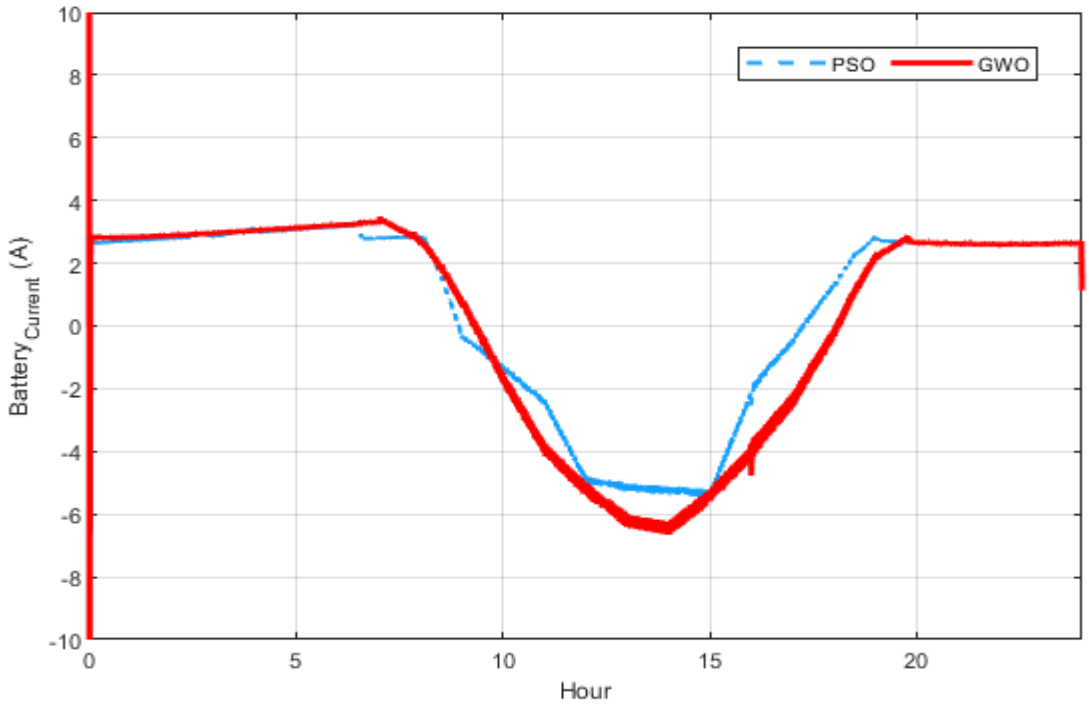

Figure 4.9 *Battery Current Behavior at 20% < SOC < 80%*

4.5.4.2 Hybrid system energy management

Figure 4.10 picts the power fluctuations during a 25-hour duration for the primary elements of the hybrid system: photovoltaic (PV) power, battery power, grid power, and load power. The photovoltaic power exhibits a standard daily pattern, progressively escalating in the morning with increasing solar irradiance, attaining a zenith about midday that may surpass 16 kW contingent upon meteorological conditions, then diminishing to almost zero by sunset. When solar generation surpasses local demand, the excess energy is either stored in batteries or transmitted to the grid. The battery is integral to energy management: it charges at an average power of approximately 3.8 kW during the day when photovoltaic production surpasses consumption (between 9 AM and 3 PM) and discharges at an average power of about 1.5 kW at night (between 6 PM and 6 AM) to meet local demand. In this system, charging is associated with negative power, whereas discharging is linked to positive power. The grid supplements energy requirements when the aggregate output from the battery and photovoltaic system is inadequate, delivering an average power of approximately 1.5 kW, particularly throughout the morning (6 AM – 9 AM) and evening (6 PM – midnight). The load power is predominantly consistent at approximately 3 kW, with a peak of 4 kW over the day, indicative of standard residential or commercial consumption. This astute synchronization of generation, storage, and

grid ensures a reliable power supply, enhances self-consumption, reduces grid reliance, and optimizes charging and discharging, thereby facilitating superior battery management. It dynamically adjusts energy management to hourly fluctuations in demand and solar generation.

The enhanced stability of GWO in managing battery current and voltage demonstrates its capacity to prolong battery lifespan and mitigate thermal stress. This discovery corroborates prior studies emphasizing the significance of improved metaheuristic optimization in enhancing energy storage management in photovoltaic-based microgrids. The proposed controller enhances safety and dependability by alleviating sudden fluctuations, surpassing traditional methods.

Two further tests were done to confirm that Controller 2, which employs logical conditions to keep the battery's SOC between 20% and 80%, works. The first instance began with an 80% charge. The second case was less than 20%. The first simulation showed that the state of charge (SOC) slowly went above 80%, which allowed us to look at how well the controller controlled the charge.

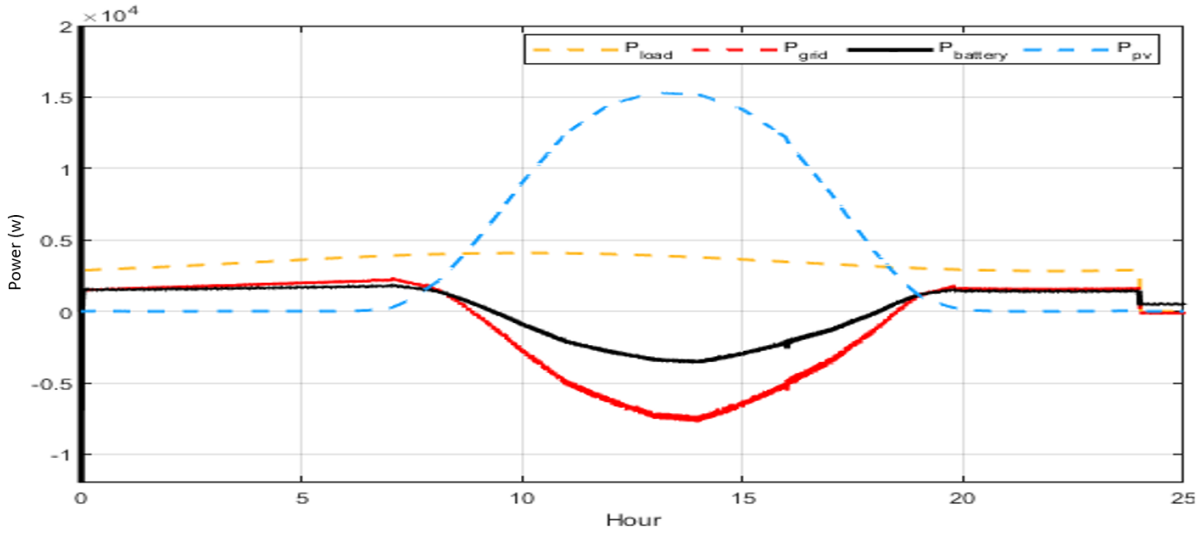

Figure 4.10 *Hybrid System Power-Based on the Proposed Method at 20% < SOC <80%*

4.5.5 SOC control verification

Two further tests were performed to validate that Controller 2, which uses logical conditions to regulate the battery's SOC between 20% and 80%, is functional. The first instance started with an 80% charge. The second scenario included less than 20%. The initial simulation revealed that the state of charge (SOC) gradually increased above 80%, allowing us to assess how successfully the controller managed the charge.

4.5.5.1 Case 1: SOC ≥ 80%

Figure 4.11 depicts a scenario in which, when the battery's state of charge exceeds 80%, both the battery and the grid give electricity to the load. As soon as PV production exceeds load demand, the battery that was depleted with a SOC of less than 80% begins to recharge. The charging continues till the state of charge reaches 80% once more. When the battery reaches this level, it is deactivated to prevent overcharging, and the excess energy from the photovoltaic panels is fed into the grid.

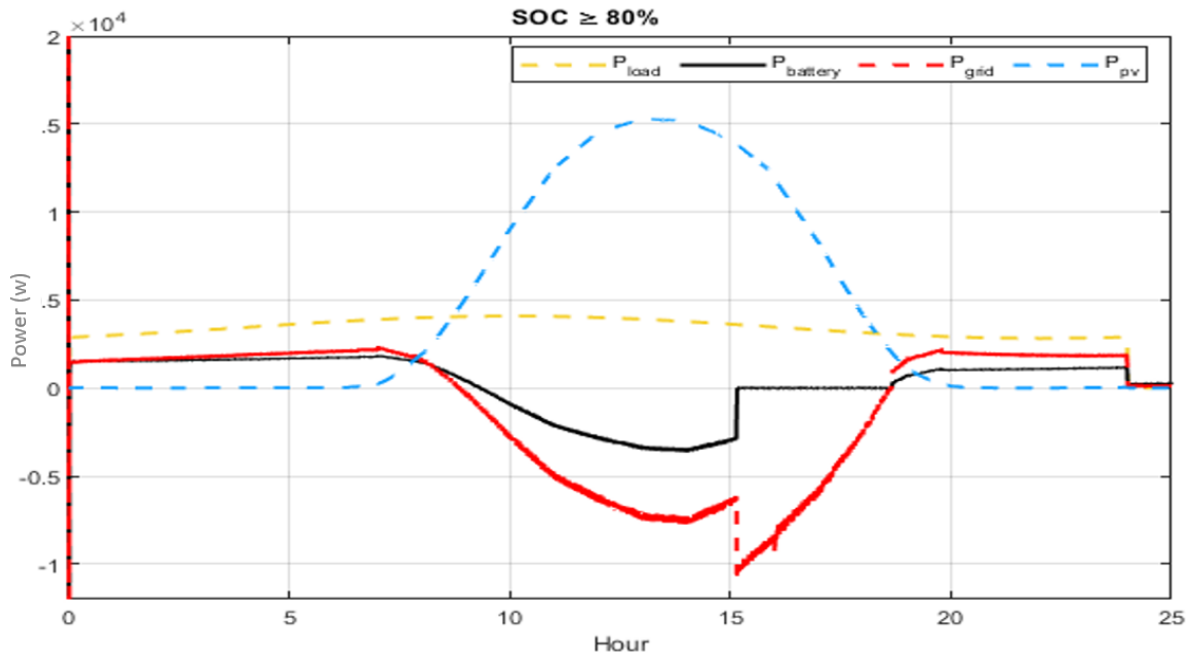

Figure 4.11 *Hybrid System Power (SOC≥80%)*

Figure 4.12 Displays the battery's State of Charge (SOC) development with a limitation of >= 80%. In the morning (between 0 and 10 h), the SOC gradually decreases, showing that the battery is discharging to meet the demand when there is insufficient PV. The minimum SOC is 79.9%.

When surplus PV production becomes available after 10 hours, the battery begins to charge, gradually increasing the SOC to 80% in around 15 hours. To prevent overcharging, the energy management system turns off the battery at this point. Energy surpluses are transferred to the grid.

The SOC remains at around 80% for 15 and 20 hours, indicating good upper SOC limit control. Due to declining solar production, a new discharge phase begins after 20 hours, lowering SOC but maintaining it above 79.8%.

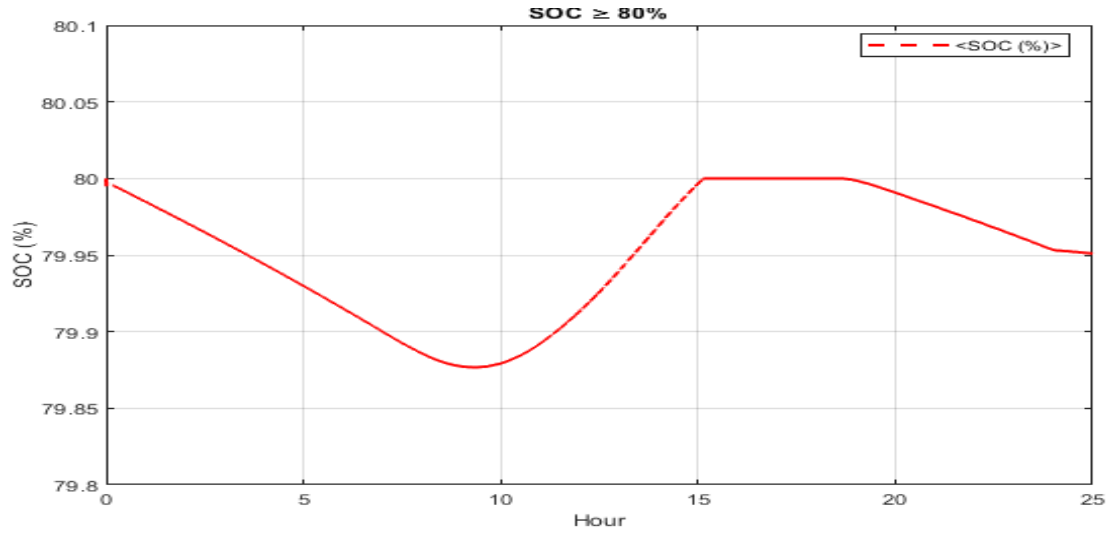

Figure 4.12 *Battery state of charge (SOC≥80%)*

4.5.5.2 Case 2: SOC < 20%

Figure 4.13 depicts the second example, in which the initial level of charge is less than 20%. To prevent deep discharge, the battery is initially rendered inactive. The grid provides all power. When photovoltaic generation is available, it is used to charge the battery, with any excess energy being transmitted to the grid.

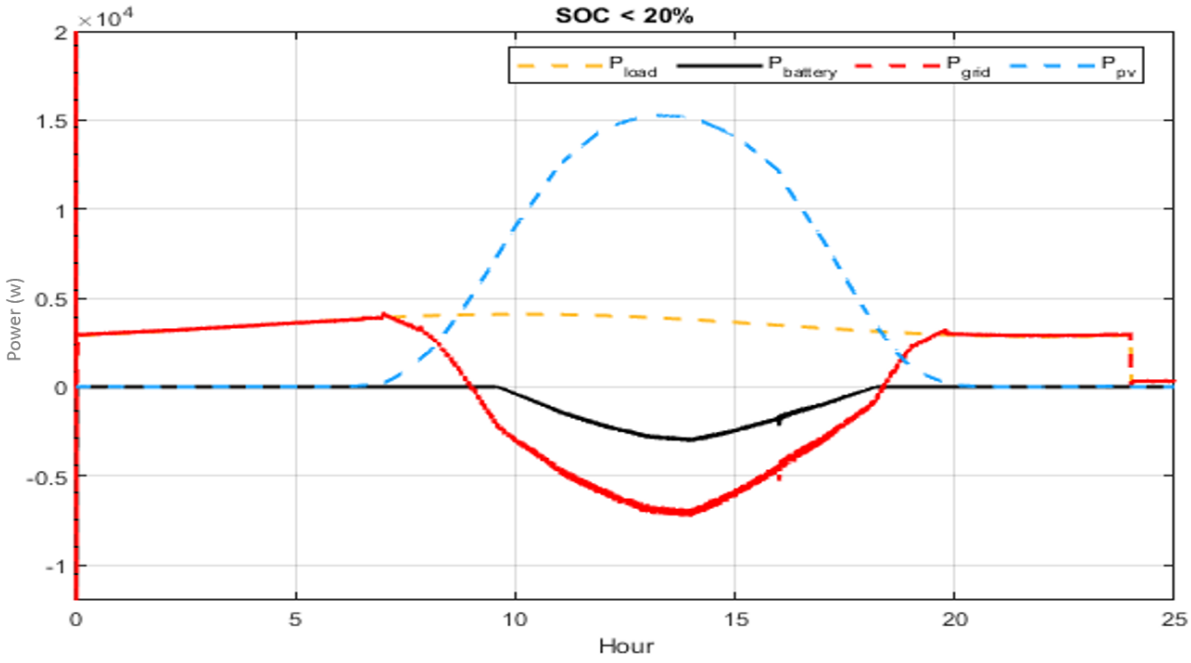

Figure 4.13 *Hybrid system power (SOC <20%)*

Figure 4.14 displays the progression of the battery's state of charge (SOC) during a 25-hour period, beginning with less than 20%. During the first 15 hours, the State of Charge (SOC) remains constant at 19%, indicating that the battery is kept dormant to avoid premature discharge and hence extend its lifespan. When solar production (PV) exceeds local demand, the battery begins rapid charging, peaking at hour 16 with a state of charge (SOC) increase of roughly 19.15% before stabilizing at this new equilibrium level. The quick SOC shift in one hour demonstrates the effectiveness of the energy management system, which ensures a safe and regulated charging operation, reducing the risk of overcharging or damage.

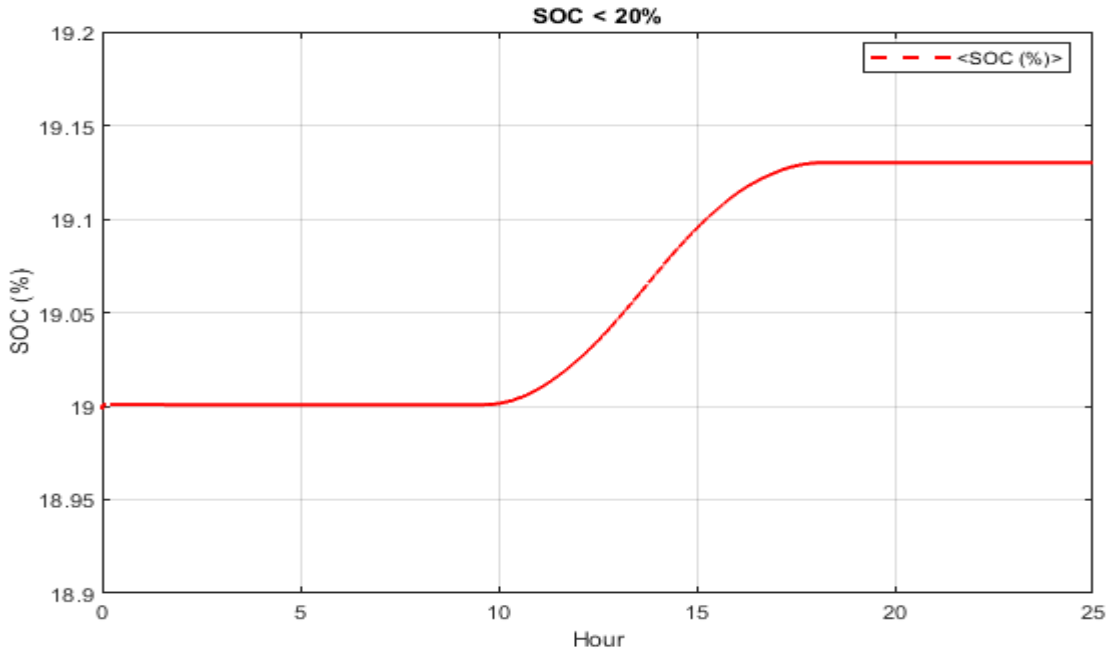

Figure 4.14 *Battery state of charge (SOC <20%)*

4.5.6 Overall Discussion and Interpretation of the Results

This pattern highlights the system's intelligent and efficient management of renewable energy resources. By effectively utilizing solar energy surplus to recharge the battery, the system ensures a continuous balance between electricity generation, consumption, and storage. This dynamic coordination not only stabilizes the energy supply but also protects the battery from excessive cycling, abrupt fluctuations, and potential degradation, thereby enhancing the longevity and reliability of the storage system. The adaptive operation ensures that energy is used optimally, prioritizing self-consumption when solar production is high and drawing from the battery only when necessary, which ultimately reduces reliance on the electrical grid.

The comparative analysis further demonstrates that the Grey Wolf Optimizer (GWO) outperforms Particle Swarm Optimization (PSO) across several key metrics. Specifically, GWO achieves faster convergence to optimal solutions, exhibits lower oscillations, and provides more accurate control over the battery's state of charge (SOC). These improvements are attributed to GWO's strategic balance between exploration and exploitation, combined with its multi-leader hierarchy, which prevents premature convergence to local optima a common limitation in many heuristic optimization methods. By maintaining this robust search mechanism, GWO is able to respond effectively to dynamic variations in solar irradiation and load demand, ensuring stable operation even under highly variable conditions.

Recent studies on renewable energy systems and microgrid control have further reinforced these observations, highlighting the algorithm's robustness and versatility in nonlinear control applications. Beyond the algorithmic performance, the proposed approach delivers tangible operational benefits: it improves voltage stability throughout the microgrid, minimizes stress on the battery to extend its lifespan, and reduces dependency on the main grid. These advantages are particularly significant for PV-based microgrids in regions such as Algeria, where solar irradiance can fluctuate considerably. By integrating such an intelligent energy management strategy, microgrids can achieve higher efficiency, greater reliability, and more sustainable operation, providing a practical solution for both urban and remote communities seeking to maximize renewable energy utilization while maintaining system resilience.

4.6 CONCLUSION

This chapter presented and analyzed the simulation results obtained for the studied hybrid microgrid, focusing on the validation of the proposed forecasting, control, and energy management strategies. The MATLAB/Simulink simulations allowed a detailed assessment of the system's dynamic behavior under realistic conditions, accounting for the natural variability of renewable resources and consumption patterns typical of the Djelfa region in Algeria.

The forecasting methods implemented for solar irradiance, ambient temperature, and electricity consumption proved effective, with the best-performing models, ANN for irradiance and temperature and linear regression for consumption, providing accurate and reliable time-series data. These forecasted inputs enabled realistic excitation of the Simulink model, ensuring that subsequent analyses of control and energy management strategies reflected true operating conditions.

The detailed modeling of the microgrid including the photovoltaic generator, lithium-ion battery, DC bus, inverter, and grid connection enabled comprehensive evaluation of DC bus voltage regulation, battery state-of-charge control, and power distribution among sources. The results demonstrated that the FOPI controller optimized with GWO achieves fast and stable voltage regulation, outperforming both PSO and conventional PID controllers in terms of convergence speed, stability, and dynamic response.

Battery behavior analysis showed that the proposed approach effectively balances charging and discharging, prevents over-cycling, and minimizes voltage and current fluctuations, thereby prolonging battery lifetime. The intelligent energy management strategy maximizes self-consumption, reduces grid dependency, and ensures reliable microgrid operation even under highly variable solar production and load demand.

Comparative evaluation of optimization algorithms confirmed the superiority of the Grey Wolf Optimizer GWO over Particle Swarm Optimization PSO, thanks to its ability to maintain an optimal balance between exploration and exploitation and to avoid premature convergence to local minima. This robustness translates into improved system stability, more precise SOC control, and enhanced overall operational safety.

In conclusion, the results of this chapter validate the effectiveness of the proposed integrated strategy for forecasting, control, and energy management in hybrid photovoltaic microgrids. The combination of accurate forecasting, FOPI control optimized with GWO, and adaptive battery management not only improves technical performance but also enhances system reliability, durability, and resilience. These findings provide a solid foundation for the practical implementation of photovoltaic microgrids in regions with high solar potential such as Algeria and offer a pathway toward more autonomous, efficient, and sustainable local energy systems.

General Conclusion

This thesis presented a comprehensive study on the control and optimization of energy storage systems within smart grid environments, with particular emphasis on lithium-ion batteries integrated into photovoltaic-based hybrid microgrids. The research addressed key challenges related to renewable energy intermittency, battery degradation, and the limitations of conventional control strategies.

An extensive state-of-the-art review was first conducted to analyze the evolution of electrical networks, the architecture of smart grids, and the characteristics of existing energy storage technologies. This analysis highlighted the strategic role of energy storage systems in enhancing grid flexibility and reliability. Among the various technologies, lithium-ion batteries were identified as the most suitable solution for modern energy management applications due to their high energy density, efficiency, and technological maturity.

The thesis then focused on the detailed modeling of lithium-ion batteries and their integration into a hybrid microgrid comprising photovoltaic generation, bidirectional DC–DC converters, and grid connection. Accurate electrical modeling was shown to be essential for capturing the dynamic behavior of the battery and for designing effective control strategies capable of preserving battery health while ensuring reliable power supply.

To overcome the shortcomings of classical PI controllers, an advanced energy management strategy based on a Fractional-Order PI (FOPI) controller optimized using the Grey Wolf Optimizer (GWO) algorithm was proposed. The use of fractional calculus allowed finer tuning of system dynamics, while the GWO algorithm enabled efficient and robust optimization of controller parameters in a nonlinear and time-varying environment.

Simulation results confirmed that the proposed FOPI–GWO control strategy significantly improves system performance in terms of transient response, overshoot reduction, steady-state accuracy, and robustness against disturbances. Moreover, the optimized control scheme effectively reduces unnecessary battery cycling and mitigates stress on the storage system, thereby contributing to the extension of battery lifetime and the improvement of overall energy efficiency.

In conclusion, this work demonstrates that the combination of fractional-order control and bio-inspired optimization represents a promising solution for advanced energy

management in smart grids. The proposed methodology provides a solid foundation for future developments, including experimental validation, real-time implementation, and the extension of the strategy to multi-storage systems, electric vehicle integration, and large-scale smart grid applications.

References

[1] M. Keskin, “Smart grids and Turkey: An overview of the current power system and smart grid development,” 2021.

[2] A. B. Adeniran, *Architecture Design and Optimization of Edge-Enabled Smart Grids*, Ph.D. dissertation, Univ. of South Florida, 2020.

[3] B. Multon, *Production d’énergie électrique par sources renouvelables*, Editions TI, 2003.

[4] J. Mitali, S. Dhinakaran, and A. A. Mohamad, “Energy storage systems: A review,” *Energy Storage and Saving*, vol. 1, no. 3, pp. 166–216, 2022.

[5] H. El Makhtoum and Y. Bentaleb, “Réseaux électriques intelligents (Smart Grids),” in *Proc. COC’2021*, 2021.

[6] D. B. Avancini *et al.*, “Energy meters evolution in smart grids: A review,” *Journal of Cleaner Production*, vol. 217, pp. 702–715, 2019.

[7] M. Y. Ali, *Energy Management System of a Microgrid with Distributed Generation*, Ph.D. dissertation, 2019.

[8] F. E. Abrahamsen, Y. Ai, and M. Cheffena, “Communication technologies for smart grid: A comprehensive survey,” *Sensors*, vol. 21, no. 23, p. 8087, 2021.

[9] S. Ishaq *et al.*, “A review on recent developments in control and optimization of microgrids,” *Energy Reports*, vol. 8, pp. 4085–4103, 2022.

[10] F. Y. Melhem, *Optimization Methods and Energy Management in Smart Grids*, Ph.D. dissertation, Univ. Bourgogne Franche-Comté, 2018.

[11] J. Klaimi, *Gestion Multi-Agents des Smart Grids Intégrant un Système de Stockage*, Ph.D. dissertation, UTT & Université Libanaise, 2017.

[12] A. S. Veerendra, M. R. B. Mohamed, and F. P. García Márquez, “Energy management control strategies for energy storage systems of hybrid electric vehicles: A review,” *Energy Storage*, vol. 6, no. 1, e573, 2024.

[13] R. Kabouche, S. Harrouni, and A. Talha, “Étude comparative des techniques de stockage de l’énergie photovoltaïque,” *Revue des Énergies Renouvelables*, pp. 115–129, 2012.

[14] N. Benabdallah, *Apport du Stockage Inertiel dans la Production Éolienne*, Ph.D. dissertation, Univ. Ibn Khaldoun–Tiaret, 2020.

[15] M. Gournis, *Perspectives de stockage d’énergie en Belgique à l’horizon 2030*, Master dissertation, University of Namur, 2019..

[16] D. H. X. de Vries, *Investigating the Potential Role of Pumped Hydro Storage in the Ethiopian Energy System*, Ph.D. dissertation, TU Delft, 2023.

[17] H. Ibrahim, *Étude et Conception d’un Générateur Hybride Éolien–Diesel avec Stockage d’Air Comprimé*, Ph.D. dissertation, UQAC, 2010.

[18] H. Benyettou and I. Laouedj, *Étude et Conception des Systèmes de Stockage d’une Station Photovoltaïque*, 2021.

[19] A. I. Zermane, *Contribution à l’Optimisation des Systèmes Photovoltaïques par le Stockage de l’Énergie*, Ph.D. dissertation, 2025.

[20] S. Souhila and M. Razika, *Étude et Caractérisation des Supercondensateurs*, Ph.D. dissertation, UMMTO, 2024.

[21] F. Benmebarek, *Étude de l’Hystérésis Magnétique dans les Matériaux Supraconducteurs*, Ph.D. dissertation, 2024.

[22] S. Laouarem, *Contrôle des Puissances par SMES*, Ph.D. dissertation, 2018.

[23] P. Lhoste, *La Technodiversité Émergente de la Mine Urbaine*, Ph.D. dissertation, Toulouse INP, 2023.

[24] A. A. Boudiba and T. Sellami, *Battery Management System – SOC Estimation*, Ph.D. dissertation, 2021.

[25] S. Abdelouhab, *New Architecture for Porous Silicon Anodes for Li-Ion Batteries*, Ph.D. dissertation, 2025.

[26] N. Boudraa and A. Branis, *Fault Prognostics of Li-Ion Batteries Using Deep Learning*, Ph.D. dissertation, Univ. Kasdi Merbah Ouargla.

[27] B. Mohammed and B. Massilva, *SOC Estimation of Li-Ion Batteries Using State Observers*, Ph.D. dissertation, UMMTO, 2024.

[28] B. Dahmane and D. Yahia, *Energy Management System for Hybrid Sources*, Ph.D. dissertation, UMMTO, 2024.

[29] S. Ouedraogo, *Optimized Energy Management Strategies in PV Microgrids*, Ph.D. dissertation, Univ. Pascal Paoli, 2023.

[30] T. J. Wurschmidt, *Optimized Battery Control Strategy for Sustainable Buildings*, Master's thesis, NTNU, 2025.

[31] M. M. Rahman *et al.*, "Assessment of energy storage technologies: A review," *Energy Conversion and Management*, vol. 223, p. 113295, 2020, doi:10.1016/j.enconman.2020.113295.

[32] A. G. Olabi *et al.*, "Critical review of energy storage systems," *Energy*, vol. 214, p. 118987, 2021, doi:10.1016/j.energy.2020.118987.

[33] T. M. Gür, "Review of electrical energy storage technologies, materials and systems," *Energy & Environmental Science*, vol. 11, 2018, doi:10.1039/C8EE01419A.

[34] C. Zhang *et al.*, "Energy storage system: Current studies on batteries and power conditioning systems," *Renewable and Sustainable Energy Reviews*, vol. 82, pp. 3070–3084, 2018, doi:10.1016/j.rser.2017.10.030.

[35] K. Itani and A. De Bernardinis, "Review on new-generation battery technologies," *Energies*, vol. 16, p. 7530, 2023, doi:10.3390/en16227530.

[36] T. Chen *et al.*, “Applications of lithium-ion batteries in grid-scale energy storage systems,” *Trans. Tianjin Univ.*, vol. 26, pp. 236–245, 2020, doi:10.1007/s12209-020-00236-w.

[37] H. C. Hesse *et al.*, “Lithium-ion battery storage for the grid,” *Energies*, vol. 10, p. 2107, 2017, doi:10.3390/en10122107.

[38] M. Förstl *et al.*, “Assessment of residential battery storage systems,” *Int. J. Energy Research*, vol. 44, pp. 4770–4782, 2020, doi:10.1002/er.4770.

[39] Z. Song, X. Guan, and M. Cheng, “Multi-objective optimization strategy for home energy management systems,” *Energy Reports*, vol. 8, pp. 1234–1248, 2022, doi:10.1016/j.egyr.2022.04.023.

[40] T. Sayfutdinov and P. Vorobev, “Optimal utilization strategy of LiFePO4 battery storage,” *Applied Energy*, vol. 316, p. 119080, 2022, doi:10.1016/j.apenergy.2022.119080.

[41] Y. Yoo and Y. Ha, “Market attractiveness analysis of battery energy storage systems in Southeast Asia,” *Renewable and Sustainable Energy Reviews*, vol. 191, p. 114095, 2024, doi:10.1016/j.rser.2023.114095.

[42] A. K. Pandey *et al.*, “Solar energy utilization in ASEAN countries,” *Sustainability*, vol. 14, p. 11193, 2022, doi:10.3390/su141811193.

[43] H. E. Moon, Y. H. Ha, and K. N. Kim, “Economic analysis of PV and reused EV batteries,” *Energies*, vol. 16, p. 311, 2023, doi:10.3390/en16010311.

[44] Vistra Corp., “Vistra Zero,” 2024. [Online]. Available: https://vistracorp.com/vistra-zero/

[45] Neoen, “Victoria Big Battery,” 2024. [Online]. Available: https://victorianbigbattery.com.au/

[46] Eneco, “EnspireME,” 2024. [Online]. Available: https://www.eneco.nl/

[47] B. Li *et al.*, “Review on photovoltaic with battery energy storage systems,” *J. Energy Storage*, vol. 61, p. 106763, 2023, doi:10.1016/j.est.2023.106763.

[48] J. Liu *et al.*, “Renewable energy design for net-zero energy buildings,” *Energy Conversion and Management*, vol. 295, p. 117768, 2023, doi:10.1016/j.enconman.2023.117768.

[49] K. E. Ouedraogo *et al.*, “Low-cost energy management systems for residential buildings,” *Energy*, vol. 271, p. 126922, 2023, doi:10.1016/j.energy.2023.126922.

[50] G. Zhao *et al.*, “Economic analysis of integrating PV and BESS in office buildings,” *Energy and Buildings*, vol. 284, p. 112885, 2023, doi:10.1016/j.enbuild.2023.112885.

[51] D. S. Obaid, A. J. Mahdi, and M. H. Alkhaffaji, “Optimal energy management of a PV–battery–grid system,” *Indonesian J. Electrical Eng. Comput. Sci.*, vol. 27, no. 3, pp. 1162–1175, 2022.

[52] O. Hafsi *et al.*, “Integration of hydrogen technology in DC microgrids,” *Sustainable Energy Technologies and Assessments*, vol. 52, p. 102121, 2022.

[53] M. Moghimi *et al.*, “Rule-based energy management system in an experimental microgrid,” in *MATEC Web of Conf.*, vol. 10011, 2016.

[54] N. Attou *et al.*, “Energy management system for hybrid microgrids,” *Electrotehnica, Electronica, Automatica*, vol. 69, no. 2, 2021.

[55] H. Aboubaida *et al.*, “Energy management and control strategy of DC microgrids,” *Simulation Modelling Practice and Theory*, vol. 124, p. 102726, 2023.

[56] G. Muriithi and S. Chowdhury, “Reinforcement learning-based energy management,” *Energies*, vol. 14, no. 9, p. 2700, 2021.

[57] R. Rigo-Mariani, *Integrated Design Methods for Microgrids with Storage*, Ph.D. dissertation, INP Toulouse, 2014.

[58] D. Allart, *Electro-Thermal Modeling of Li-Ion Batteries*, Ph.D. dissertation, Normandie Univ., 2017.

[59] P. von Hohendorff Seger, *Uncertainty Modeling and Energy Management of Second-Life Li-Ion Batteries*, Ph.D. dissertation, Univ. Grenoble Alpes, 2022.

[60] K. Amin, S. K. Cho, and S. J. Kwon, “SOC and SOH estimation using adaptive observers,” *J. Energy Storage*, vol. 21, pp. 270–280, 2019.

[61] D. Andrea, *Battery Management Systems for Large Lithium-Ion Battery Packs*, Norwood, MA, USA: Artech House, 2010.

[62] H. Zhang, X. Xu, and L. Xu, “A method for internal resistance estimation of lithium-ion batteries,” *Journal of Power Sources*, vol. 266, pp. 561–566, 2014.

[63] M. W. Verbrugge *et al.*, “Electrical impedance spectroscopy and its application to battery systems,” *Journal of The Electrochemical Society*, vol. 156, no. 11, pp. A927–A936, 2009.

[64] A. Mukhopadhyay and L. Zhang, “Battery terminal voltage estimation using a model-based approach,” *Journal of Power Sources*, vol. 252, pp. 376–385, 2014.

[65] Z. Dang, Y. Wang, H. Li, and Z. Chen, “Open-circuit voltage hysteresis modeling for lithium-ion batteries,” *Energies*, vol. 10, no. 10, p. 1447, 2017.

[66] MIT Electric Vehicle Team, *Electric Vehicle Basics*, MIT, 2008.

[67] A. Li, “Analyse expérimentale et modélisation d’éléments de batterie et de leurs assemblages,” Ph.D. dissertation, 2013.

[68] S. Piller, M. Perrin, and A. Jossen, “Methods for state-of-charge determination and their applications,” *Journal of Power Sources*, vol. 96, no. 1, pp. 113–120, 2001.

[69] A. Eddahech, *Modélisation du vieillissement et détermination de l’état de santé des batteries Li-ion*, Ph.D. dissertation, Univ. Bordeaux, 2013.

[70] N. Kularatna, “Battery management systems and SOC development for EVs,” *IEEE Potentials*, vol. 34, no. 1, pp. 14–20, 2015.

[71] Z. Chen, C. C. Mi, and Y. Fu, “State of health estimation for lithium-ion batteries using grey relational grade analysis,” *IEEE Trans. Vehicular Technology*, vol. 62, no. 7, pp. 3521–3530, 2013.

[72] X. Chen *et al.*, “State of health estimation and degradation modes analysis of pouch NMC532/graphite Li-ion batteries,” *Journal of Power Sources*, vol. 498, p. 229884, 2021, doi:10.1016/j.jpowsour.2021.229884.

[73] M. S. H. Lipu *et al.*, “State-of-charge estimation for lithium-ion batteries: A review,” *IEEE Access*, vol. 6, pp. 18362–18381, 2018.

[74] M. Noura *et al.*, “A review on battery management systems for electric vehicles,” *Renewable and Sustainable Energy Reviews*, vol. 134, p. 110222, 2020.

[75] S. Cailliez, *Modélisation du comportement et du vieillissement d’une batterie automobile*, Ph.D. dissertation, École Centrale de Nantes, 2023.

[76] Y. Ghoulame, *Multi-Physics Modeling and Intelligent Energy Management of Hybrid Storage Systems*, Ph.D. dissertation, Univ. Strasbourg, 2023.

[77] G. Javid, *SOC Estimation and Optimized Management of Li-Ion Batteries*, Ph.D. dissertation, Univ. Haute Alsace, 2021.

[78] C. Lorenzo, *Multi-Criteria Optimization of Hybrid Hydrogen-Electric Trains*, Ph.D. dissertation, Univ. Bourgogne Franche-Comté, 2021.

[79] A. Ramakrishnan *et al.*, “Review on Li-ion batteries with battery management systems in electric vehicles,” *Advances in Materials Science and Engineering*, 2022.

[80] R. Sadoun, *Hybrid Electrical Energy Sources for Urban Electric Vehicles*, Ph.D. dissertation, École Centrale de Lille, 2013.

[81] A. Adel, *Fractional-Order Modeling of Li-Ion Batteries for SOC and SOH Estimation*, Ph.D. dissertation, Univ. Bordeaux, 2025.

[82] J. Hemdani, *Intelligent SOC and SOH Monitoring Systems for EV Batteries*, Ph.D. dissertation, Univ. Paris-Saclay, 2025.

[83] D. Andrea, *Battery Management Systems for Large Lithium-Ion Battery Packs*, Artech House, 2010.

[84] H. Aoudjeregba, *Control of Hybrid Renewable Energy Systems*, Ph.D. dissertation, 2025.

[85] N. Hata, *Control of Grid-Connected Photovoltaic Systems*, Ph.D. dissertation, 2025.

[86] Y. Tong *et al.*, "Bidirectional DC–DC converter topologies for hybrid energy storage systems in EVs," *Energies*, vol. 18, no. 9, p. 2312, 2025.

[87] P. Poolphaka, *High-Frequency Permanent Magnet Conversion Chains*, Ph.D. dissertation, Univ. Lorraine, 2024.

[88] F. Zayas-Gato *et al.*, *PID Controller Design*, Univ. of A Coruña, 2020.

[89] Control Automático Educación, "Derivative control action—PID," 2023. [Online]. Available: https://controlautomaticoeducacion.com/

[90] FIRST Robotics Competition, "Introduction to PID," 2023. [Online]. Available: https://docs.wpilib.org/

[91] T. Nouaoui, *Advanced Control Techniques for PMSM-Based Systems*, Ph.D. dissertation, 2025.

[92] N. Djedjiga and T. Malia, *FPGA Implementation of Neuro-Fuzzy Control*, Ph.D. dissertation, UMMTO, 2024.

[93] Y. K. A. Langueh, *Neural Network and Fuzzy Logic Algorithms on FPGA for MPPT*, Ph.D. dissertation, UQAR, 2024.

[94] Y. Mansour, *Intelligent Controllers for Voltage Regulation in Power Networks*, Ph.D. dissertation, UQAT, 2024.

[95] M. Jain *et al.*, "Variants and advancements of PSO algorithm," *Applied Sciences*, vol. 12, no. 17, p. 8392, 2022.

[96] M. Shoaei *et al.*, "Applications of AI in renewable energy systems," *Energy Conversion and Management*, vol. 306, p. 118207, 2024.

[97] C. Garron, *Optimization of DC Networks in Buildings*, Ph.D. dissertation, Univ. Grenoble Alpes, 2025.

[98] T. Abdelhalim *et al.*, “Enhanced DC bus stability using optimized FOPID controller,” in *Proc. IC2EM*, IEEE, 2023.

[99] Y. Cui, *Improved Artificial Bee Colony Algorithms*, Ph.D. dissertation, Centrale Lille, 2022.

[100] N. M. Hatta *et al.*, “Recent studies on Grey Wolf Optimizer,” *Artificial Intelligence Review*, vol. 52, no. 4, pp. 2651–2683, 2019.

[101] S. Ouedraogo, *Développement de Stratégies Optimisées de Gestion de l’Énergie Intermittente dans un Micro-Réseau Photovoltaïque avec Stockage*, Ph.D. dissertation, Université Pascal Paoli, 2023.

[102] L. Bournival, *Conception d’un Banc d’Essai pour Contrôleurs MPPT Intelligents*, Ph.D. dissertation, Université du Québec en Abitibi-Témiscamingue, 2025.

[103] A. Teta, M. M. Rezaoui, A. Kouzou, and A. Djalab, “Fuzzy logic based MPPT for grid-connected PV systems with Z-source inverter,” in *Proc. Int. Conf. on Artificial Intelligence in Renewable Energetic Systems*, Springer, 2018, pp. 139–147.

[104] T. Mesbahi *et al.*, “Advanced model of hybrid energy storage systems integrating lithium-ion batteries and supercapacitors,” *IEEE Trans. Industrial Electronics*, vol. 68, no. 5, pp. 3962–3972, 2020.

[105] A. Al-Lami and Á. Török, “Regional forecasting of CO_2 emissions of transportation in Central Europe,” *Energy Reports*, vol. 13, pp. 1215–1224, 2025.

[106] S. K. Towfek, N. Khodadadi, and L. Abualigah, “AI in higher education using PSO-guided optimization,” *Journal of Artificial Intelligence Engineering Practice*, vol. 1, no. 1, pp. 1–17, 2024.

[107] U. Habib, M. M. Latif, and K. Zahid, “Real-time optimization of solar PV integrated smart grids,” *Kashf Journal of Multidisciplinary Research*, vol. 2, no. 5, pp. 103–116, 2025.

[108] M. Zheng and X. Luo, “Joint SOC and SOH estimation using SVM, CNN, and LSTM models,” *International Journal of Electrochemical Science*, vol. 19, no. 9, p. 100747, 2024.

[109] N. Ladaci, A. Saadia, and A. Belaadi, “ANN and RSM prediction of water uptake of recycled HDPE biocomposites,” *Journal of Natural Fibers*, vol. 21, no. 1, p. 2356697, 2024.

[110] J. Thongjamroon, S. Phimphisan, and N. Sriwiboon, “Explainable CNN–LSTM framework for crude oil price forecasting,” *Journal of Robot Control*, vol. 6, no. 5, pp. 2109–2116, 2025.

[111] M. Maissa and L. Kouider, “Direct power control technique for grid-tied VSI inverter fed by photovoltaic systems,” in *Proc. ICRSEtoSET*, IEEE, 2023.

[112] M. Maissa, L. Kouider, and T. Ali, “DPC control for grid-tied inverters under parameter variations,” in *Proc. IC2EM*, IEEE, 2023.

[113] J. Thirumaran and S. Shylaja, “Medical image processing—An introduction,” *International Journal of Science and Research*, vol. 4, no. 11, pp. 1197–1199, 2015.